The Intracellular Kinetics of HIV-1 Replication

Mowgli Holmes

Submitted in partial fulfillment of the
requirements for the degree of
Doctor of Philosophy
under the Executive Committee
of the Graduate School of Arts and Sciences

Columbia University

2013

ABSTRACT

The Intracellular Kinetics of HIV-1 Replication

Mowgli Holmes

The rate of HIV-1 replication has an impact on the viral loads patients have and the

time it takes for an infection to progress to AIDS. This replication rate is defined

partly by the time it takes an infected cell to begin producing new infectious virus,

and this, in turn, is defined by the time required for each step of the viral life cycle

inside cells. Many of the stages of the HIV-1 life cycle have been well-characterized

mechanistically, but the timing with which they occur has not. HIV-1 is under strong

pressure to replicate rapidly, yet evidence indicates that there are stages at which

there is active viral auto-inhibition of the rate of replication. We therefore sought to

characterize the timing of each major stage of the viral life cycle and to determine

how they are correlated with one another. Using a variety of techniques including

quantitative microscopy we tracked the timing of these events, both in bulk infected

cultures and in single infected cells, and generated a time line of the HIV-1

replication cycle. We find that there is a delay of about 11 hours between integration

and gene expression, whereas early and late gene expression are separated by only

about 3 hours. In addition we find that a critical event prior to assembly, the virus-

directed removal of the host restriction factor APOBEC3G, takes place within 2.5

hours following late gene expression. One of the major processes HIV-1 must complete before it can produce new virions is the clearance of antiviral restriction factors that can block the production of new infectious virus. We present evidence in support of the hypothesis that the assembly and release of virions, which is inhibited by the presence of the MA domain of the Gag protein, is delayed precisely in order to allow restriction factor clearance to reach completion before the assembly process begins.

Table of Contents

List of Figures.

List of Abbreviations.

HIV-1	Human Immunodeficiency Virus-1
CTL	cytotoxic T lymphocytes
WT	wild-type
PIC	pre-integration complex
RTC	reverse transcription complex
PFA	paraformaldehyde
PBMC	peripheral blood mononuclear cells
MOI	multiplicity of infection
A3G	APOBEC3G
PIP2	phosphatidylinositol-4,5 bisphosphate
ELV	Elvitegravir
EFV	Efavirenz
NEL	Nelfinavir
MA	matrix
CA	capsid
IN	integrase
RT	reverse transcriptase

Acknowledgments

Many, many people helped me with this thesis and this PhD. Most of all I thank my advisor, Paul Bieniasz, for sticking it out, for being all-seeing, and for teaching me what science I know.

Next I thank David Fidock, for making this happen. Really: thank you.

I'm very grateful to my thesis committee, Christian Schindler, Steve Goff, and Saul Silverstein. Steve was a friendly source of knowledge many times when I most needed it. Christian I especially thank for not ever letting things get past him, and for helping me to switch gears when I needed to. Saul I thank for being willing to do all the work he did on this thesis itself. It might not have happened otherwise.

I also thank David Volsky, who is the nicest guy I ever worked for or with. I'm grateful to the entire Volsky lab for all their help and support (especially Galina).

The members of the Bieniasz lab are a wonderful and fascinating and incredibly generous group of people. Many thanks to every one of them, for taking me in, and sorting me out, or trying to. Special thanks to Mudathir, for recommending slowness as a means toward speed.

Above all I thank my lovely wife, for doing all the actual work.

Chapter 1. Introduction

The dynamics of HIV-1 infection in patients

The work presented here is concerned with the timing of the events of the HIV-1 intracellular replication cycle. The temporal course of HIV-1 infection has been studied at another scale, in patients, for over 25 years. HIV-1 causes a prolonged and incurable infection which, untreated, leads to the fatal complications of AIDS. After an initial acute phase of infection, viral load drops sharply, typically by more than 100-fold, and remains low and primarily stable for as long as a decade[1-4]. Patients remain asymptomatic during this extended period of clinical latency, but over its course the number of CD4-positive T-cells gradually declines[5-7]. These are the primary target cells of HIV-1 and play a central role in the immune system as a whole. Eventually they drop below a critical threshold, and as they do viral loads begin to rise sharply[8-13]. At this point, in the absence of a functioning immune system, patients are vulnerable to a wide range of normally unthreatening pathogens. HIV-1 is fatal if untreated, but untreated patients live for an average of ten years[1,14-16].

It was initially believed that the clinical latency period was also one of viral latency. This is not the case; viral replication is ongoing and vigorous during this time[17,18], producing as many as 10^{10} virions per day in an infected patient[19]. A quasi-steady state is in place for this period, in which the virus is cleared at close to the same rate at which it is produced[18,20,21]. During clinical latency a conflict takes place between HIV-1 and the immune system, central to which is the killing of HIV-1-infected cells by CD8-positive cytotoxic T lymphocytes (CTL) that are specifically directed against HIV-1 antigens[22,23]. During the asymptomatic period, the immune system continuously generates CTL responses against particular HIV-1 epitopes displayed on infected cells. These responses partially suppress viral loads, but they are balanced by the high replication rate of the virus, and by the fact that HIV-1 continuously generates mutations in the targeted epitopes[24-26]. These CTL escape mutants can then replicate more freely until new CTL responses are generated against them[27,28].

A B-cell-mediated response is also mounted against HIV-1. Both neutralizing antibodies[29-34] and antibody-mediated cell-dependent toxicity[35-40] are thought to play a role in the ability of the immune system to slow the progression to the disease state. Most patients appear to develop antibodies targeting the Env (Envelope) protein of HIV-1. However, viral escape from these is rapid and often incurs no fitness cost to the virus[41-43]. The Env protein is highly variable in primary sequence and is heavily glycosylated[44-48]. This "glycan shield" serves to conceal

many of the available epitopes, and modifications of the pattern of sugar attachment

sites is frequently the pathway utilized to achieve viral escape from humoral

immune surveillance[49,50]. The immune system adapts in turn to increasing Env

diversity in the viral population. B cell responses are composed of many different

clonal lines, and many anti-HIV-1 antibodies show evidence of extensive somatic

hypermutation[51-55]. A small fraction of infected patients do generate potent and

broadly neutralizing antibodies[56-60], and escape from some of these may entail

fitness decreases for the virus[61,62]. Such antibodies have been cloned from post-

germinal center Env-specific B cells of infected patients[52,63]. Used in combination

they are capable of suppressing infection in humanized mice[64]. These may serve as

the basis for new approaches to vaccine development or passive vaccination

therapies, perhaps in conjunction with rational design techniques. Such antibodies

have proven very hard to elicit through vaccination, as they are typically highly

divergent from the available germline antibody sequences[65].

The human immune system is capable of mounting a multi-pronged and temporarily

effective defense against HIV-1, but over time multiple processes take place that

lead to increasing failure to control the infection, and ultimately to the destruction

of the immune system as a whole. The diversity of the viral population begins to

outstrip the sequence diversity available to the adaptive immune system[66-68]. CD4+

T cells are depleted, lowering the amount of critical T cell help available to both the

cytotoxic and humoral responses[69-71]. Both T and B cells show signs of chronic

overactivation, dysregulation, and lymphopoetic exhaustion[9,12,72-75]. The relative importance of these processes is not well understood. In addition, the rate at which progression to AIDS occurs is highly variable between patients, and is largely a function of the individual "set point" — the viral load level at the end of the acute phase[76-78]. This set point is strongly influenced by the efficacy of the HIV-1-directed CTL response, and by the fitness of the particular strain of virus in the patient[79-82]. Lower set-points can lead to a longer duration of the clinical latency period; but in the absence of treatment the latent period almost always comes to an end, the immune system ceases to provide protection, and opportunistic infections lead to patient death.

Kinetic adaptation

HIV-1 infection maintains the human immune system in a draw-out evolutionary battle that it cannot win. RNA viruses in general are extremely plastic in response to selection pressure[83-85]. HIV-1 has an error-prone reverse-transcriptase enzyme[86,87] and a propensity for genetic recombination[88-90], both of which drive efficient adaptation. After an initial bottleneck during transmission[91], the expansion of the viral population generates broad sequence variation[28], allowing HIV-1 to respond to most immunological or pharmacological pressures placed on it very rapidly. This high rate of evolution operates at several levels and timescales[51]. It allows

adaptation of HIV-1 to selection pressures in a host, within days or weeks[18,92]. It has

allowed HIV-1 to adapt to the human population in general[93-95], in a span probably

measured in years or decades. It has also allowed the Retroviridae as a whole to

become exquisitely adapted to mammals, over millenia[96-99].

Both theoretical and experimental studies have indicated that viral virulence and

replication rate are responsive to selection pressure in host populations[27,100-105], and

that in the case of HIV-1 there is variation in virulence and replication rate, both

between and within individual patients, and that these are heritable upon

transmission[106-108]. Viral phenotypes of this type, operating at the organism or

species level, have molecular correlates at the level of intracellular replication. For

instance, certain genotypes may lead to higher rates of viral production from cells,

which may ultimately contribute to an organism-level increase in virulence or

changes to the dynamics of disease progression. Selection may operate at either one

of these levels.

This idea of multi-level selection, once very controversial, has become more

accepted of late[109-112]. At its most basic it challenges the Darwinian idea of the fittest

individual as the unit of selection, by proposing that selection can operate on groups

or populations as well as individuals. Only in this context can population-level

phenotypes be seen as adaptive or maladaptive. Viral evolution is a special case of

this, and has been formulated in terms of the idea of the "quasispecies"[113-117], in

which the high mutation rates of RNA viruses are thought to generate populations where diversity and complementation play fundamentally different roles than they do in other organisms. Whether or not RNA viruses exhibit the necessary diversity and mutation rates to qualify as a quasispecies, and to demonstrate group "cooperation", has been called into question[118,119]. However, quasispecies theory simply describes a special case of group selection, and it does not require acceptance of quasispecies theory as a whole to acknowledge that selection operates at multiple levels in viral populations as well as in others. The fate of both host cells and host organisms will have an impact on which viral sequences survive in host populations, and evidence has accumulated of selection for viral genotypes that minimize single-genome reproductive success and but maximize viral persistence[27,120,121]. It is therefore possible that the characteristic temporal dynamics of HIV-1 replication leading to AIDS may themselves be an adaptation to selection pressures operating at the level of transmission or immune surveillance.

Such a hypothesis would be complicated to prove or falsify, not because HIV-1 disease progression in this case would be a "group level" phenotype of a viral population, but because any phenotype may be the result of non-adaptive processes. At one point it was widely believed among evolutionary biologists that most phenotypes were adaptive, and that adequate proof of this consisted of demonstrating a level of functionality that made chance an unlikely cause[122]. It is now generally understood that the burden of proof is higher, and that constraint,

pathology, drift and pleiotropy all need to be ruled out in order to prove adaptation[123-126]. The kinetic or dynamic pattern of a process is a phenotype, like any other, and just as likely to reflect adaptation. In the case of HIV-1, kinetic phenotypes may operate, or be selected for, at either the population or virion level, but in either case they may have been shaped by selection and may serve an adaptive role. Kinetic phenotypes are frequently assumed to reflect constraint, but this is not necessarily the case. The same is true of group-level phenotypes in general, such as virulence or disease dynamics: they may be assumed to be the result of pleiotropy, a selectively neutral or even negative "side-effect" of adaptive genetic changes[124,127-129], or the result of structural or biochemical constraint[130], but this assumption may be incorrect.

The time course of AIDS is a function, if not a simple one, of the molecular interactions between the host and the infecting strain of HIV-1. The replication rate of the virus is one key determinant of the viral set point and of the entire course of the disease. This replication rate in turn is determined by the rates of each process in the viral lifecycle. This thesis will investigate the kinetic pattern of the events of a single replication cycle of HIV-1. The timing of these events is ultimately manifested in the kinetics of virion production from each cell, which in turn impacts the balance between viral replication and immunological control that shapes the course of the disease. Whether the kinetics of any of these particular processes are the result of adaptation, constraint, or neutrality is not known, and has rarely been investigated.

But because kinetic processes can be highly regulated, can be altered by sequence variation, and can have broad functional consequences, it is quite possible for them to be structured over time by natural selection.

The dynamics of HIV-1 infection in cells

The lifetime of an untreated patient infected with HIV-1 may be near a decade. The lifetime of a single typical cell infected with HIV-1 is roughly 48 hours[19,78,79,131,132]. The life-cycle of HIV-1 is about 24 hours: the time it takes to enter a cell, integrate into its genome, and begin to release hundreds of new virions ready to infect new cells. The approximate durations of the major events of the HIV-1 life-cycle in a cell have been known for many years. But most have not been carefully defined; for many of the events there is no kinetic information of any kind available; and the mechanisms of kinetic regulation by HIV-1 are unknown.

The 48 hours that infected CD4-positive T cells in patients are thought to survive is not long. As will be shown here, HIV-1 takes a minimum of 18 hours to begin releasing new virions from infected cells. Because of the short lifetime of HIV-1-infected cells, the virus would be expected to have been under pressure to replicate as rapidly as possible, and to trigger each necessary stage inside cells the instant it becomes possible to do so. Although this may be the case for several stages, there is

evidence that several are subject to kinetic self-regulation and even auto-inhibition. Post-entry uncoating[133-135], the phases of gene expression[136-138], and virion assembly itself[139,140] are all processes over which HIV-1 exerts tight temporal regulation. They take place in a characteristic time-frame and, as we will attempt to show, disrupting or accelerating that timing can be harmful to the virus.

There is a reasonable objection to the notion that any characteristic time course is an example of "kinetic regulation." It may simply reflect constraint, rather than adaptation. The fact that events take a certain amount of time does not necessarily imply that the timing itself is being regulated or has been specifically selected for. On the other hand, it may be possible in some cases to provide evidence for such selection. The rates of each individual biochemical reaction in a pathway are themselves plastic and adaptable. Thus, where there is pressure for events to take place more rapidly, or more slowly, they can be optimized to do so. In many cases enzymes do not operate as efficiently as possible. Directed molecular evolution studies show that it is often possible to apply selection pressure to enzymes that causes them to develop improved rate constants[141,142]. Likewise for binding constants that can affect the rates at which molecules engage and disengage with their ligands[143]. The ease with which these modifications can be evolved indicates that biomolecules frequently exist at fitness optima that do not correspond to a kinetic maximum, and also that they are not necessarily separated from higher kinetic rates by any strict structural constraints.

All these considerations can provide guidelines for how to assess whether the actual kinetics of a process are serving an adaptive function. As with any function, regulation of timing should be alterable by mutation, and the study of these mutations should provide an indication of the associated fitness costs. Lacking such mutants, we can still examine how the timing of individual processes fits with other processes, and attempt to rule out constraint or neutrality by assessing whether the process could feasibly be accelerated or decelerated without reducing fitness. Their rapid rates of growth and evolution, and the temporal and immunological pressures they operate under, make retroviruses an ideal system to identify such kinetic adaptation. For the most part we do not understand why the phases of HIV-1 replication operate with the timing that they do. Defining the causes and consequences of those kinetics has the potential to reveal important information about the constraints HIV-1 is operating under, and viral mechanisms for dealing with those constraints that have not been previously apparent.

References, Chapter 1

1. Giesecke, J., Scalia-Tomba, G., Håkansson, C., Karlsson, A. & Lidman, K. Incubation time of AIDS: progression of disease in a cohort of HIV-infected homo- and bisexual men with known dates of infection. *Scand. J. Infect. Dis.* **22**, 407–411 (1990).

2. Langlade-Demoyen, P. *et al.* Immune recognition of AIDS virus antigens by human and murine cytotoxic T lymphocytes. *J. Immunol.* **141**, 1949–1957 (1988).

3. Rutherford, G. W. *et al.* Course of HIV-I infection in a cohort of homosexual and bisexual men: an 11 year follow up study. *BMJ* **301**, 1183–1188 (1990).

4. Longini, I. M. *et al.* Statistical analysis of the stages of HIV infection using a Markov model. *Stat Med* **8**, 831–843 (1989).

5. Giorgi, J. V. *et al.* Selective alterations in immunoregulatory lymphocyte subsets in early HIV (human T-lymphotropic virus type III/lymphadenopathy-associated virus) infection. *J. Clin. Immunol.* **7**, 140–150 (1987).

6. Gerstoft, J. *et al.* The immunological and clinical outcome of HIV infection: 31 months of follow-up in a cohort of homosexual men. *Scand. J. Infect. Dis.* **19**, 503–509 (1987).

7. Frazer, I. H. *et al.* Immunological abnormalities in asymptomatic homosexual men: correlation with antibody to HTLV-III and sequential changes over two years. *Q. J. Med.* **61**, 921–933 (1986).

8. Lifson, J. D. *et al.* Induction of CD4-dependent cell fusion by the HTLV-III/LAV envelope glycoprotein. *Nature* **323**, 725–728 (1986).

9. Wodarz, D., Klenerman, P. & Nowak, M. A. Dynamics of cytotoxic T-lymphocyte exhaustion. *Proc. Biol. Sci.* **265**, 191–203 (1998).

10. Pinching, A. J. Factors affecting the natural history of human immunodeficiency virus infection. *Immunodefic Rev* **1**, 23–38 (1988).

11. Robinson, H. L. T cells versus HIV-1: fighting exhaustion as well as escape.

Nat. Immunol. **4**, 12–13 (2003).

12. Hazenberg, M. D. *et al.* T-cell division in human immunodeficiency virus (HIV)-1 infection is mainly due to immune activation: a longitudinal analysis in patients before and during highly active antiretroviral therapy (HAART). *Blood* **95**, 249–255 (2000).

13. Doehle, B. P., Hladik, F., McNevin, J. P., McElrath, M. J. & Gale, M. Human immunodeficiency virus type 1 mediates global disruption of innate antiviral signaling and immune defenses within infected cells. *J. Virol.* **83**, 10395–10405 (2009).

14. Rezza, G. *et al.* The natural history of HIV infection in intravenous drug users: risk of disease progression in a cohort of seroconverters. *AIDS* **3**, 87–90 (1989).

15. Koblin, B. A. *et al.* Long-term survival after infection with human immunodeficiency virus type 1 (HIV-1) among homosexual men in hepatitis B vaccine trial cohorts in Amsterdam, New York City, and San Francisco, 1978-1995. *Am. J. Epidemiol.* **150**, 1026–1030 (1999).

16. Longini, I. M., Clark, W. S., Gardner, L. I. & Brundage, J. F. The dynamics of CD4+ T-lymphocyte decline in HIV-infected individuals: a Markov modeling approach. *J. Acquir. Immune Defic. Syndr.* **4**, 1141–1147 (1991).

17. Coombs, R. W. *et al.* Plasma viremia in human immunodeficiency virus infection. *N. Engl. J. Med.* **321**, 1626–1631 (1989).

18. Wei, X. *et al.* Viral dynamics in human immunodeficiency virus type 1 infection. *Nature* **373**, 117–122 (1995).

19. Perelson, A. S., Neumann, A. U., Markowitz, M., Leonard, J. M. & Ho, D. D. HIV-1 dynamics in vivo: virion clearance rate, infected cell life-span, and viral generation time. *Science* **271**, 1582–1586 (1996).

20. Perelson, A. S., Kirschner, D. E. & de Boer, R. Dynamics of HIV infection of CD4+ T cells. *Math Biosci* **114**, 81–125 (1993).

21. Coffin, J. M. HIV population dynamics in vivo: implications for genetic variation, pathogenesis, and therapy. *Science* **267**, 483–489 (1995).

22. Koup, R. A. *et al.* Temporal association of cellular immune responses with the initial control of viremia in primary human immunodeficiency virus type

1 syndrome. *J. Virol.* **68**, 4650–4655 (1994).

23. Borrow, P., Lewicki, H., Hahn, B. H., Shaw, G. M. & Oldstone, M. B. Virus-specific CD8+ cytotoxic T-lymphocyte activity associated with control of viremia in primary human immunodeficiency virus type 1 infection. *J. Virol.* **68**, 6103–6110 (1994).

24. Koup, R. A. Virus escape from CTL recognition. *J. Exp. Med.* **180**, 779–782 (1994).

25. Goulder, P. J. *et al.* Patterns of immunodominance in HIV-1-specific cytotoxic T lymphocyte responses in two human histocompatibility leukocyte antigens (HLA)-identical siblings with HLA-A*0201 are influenced by epitope mutation. *J. Exp. Med.* **185**, 1423–1433 (1997).

26. Borrow, P. *et al.* Antiviral pressure exerted by HIV-1-specific cytotoxic T lymphocytes (CTLs) during primary infection demonstrated by rapid selection of CTL escape virus. *Nat. Med.* **3**, 205–211 (1997).

27. Ojosnegros, S., Beerenwinkel, N. & Domingo, E. Competition-colonization dynamics: An ecology approach to quasispecies dynamics and virulence evolution in RNA viruses. *Commun Integr Biol* **3**, 333–336 (2010).

28. Henn, M. R. *et al.* Whole genome deep sequencing of HIV-1 reveals the impact of early minor variants upon immune recognition during acute infection. *PLoS Pathog.* **8**, e1002529 (2012).

29. Wang, Q. *et al.* High level serum neutralizing antibody against HIV-1 in Chinese long-term non-progressors. *Microbiol. Immunol.* **52**, 209–215 (2008).

30. Rodriguez, S. K. *et al.* Comparison of heterologous neutralizing antibody responses of human immunodeficiency virus type 1 (HIV-1)- and HIV-2-infected Senegalese patients: distinct patterns of breadth and magnitude distinguish HIV-1 and HIV-2 infections. *J. Virol.* **81**, 5331–5338 (2007).

31. Stiegler, G. *et al.* Antiviral activity of the neutralizing antibodies 2F5 and 2G12 in asymptomatic HIV-1-infected humans: a phase I evaluation. *AIDS* **16**, 2019–2025 (2002).

32. Cecilia, D., Kleeberger, C., Muñoz, A., Giorgi, J. V. & Zolla-Pazner, S. A longitudinal study of neutralizing antibodies and disease progression in HIV-1-infected subjects. *J. Infect. Dis.* **179**, 1365–1374 (1999).

33.   Turbica, I. *et al.* Temporal development and prognostic value of antibody response to the major neutralizing epitopes of gp120 during HIV-1 infection. *J. Med. Virol.* **52**, 309–315 (1997).

34.   Yamanaka, T. *et al.* Correlation of titer of antibody to principal neutralizing domain of HIVMN strain with disease progression in Japanese hemophiliacs seropositive for HIV type 1. *AIDS Res. Hum. Retroviruses* **13**, 317–326 (1997).

35.   Wren, L. H. *et al.* Specific antibody-dependent cellular cytotoxicity responses associated with slow progression of HIV infection. *Immunology* **138**, 116–123 (2013).

36.   Chung, A. W. *et al.* Activation of NK cells by ADCC antibodies and HIV disease progression. *J. Acquir. Immune Defic. Syndr.* **58**, 127–131 (2011).

37.   Baum, L. L. *et al.* HIV-1 gp120-specific antibody-dependent cell-mediated cytotoxicity correlates with rate of disease progression. *J. Immunol.* **157**, 2168–2173 (1996).

38.   Dalgleish, A. *et al.* Failure of ADCC to predict HIV-associated disease progression or outcome in a haemophiliac cohort. *Clin. Exp. Immunol.* **81**, 5–10 (1990).

39.   Tyler, D. S. *et al.* Alterations in antibody-dependent cellular cytotoxicity during the course of HIV-1 infection. Humoral and cellular defects. *J. Immunol.* **144**, 3375–3384 (1990).

40.   Ojo-Amaize, E. *et al.* Serum and effector-cell antibody-dependent cellular cytotoxicity (ADCC) activity remains high during human immunodeficiency virus (HIV) disease progression. *J. Clin. Immunol.* **9**, 454–461 (1989).

41.   Euler, Z. *et al.* Cross-reactive neutralizing humoral immunity does not protect from HIV type 1 disease progression. *J. Infect. Dis.* **201**, 1045–1053 (2010).

42.   van Gils, M. J. *et al.* Rapid escape from preserved cross-reactive neutralizing humoral immunity without loss of viral fitness in HIV-1-infected progressors and long-term nonprogressors. *J. Virol.* **84**, 3576–3585 (2010).

43.   Quakkelaar, E. D. *et al.* Escape of human immunodeficiency virus type 1 from broadly neutralizing antibodies is not associated with a reduction of viral replicative capacity in vitro. *Virology* **363**, 447–453 (2007).

44.   Neurath, A. R. & Strick, N. Confronting the hypervariability of an immunodominant epitope eliciting virus neutralizing antibodies from the envelope glycoprotein of the human immunodeficiency virus type 1 (HIV-1). *Mol. Immunol.* **27**, 539–549 (1990).

45.   Callahan, K. M., Fort, M. M., Obah, E. A., Reinherz, E. L. & Siliciano, R. F. Genetic variability in HIV-1 gp120 affects interactions with HLA molecules and T cell receptor. *J. Immunol.* **144**, 3341–3346 (1990).

46.   Kozarsky, K. *et al.* Glycosylation and processing of the human immunodeficiency virus type 1 envelope protein. *J. Acquir. Immune Defic. Syndr.* **2**, 163–169 (1989).

47.   Montefiori, D. C., Robinson, W. E. & Mitchell, W. M. Role of protein N-glycosylation in pathogenesis of human immunodeficiency virus type 1. *Proc. Natl. Acad. Sci. U.S.A.* **85**, 9248–9252 (1988).

48.   Lifson, J., Coutré, S., Huang, E. & Engleman, E. Role of envelope glycoprotein carbohydrate in human immunodeficiency virus (HIV) infectivity and virus-induced cell fusion. *J. Exp. Med.* **164**, 2101–2106 (1986).

49.   Dacheux, L. *et al.* Evolutionary dynamics of the glycan shield of the human immunodeficiency virus envelope during natural infection and implications for exposure of the 2G12 epitope. *J. Virol.* **78**, 12625–12637 (2004).

50.   Wei, X. *et al.* Antibody neutralization and escape by HIV-1. *Nature* **422**, 307–312 (2003).

51.   Hill, A. L., Rosenbloom, D. I. S. & Nowak, M. A. Evolutionary dynamics of HIV at multiple spatial and temporal scales. *J. Mol. Med.* **90**, 543–561 (2012).

52.   Scheid, J. F. *et al.* Broad diversity of neutralizing antibodies isolated from memory B cells in HIV-infected individuals. *Nature* **458**, 636–640 (2009).

53.   Cagigi, A. *et al.* CD27(-) B-cells produce class switched and somatically hyper-mutated antibodies during chronic HIV-1 infection. *PLoS ONE* **4**, e5427 (2009).

54.   Balin, S. J., Ross, T. M., Platt, J. L. & Cascalho, M. HIV genes diversify in B cells. *Curr. HIV Res.* **6**, 10–18 (2008).

55.   Torán, J. L. *et al.* Improvement in affinity and HIV-1 neutralization by somatic mutation in the heavy chain first complementarity-determining

region of antibodies triggered by HIV-1 infection. *Eur. J. Immunol.* **31**, 128–137 (2001).

56. Gray, E. S. *et al.* Broad neutralization of human immunodeficiency virus type 1 mediated by plasma antibodies against the gp41 membrane proximal external region. *J. Virol.* **83**, 11265–11274 (2009).

57. Shen, X. *et al.* In vivo gp41 antibodies targeting the 2F5 monoclonal antibody epitope mediate human immunodeficiency virus type 1 neutralization breadth. *J. Virol.* **83**, 3617–3625 (2009).

58. Tomaras, G. D. *et al.* Initial B-cell responses to transmitted human immunodeficiency virus type 1: virion-binding immunoglobulin M (IgM) and IgG antibodies followed by plasma anti-gp41 antibodies with ineffective control of initial viremia. *J. Virol.* **82**, 12449–12463 (2008).

59. Derdeyn, C. A. *et al.* Envelope-constrained neutralization-sensitive HIV-1 after heterosexual transmission. *Science* **303**, 2019–2022 (2004).

60. Robert-Guroff, M. *et al.* Spectrum of HIV-1 neutralizing antibodies in a cohort of homosexual men: results of a 6 year prospective study. *AIDS Res. Hum. Retroviruses* **4**, 343–350 (1988).

61. Sather, D. N. *et al.* Broadly neutralizing antibodies developed by an HIV-positive elite neutralizer exact a replication fitness cost on the contemporaneous virus. *J. Virol.* **86**, 12676–12685 (2012).

62. Bar, K. J. *et al.* Early low-titer neutralizing antibodies impede HIV-1 replication and select for virus escape. *PLoS Pathog.* **8**, e1002721 (2012).

63. Scheid, J. F. *et al.* A method for identification of HIV gp140 binding memory B cells in human blood. *J. Immunol. Methods* **343**, 65–67 (2009).

64. Klein, F. *et al.* HIV therapy by a combination of broadly neutralizing antibodies in humanized mice. *Nature* **492**, 118–122 (2012).

65. Xiao, X., Chen, W., Feng, Y. & Dimitrov, D. S. Maturation Pathways of Cross-Reactive HIV-1 Neutralizing Antibodies. *Viruses* **1**, 802–817 (2009).

66. Rachinger, A. *et al.* HIV-1 envelope diversity one year after seroconversion predicts subsequent disease progression. *AIDS* (2012).doi:10.1097/QAD.0b013e328354f539

67.   Ganusov, V. V. *et al.* Fitness costs and diversity of the cytotoxic T lymphocyte (CTL) response determine the rate of CTL escape during acute and chronic phases of HIV infection. *J. Virol.* **85**, 10518–10528 (2011).

68.   Nowak, M. A. *et al.* Antigenic diversity thresholds and the development of AIDS. *Science* **254**, 963–969 (1991).

69.   Duvall, M. G. *et al.* Maintenance of HIV-specific CD4+ T cell help distinguishes HIV-2 from HIV-1 infection. *J. Immunol.* **176**, 6973–6981 (2006).

70.   Heeney, J. L. The critical role of CD4(+) T-cell help in immunity to HIV. *Vaccine* **20**, 1961–1963 (2002).

71.   Ostrowski, M. A. *et al.* The role of CD4+ T cell help and CD40 ligand in the in vitro expansion of HIV-1-specific memory cytotoxic CD8+ T cell responses. *J. Immunol.* **165**, 6133–6141 (2000).

72.   Sauce, D. *et al.* HIV disease progression despite suppression of viral replication is associated with exhaustion of lymphopoiesis. *Blood* **117**, 5142–5151 (2011).

73.   Appay, V. & Rowland-Jones, S. L. Premature ageing of the immune system: the cause of AIDS? *Trends Immunol.* **23**, 580–585 (2002).

74.   Krakauer, D. C. & Nowak, M. T-cell induced pathogenesis in HIV: bystander effects and latent infection. *Proc. Biol. Sci.* **266**, 1069–1075 (1999).

75.   Liu, Z. *et al.* CD8+ T-lymphocyte activation in HIV-1 disease reflects an aspect of pathogenesis distinct from viral burden and immunodeficiency. *J. Acquir. Immune Defic. Syndr. Hum. Retrovirol.* **18**, 332–340 (1998).

76.   Rodríguez, B. *et al.* Predictive value of plasma HIV RNA level on rate of CD4 T-cell decline in untreated HIV infection. *JAMA* **296**, 1498–1506 (2006).

77.   Schacker, T. W., Hughes, J. P., Shea, T., Coombs, R. W. & Corey, L. Biological and virologic characteristics of primary HIV infection. *Ann. Intern. Med.* **128**, 613–620 (1998).

78.   Ho, D. D. *et al.* Rapid turnover of plasma virions and CD4 lymphocytes in HIV-1 infection. *Nature* **373**, 123–126 (1995).

79.   Klenerman, P. *et al.* Cytotoxic T lymphocytes and viral turnover in HIV type 1 infection. *Proc. Natl. Acad. Sci. U.S.A.* **93**, 15323–15328 (1996).

80.   Mellors, J. W. *et al.* Prognosis in HIV-1 infection predicted by the quantity of virus in plasma. *Science* **272**, 1167–1170 (1996).

81.   Trkola, A. *et al.* Human immunodeficiency virus type 1 fitness is a determining factor in viral rebound and set point in chronic infection. *J. Virol.* **77**, 13146–13155 (2003).

82.   Streeck, H. *et al.* Human immunodeficiency virus type 1-specific CD8+ T-cell responses during primary infection are major determinants of the viral set point and loss of CD4+ T cells. *J. Virol.* **83**, 7641–7648 (2009).

83.   Domingo, E., Escarmís, C., Sevilla, N. & Baranowski, E. Population dynamics in the evolution of RNA viruses. *Adv. Exp. Med. Biol.* **440**, 721–727 (1998).

84.   Clarke, D. K. *et al.* Genetic bottlenecks and population passages cause profound fitness differences in RNA viruses. *J. Virol.* **67**, 222–228 (1993).

85.   Ewald, P. W. Evolution of mutation rate and virulence among human retroviruses. *Philos. Trans. R. Soc. Lond., B, Biol. Sci.* **346**, 333–41– discussion 341–3 (1994).

86.   Roberts, J. D., Bebenek, K. & Kunkel, T. A. The accuracy of reverse transcriptase from HIV-1. *Science* **242**, 1171–1173 (1988).

87.   Nowak, M. HIV mutation rate. *Nature* **347**, 522 (1990).

88.   Zhang, M. *et al.* The role of recombination in the emergence of a complex and dynamic HIV epidemic. *Retrovirology* **7**, 25 (2010).

89.   Galetto, R. & Negroni, M. Mechanistic features of recombination in HIV. *AIDS Rev* **7**, 92–102 (2005).

90.   Yu, H., Jetzt, A. E., Ron, Y., Preston, B. D. & Dougherty, J. P. The nature of human immunodeficiency virus type 1 strand transfers. *J. Biol. Chem.* **273**, 28384–28391 (1998).

91.   Edwards, C. T. T. *et al.* Population genetic estimation of the loss of genetic diversity during horizontal transmission of HIV-1. *BMC Evol. Biol.* **6**, 28 (2006).

92.   Richman, D. D. *et al.* Nevirapine resistance mutations of human immunodeficiency virus type 1 selected during therapy. *J. Virol.* **68**, 1660–1666 (1994).

93. Wain, L. V. *et al.* Adaptation of HIV-1 to its human host. *Mol. Biol. Evol.* **24**, 1853–1860 (2007).

94. Soares, A. E. R., Soares, M. A. & Schrago, C. G. Positive selection on HIV accessory proteins and the analysis of molecular adaptation after interspecies transmission. *J. Mol. Evol.* **66**, 598–604 (2008).

95. Leslie, A. J. *et al.* HIV evolution: CTL escape mutation and reversion after transmission. *Nat. Med.* **10**, 282–289 (2004).

96. Best, S., Le Tissier, P. R. & Stoye, J. P. Endogenous retroviruses and the evolution of resistance to retroviral infection. *Trends Microbiol.* **5**, 313–318 (1997).

97. Wang, H. & Lambowitz, A. M. The Mauriceville plasmid reverse transcriptase can initiate cDNA synthesis de novo and may be related to reverse transcriptase and DNA polymerase progenitor. *Cell* **75**, 1071–1081 (1993).

98. Gifford, R. J. Viral evolution in deep time: lentiviruses and mammals. *Trends Genet.* **28**, 89–100 (2012).

99. Katzourakis, A., Gifford, R. J., Tristem, M., Gilbert, M. T. P. & Pybus, O. G. Macroevolution of complex retroviruses. *Science* **325**, 1512 (2009).

100. Lederberg, J. Emerging infections: an evolutionary perspective. *Emerging Infect. Dis.* **4**, 366–371 (1998).

101. Gilchrist, M. A., Coombs, D. & Perelson, A. S. A. S. Optimizing within-host viral fitness: infected cell lifespan and virion production rate. *J. Theor. Biol.* **229**, 281–288 (2004).

102. Bolker, B. M., Nanda, A. & Shah, D. Transient virulence of emerging pathogens. *J R Soc Interface* **7**, 811–822 (2010).

103. Lenski, R. E. & May, R. M. The evolution of virulence in parasites and pathogens: reconciliation between two competing hypotheses. *J. Theor. Biol.* **169**, 253–265 (1994).

104. Kubinak, J. L., Ruff, J. S., Hyzer, C. W., Slev, P. R. & Potts, W. K. Experimental viral evolution to specific host MHC genotypes reveals fitness and virulence trade-offs in alternative MHC types. *Proceedings of the National Academy of Sciences* **109**, 3422–3427 (2012).

105.   Alizon, S. & van Baalen, M. Acute or chronic? Within-host models with immune dynamics, infection outcome, and parasite evolution. *Am. Nat.* **172**, E244–56 (2008).

106.   Ashton, L. J. *et al.* HIV infection in recipients of blood products from donors with known duration of infection. *Lancet* **344**, 718–720 (1994).

107.   Woolhouse, M. E. J., Webster, J. P., Domingo, E., Charlesworth, B. & Levin, B. R. Biological and biomedical implications of the co-evolution of pathogens and their hosts. *Nat. Genet.* **32**, 569–577 (2002).

108.   Levin, B. R., Bull, J. J. & Stewart, F. M. The intrinsic rate of increase of HIV/AIDS: epidemiological and evolutionary implications. *Math Biosci* **132**, 69–96 (1996).

109.   Eldakar, O. T. & Wilson, D. S. Eight criticisms not to make about group selection. *Evolution* **65**, 1523–1526 (2011).

110.   Traulsen, A., Shoresh, N. & Nowak, M. A. Analytical results for individual and group selection of any intensity. *Bull. Math. Biol.* **70**, 1410–1424 (2008).

111.   Wilson, D. S. A theory of group selection. *Proc. Natl. Acad. Sci. U.S.A.* **72**, 143–146 (1975).

112.   Frank, S. A. Natural selection. III. Selection versus transmission and the levels of selection. *J. Evol. Biol.* **25**, 227–243 (2012).

113.   Nowak, M. A., May, R. M. & Anderson, R. M. The evolutionary dynamics of HIV-1 quasispecies and the development of immunodeficiency disease. *AIDS* **4**, 1095–1103 (1990).

114.   Goodenow, M. *et al.* HIV-1 isolates are rapidly evolving quasispecies: evidence for viral mixtures and preferred nucleotide substitutions. *J. Acquir. Immune Defic. Syndr.* **2**, 344–352 (1989).

115.   Steinhauer, D. A. & Holland, J. J. Rapid evolution of RNA viruses. *Annu. Rev. Microbiol.* **41**, 409–433 (1987).

116.   Domingo, E. *et al.* The quasispecies (extremely heterogeneous) nature of viral RNA genome populations: biological relevance--a review. *Gene* **40**, 1–8 (1985).

117.   Epstein, I. R. & Eigen, M. Selection and self-organization of self-reproducing

macromolecules under the constraint of constant flux. *Biophysical chemistry* **10**, 153–160 (1979).

118.   Holmes, E. C. Does hepatitis C virus really form quasispecies? *Infect. Genet. Evol.* **10**, 431–432 (2010).

119.   Jenkins, G. M., Worobey, M., Woelk, C. H. & Holmes, E. C. Evidence for the non-quasispecies evolution of RNA viruses [corrected]. *Mol. Biol. Evol.* **18**, 987–994 (2001).

120.   Vignuzzi, M., Stone, J. K., Arnold, J. J., Cameron, C. E. & Andino, R. Quasispecies diversity determines pathogenesis through cooperative interactions in a viral population. *Nature* **439**, 344–348 (2006).

121.   Krakauer, D. C. & Komarova, N. L. Levels of selection in positive-strand virus dynamics. *J. Evol. Biol.* **16**, 64–73 (2003).

122.   Gould, S. J. & Lewontin, R. C. The spandrels of San Marco and the Panglossian paradigm: a critique of the adaptationist programme. *Proc. R. Soc. Lond., B, Biol. Sci.* **205**, 581–598 (1979).

123.   Ellison, P. T. & Jasienska, G. Constraint, pathology, and adaptation: how can we tell them apart? *Am. J. Hum. Biol.* **19**, 622–630 (2007).

124.   Wagner, G. P. *et al.* Pleiotropic scaling of gene effects and the 'cost of complexity'. *Nature* **452**, 470–472 (2008).

125.   Remold, S. K., Rambaut, A. & Turner, P. E. Evolutionary genomics of host adaptation in vesicular stomatitis virus. *Mol. Biol. Evol.* **25**, 1138–1147 (2008).

126.   Harris, E. E. Nonadaptive processes in primate and human evolution. *Am. J. Phys. Anthropol.* **143 Suppl 51**, 13–45 (2010).

127.   Presloid, J. B., Ebendick-Corpus, B. E., Zárate, S. & Novella, I. S. Antagonistic pleiotropy involving promoter sequences in a virus. *J. Mol. Biol.* **382**, 342–352 (2008).

128.   Griswold, C. K. & Whitlock, M. C. The genetics of adaptation: the roles of pleiotropy, stabilizing selection and drift in shaping the distribution of bidirectional fixed mutational effects. *Genetics* **165**, 2181–2192 (2003).

129.   Kirchhoff, F. Is the high virulence of HIV-1 an unfortunate coincidence of

primate lentiviral evolution? *Nat. Rev. Microbiol.* **7**, 467–476 (2009).

130. Wlasiuk, G. & Nachman, M. W. Adaptation and constraint at Toll-like receptors in primates. *Mol. Biol. Evol.* **27**, 2172–2186 (2010).

131. Markowitz, M. *et al.* A novel antiviral intervention results in more accurate assessment of human immunodeficiency virus type 1 replication dynamics and T-cell decay in vivo. *J. Virol.* **77**, 5037–5038 (2003).

132. Dixit, N. M., Markowitz, M., Ho, D. D. & Perelson, A. S. Estimates of intracellular delay and average drug efficacy from viral load data of HIV-infected individuals under antiretroviral therapy. *Antivir. Ther. (Lond.)* **9**, 237–246 (2004).

133. Forshey, B. M., Schwedler, von, U., Sundquist, W. I. & Aiken, C. Formation of a human immunodeficiency virus type 1 core of optimal stability is crucial for viral replication. *J. Virol.* **76**, 5667–5677 (2002).

134. Kim, J., Tipper, C. & Sodroski, J. Role of TRIM5α RING domain E3 ubiquitin ligase activity in capsid disassembly, reverse transcription blockade, and restriction of simian immunodeficiency virus. *J. Virol.* **85**, 8116–8132 (2011).

135. Hulme, A. E., Perez, O. & Hope, T. J. Complementary assays reveal a relationship between HIV-1 uncoating and reverse transcription. *Proceedings of the National Academy of Sciences* **108**, 9975–9980 (2011).

136. Kim, S. Y., Byrn, R., Groopman, J. & Baltimore, D. Temporal aspects of DNA and RNA synthesis during human immunodeficiency virus infection: evidence for differential gene expression. *J. Virol.* **63**, 3708–3713 (1989).

137. Ranki, A., Lagerstedt, A., Ovod, V., Aavik, E. & Krohn, K. J. Expression kinetics and subcellular localization of HIV-1 regulatory proteins Nef, Tat and Rev in acutely and chronically infected lymphoid cell lines. *Arch. Virol.* **139**, 365–378 (1994).

138. Malim, M. H., Hauber, J., Le, S. Y., Maizel, J. V. & Cullen, B. R. The HIV-1 rev trans-activator acts through a structured target sequence to activate nuclear export of unspliced viral mRNA. *Nature* **338**, 254–257 (1989).

139. Paillart, J. C. & Göttlinger, H. G. Opposing effects of human immunodeficiency virus type 1 matrix mutations support a myristyl switch model of gag membrane targeting. *J. Virol.* **73**, 2604–2612 (1999).

140. Reil, H., Bukovsky, A. A., Gelderblom, H. R. & Göttlinger, H. G. Efficient HIV-1 replication can occur in the absence of the viral matrix protein. *EMBO J.* **17**, 2699–2708 (1998).

141. Griffiths, A. D. & Tawfik, D. S. Directed evolution of an extremely fast phosphotriesterase by in vitro compartmentalization. *EMBO J.* **22**, 24–35 (2003).

142. Wan, L., Twitchett, M. B., Eltis, L. D., Mauk, A. G. & Smith, M. In vitro evolution of horse heart myoglobin to increase peroxidase activity. *Proc. Natl. Acad. Sci. U.S.A.* **95**, 12825–12831 (1998).

143. Bonsor, D. A. & Sundberg, E. J. Dissecting protein-protein interactions using directed evolution. *Biochemistry* **50**, 2394–2402 (2011).
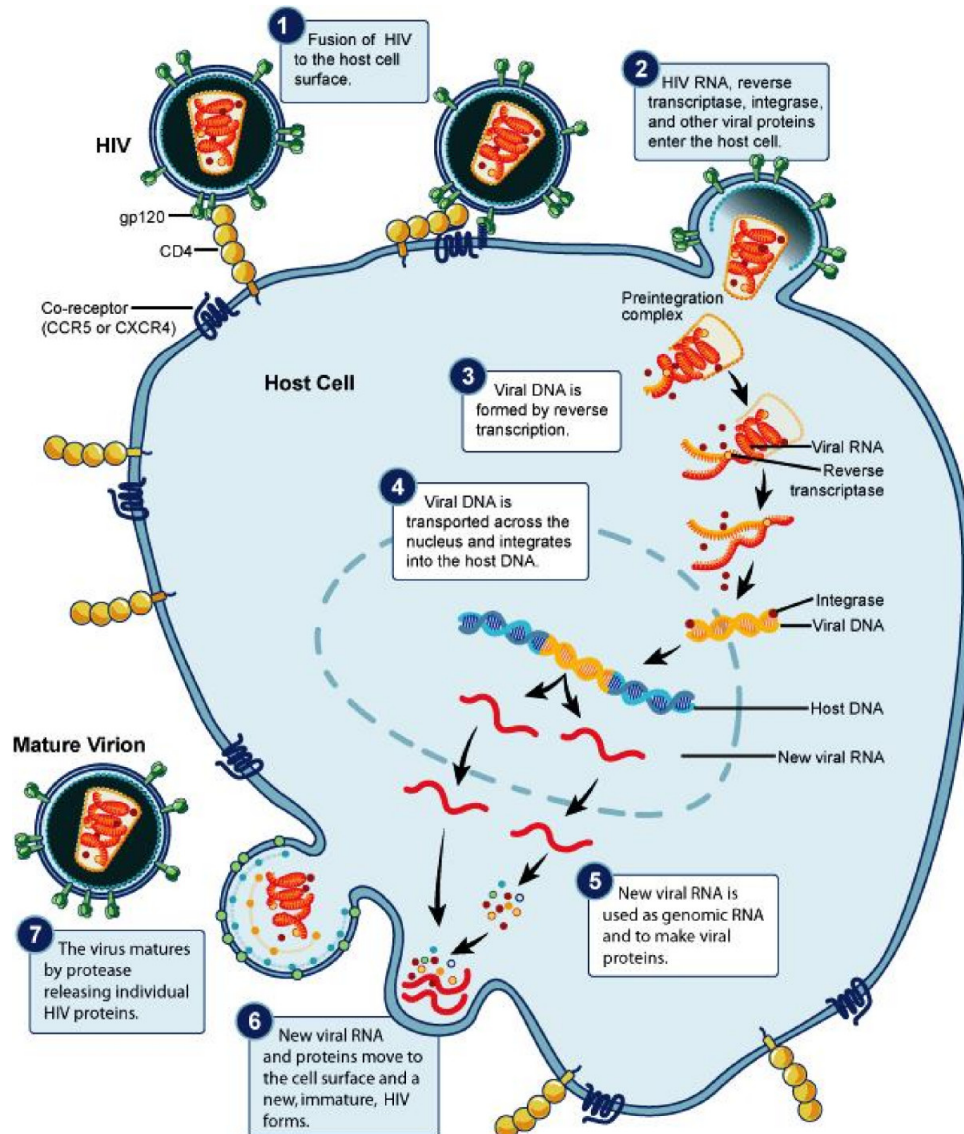
Chapter 2. The viral life-cycle.

Fig. 2.1. The life cycle of HIV-1. The major steps of intracellular replication are indicated and described in the text boxes. Source: Wayengera, M. On the general theory of the origins of retroviruses. *Theor Biol Med Model* **7**, 5 (2010). Used under a Creative Commons Attribution license: http://creativecommons.org/licenses/by/2.0.

Retroviruses are RNA viruses with a single-stranded positive-sense genome. After entering a cell, the RNA genome is reverse-transcribed into DNA and integrated into the host cell chromatin. The viral promoter drives expression of viral mRNAs, some of which are translated to produce proteins and some of which are are used as new copies of the RNA genome. The primary viral structural protein, Gag, binds the RNA genome and packages it into assembling virions. Gag is targeted to sites on the plasma membrane where it multimerizes and with the help of numerous host proteins drives the membrane curvature and budding that releases new infectious virions into the extracellular medium.

The integration point provides the basis for a functional division of the retroviral life-cycle into two distinct phases. The first half extends from the point of entry into a target cell up until the point of integration. The second half begins with gene expression from the integrated viral genome and ends with the production of infectious virions competent for reinfection of target cells and the reinitiation of the cycle. These segments have been logically distinct for researchers, partly because they require and are amenable to very different types of assays and screens. Newly discovered functions of the virus are frequently first described by the generation of mutations in specific regions of the viral genome, and the assessment of whether these lead to "incoming" deficits, or "outgoing" ones. The first half, or incoming, phase has been effectively studied by the use of reporter viruses that carry an easily detectable gene (often GFP; in earlier work, often an enzyme such as CAT). Viral

gene expression requires integration (in general; special cases may exist in which there is limited expression from unintegrated DNA[1-6]) and successful navigation of all the prior steps. Viruses carrying a reporter gene therefore provide a straightforward tool for assessing the health of the first half of the life-cycle after any given perturbation of the virus or the cells themselves.

It is not as straightforward to study the second half of the life-cycle, especially in isolation from the first half. Infection of target cells with wild-type (WT) virus leads to the production of infectious virions, but failure to do so with a particular mutant does not indicate which half of the life-cycle is affected. Transfection of viral genomes, either on one plasmid or separated into several, has been one approach to the study of the outgoing phase. This approach ensures the production of viral RNA and proteins; their successful assembly can then be monitored by following virion production. Western blotting or ELISA, or even enzymatic reporter systems[7-11], can be used to follow the appearance of new virions in the supernatant. Reporter viruses can also be used to study the outgoing phase by transfection of all the components necessary for infectious virus production. Assembly and release are then monitored by titrating the viral supernatant on target cells.

The primary techniques used to produce the data presented in the following chapters represent alterations of these basic approaches to allow analysis of later stages in the life-cycle. To study assembly, we will use infections with full-length

replication-competent viruses that also carry a reporter gene that allows for determination of infection efficiency (the first half of the lifecycle). The use of infections rather than transfections is preferable, as the kinetics of virion production by transfected viral plasmids does not mirror those found upon infection. We will use non-replication-competent versions of reporter viruses to study gene expression. Rather than using the reporter genes as simple readouts of successful infection, we will follow their expression over time in order to observe the actual timing of protein production directed by the integrated provirus. This thesis will focus on events in the second half of the HIV-1 life-cycle. A brief overview of the incoming phase is below. The major events of the outgoing phase will be reviewed in Chapters 3 and 5.

Entry

Entry of HIV-1 virions into cells is initiated by the interaction of the viral Env protein and the cell surface molecule CD4[4,5]. Env is a highly variable and glycosylated molecule that is the only virus-encoded component exposed on the surface of the virion. It is composed of a noncovalent heterodimer of the viral gp120 and gp41 proteins, anchored in the virion membrane by gp41, and arranged in trimeric spikes[12,13]. The heavy glycosylation[14,15]and the variability in its exposed loop regions[16-19] causes the development of broadly neutralizing antibodies to HIV-1

virions to be extremely difficult[18,20,21]. Initial binding of cells to virus may occur non-specifically, leading to an experimental delay between addition of virus to cells and entry. After this initial lag time, gp120 engages CD4 and coreceptors[22]. Adsorption of virus to cells at lower temperatures, followed by switching to 37°C, can remove this lag time and result in more synchronous infection events[23-25]. The CD4-gp120 interaction takes place and causes a conformational change that promotes gp120 engagement with a coreceptor (either CCR5 or CXCR4)[26-31]. Coreceptor binding results in a dramatic structural rearrangement of gp41, first to a "pre-hairpin" conformation, which has a relatively long half-life, and then to a six-helix bundle[32,33]. The free energy released from this final transformation drives rapid membrane fusion, but is thought to require the cooperativity of multiple subunits[34]. The efficiency of entry is thus dependent on at least two separate rate-limiting steps. It is also strongly counteracted at the same time by an ongoing process of viral deactivation, via endocytosis[35]. The balance between these various kinetic processes determines the ultimate efficiency of entry into the cell; and these in turn are under potentially conflicting selection pressures because the first rate-limiting step is strongly affected by the co-receptor binding affinity of the highly variable V3 loop of gp120[35]. This domain is also under selective pressure from the humoral immune system, which may explain the existence of suboptimal kinetics. V3 sequences that lead to antibody escape may not be ideal for co-receptor binding. Antagonistic pleiotropy such as this may be a common source of such phenotypes.

Trafficking

After new virions bud from cells their contents are rearranged in a maturation process, driven by the viral protease, that creates a condensed ribonucleoprotein complex surrounded by a conical shell composed of the CA protein[36,37]. HIV-1 fusion occurs at the plasma membrane, depositing this core structure into the cytoplasm. The viral core then loses its CA coat[38,39] and forms the reverse transcription complex (RTC) — in which the RNA genome will be copied into double-stranded DNA. This structure must travel through the cytoplasm to reach and enter the nucleus. At some point during this time it will become an integration-competent DNA-containing complex referred to as the pre-integration complex (PIC)[40]. These three processes, uncoating, reverse-transcription, and cytoplasmic trafficking, may not be entirely separable. In most cases perturbing one has repercussions on the others, and they almost certainly overlap in their timing[41-45].

HIV-1 engages in multiple interactions with the host cell cytoskeleton, during both the post-entry and assembly phases of its life-cycle[46-50]. These interactions appear to begin even before entry, with a series of receptor-mediated interactions with the cortical actin network beneath the plasma membrane[51]. CD4-gp120 binding leads to intracellular signaling that deactivates the actin-disassembling molecule cofilin, and leads to actin-mediated clustering of the CXCR4 or CCR5 coreceptors, strongly enhancing entry[51-53]. Then, remarkably, it appears that CD4-CXCR4 binding sends a

second intracellular signal to the cytoskeleton, resulting in the *activation* of cofilin and the depolymerization of the surrounding cortical actin[53,54]. The cortical actin that the viral core will be released into may at this stage represent a restrictive feature of the cell that requires remodeling in order to allow physical passage through it, and the activation of cofilin is thought to aid in this. The viral accessory protein Nef interacts with actin-related proteins and has also been implicated in this process[55]. Nef enhances infectivity in some cell types, in a manner that results in enhanced reverse-transcription[56]. This phenotype is absent if actin is disrupted, or if virus is pseudotyped and delivered to cells via the endocytic system[57], which is thought to allow bypassing of the cortical actin network.

However, actin may also be required for some viral processes post-entry. The RTC traffics to the nucleus using dynein-driven retrograde transport along microtubules, but appears to utilize actin for active transport as well[48,58,59]. Only disruption of both types of filament lead to complete inhibition of RTC transport, and one study[58] found a clear shift from characteristic microtuble-associated motion to motion typical of actin transport as the RTC neared the nucleus. It is likely that prior to microtubule association actin is also used for initial transport steps[60]. Entry that bypasses actin can also result in reduced reverse transcription[61], and and interruption of actin polymerization can do so as well[49]. Blocking actin polymerization near the time of entry causes RTCs to accumulate near the PM, whereas blocking it later causes them to accumulate near the nucleus[58].

Clearly HIV-1 has a complex set of interactions with the cytoskeleton. Almost every viral component of the RTC has been suggested to interact with the cytoskeletal system: Nef[62]; the reverse transcriptase (RT) enzyme itself[63]; the Integrase (IN) protein that will later mediate integration[5]; the Nucleocapsid (NC) protein, an RNA chaperone that is responsible for RNA packaging during assembly and coats the genome after virion maturation[64]; and the viral Matrix (MA) protein, which has been shown to mediate a critical association between the RTC and actin[49]. Certainly it is likely that some of these viral proteins are not themselves directly associated with the cytoskeleton, and are simply associated with the viral complex. However, a growing number of cellular cytoskeleton-related proteins have been discovered to alter HIV-1 infectivity in the pre-integration half of the lifecycle[47,52,65-68]. Some of these have complex and even contradictory activities; in fact some that were initially thought to restrict HIV-1 infectivity by blocking microtubule trafficking[67] have been found instead (or also) to *enhance* infectivity, via actin regulation[52]. It appears that after entry the HIV-1 core complex clears its way through the cortical actin; then uses actin itself for transport to microtubules; is mobilized on these toward the center of the cell; and then switches again to local actin transport to enter the nucleus. Microtubule associated motion can be quite fast, on the order of 1μm/s, whereas motion on actin filaments is about tenfold slower[69]. In any case it appears that the actual travel time to the nucleus can be quite brief, and is not the rate-limiting step. The reverse transcription process is much slower[70,71].

Reverse transcription

The viral reverse transcriptase (RT) enzyme is a product of the pol gene, and packaged into virions as a component of the GagPol polyprotein. After assembly the viral protease (PR) cleaves Gag and GagPol molecules into their constituent parts, allowing condensation and maturation of the core[36]. The mature RT enzyme is is now capable of beginning reverse transcription, and in fact some RT products can be detected within virions[72-74]. However, the process does not proceed significantly until exposure of the core to the intracellular evironment, because of the requirement for both higher concentrations of dNTPs, and the presence of necessary cellular cofactors[75-78]. The complete double-stranded DNA genome that will form the provirus is constructed in a tightly regulated multi-step process[79]. A tRNA packaged during assembly in the producer cell is used to prime reverse transcription of the RNA into DNA. The viral RT both degrades the template RNA and, finally, acts as a DNA-dependent DNA polymerase to create the double stranded DNA product. There are two obligatory strand transfers in the process — points at which the primer and nascent DNA move to a different region of the RNA template , or to the other copy of the RNA template[80,81]. In addition the RT enzyme is not highly processive[82] and can dissociate from one RNA template and switch to the other at many different possible sites[80,83]. In the event that co-infection of the producer cell leads to the packaging of non-identical genomes, this template switching can result

in genetic recombination, giving rise to a chimeric provirus. In addition the RT, unlike most cellular polymerases, lacks a proof-reading domain and is extremely error prone[84-87]. Thus reverse transcriptase is responsible for the both the high mutation rate and recombination rates of HIV-1, leading to its pronounced ability to evolve rapidly in response to selection pressures either within individual hosts[88,89] or within populations[90].

Uncoating and TRIM5α

The initially intact CA shell is shed from the viral core at some point between entry into the cell and entry into the nucleus. This uncoating process is thought to be subject to careful temporal regulation, and interference with that regulation invariably disrupts reverse transcription and infectivity[41,42,45,91]. However, the actual timing of uncoating remains controversial. Early biochemical descriptions of RTCs and PICs found little evidence of associated CA, and it was plausible that immediate uncoating was required for initiation of reverse-transcription[38,92,93]. Nor was CA found in EM studies[94]. There are many possible explanations for such negative results though, and biochemical fractionation approaches to isolation of these complexes may well be too harsh to preserve low-strength CA interactions with viral complexes. Later microscopy studies have shown putative RTCs or PICs in cells at later time points, some having traveled as far as the nucleus, still containing

large amounts of CA[42,48,58,95,96]. These approaches are also not definitive; however, much more is known about the functional relationship of uncoating to the reverse transcription process that takes place during this time. In vitro approaches to the study of virion cores led to the discovery that CA mutants conferring either enhanced or diminished core stability interfere with reverse transcription, and that core disassembly takes place in a biphasic manner[44,45]. Although not indicative of *when* uncoating takes place, these studies support the idea that it is regulated in a controlled and stepwise fashion. Further support for this view came in the form of an extraordinary tool for the study of this part of the lifecycle, the cellular restriction factor TRIM5 α [91].

TRIM5 α is an antiretroviral molecule that blocks infection by a wide range of retroviruses in a species-specific fashion[97-99]. Human TRIM5 α does not restrict HIV-1, but it strongly blocks several other viruses including N-MLV and EIAV. HIV-1 is restricted by TRIM5 α from many Old World Monkeys, and by a version, TRIMCyp, found in Owl monkeys and in some macaque species[100-103]. TRIMCyp is a TRIM5-cyclophilin a (CypA) fusion protein resulting from a retrotransposition event [102,103]; it carries the cellular CypA protein, which binds to many retroviral CA proteins, in place of its own CA-binding domain. It has proven extremely useful for the study of TRIM5-mediated restriction, because a known small-molecule inhibitor

of CypA-CA interaction, cyclosporine, can be used to modulate TRIMCyp-CA binding at will[71,104,105].

Rhesus macaque TRIM5α (TRIM5α$_{Rh}$) interacts with HIV-1 CA after entry and blocks infectivity by roughly 100-fold[91,99]. The species specificity of the interaction depends on a region within the TRIM5α SPRY domain that can be altered to target other species with very minor changes[106,107] and shows strong signs of positive selection[108,109]. The mechanism of restriction appears to involve an acceleration of the process of CA disassembly. When restrictive cells are infected by HIV-1, reverse transcription is blocked and fractionation of the cells reveals that the normal level of dense core-associated CA is absent and only soluble CA is detectable[110,111]. The restriction is saturable and can be partially overcome by high levels of virus or by pretreatment with intact virus-like particles (VLPs) made by transfection of cells with Gag-Pol and Env vectors alone[43,111-113]. These form CA shells with normal hexameric surface structure. If they are made with Gag mutants that display impaired stability, saturation does not take place, indicating that TRIM5α targets the intact CA lattice[43]. TRIM5α is thought to also form hexameric multimers, and to tightly coat the outside of the CA core[114-116]. TRIM5α has an integral E3 ligase domain, and microscopy data indicate that it recruits the proteasome directly to the viral core[117]. If the proteasome is blocked by proteasome inhibitors, or by mutations of the TRIM5α RING (E3 ligase) domain, disassembly does not take place but full

reverse transcription is able to proceed[71,118-121]. However, this does not lead to successful infection. The normal mode of restriction may involve forced uncoating or degradation, but it appears that there are multiple restrictive processes involved. Alternatively it is possible that uncoating, degradation, and even reverse-transcription inhibition are simply downstream sequelae of the critical events that actually mediate restriction.

Even though restriction is separable from uncoating, reverse-transcription is not[42]. Under all conditions in which TRIM5 α blocks reverse-transcription it also leads to accelerated uncoating. Conversely, all viral mutants or cellular conditions that avoid uncoating in the presence of restrictive TRIM5 α also allow reverse-transcription[43,120-122]. This has led to the theory that the CA coat remains in place around the RTC throughout reverse-transcription, and that the reverse-transcription process is dependent upon this protection. This idea is appealing, as the RT enzyme is not highly processive and tends to dissociate from its template[82,123]. It is possible that if the small amount of RT in the virion were not confined and kept at high local concentration, it would be difficult to complete the process. At the same time, the dimensions of the CA lattice are such that dNTPs would be allowed access to the interior of the core[124]. Evidence that inhibition of reverse-transcription delays uncoating[95] also supports this theory, and suggests that initiation of proper uncoating might be dependent on a signal that reverse-transcription is complete.

The notion that core disassembly is a temporally regulated process and that accelerated uncoating is restrictive has led to the use of TRIM5 α -insensitivity as a proxy for normal uncoating. In these experiments, TRIMCyp-expressing cells are infected, allowing the use of cyclosporine A (CsA) to block TRIMCyp-CA interaction[124]. Because CsA blocks this restrictive interaction, in its presence infection proceeds normally. Washing out the CsA at various times postinfection allows TRIMCyp to target CA and block any further reverse-transcription. At a certain point, however, the RTC becomes resistant to inhibition. If TRIMCyp in fact causes destructive accelerated uncoating, then this point of resistance should correlate with the timing of the normal uncoating process, because presumably at that point there is no longer a CA lattice for TRIMCyp to target; and even if it could, uncoating should not be harmful to the virus at this point.

Experiments of this nature have defined the kinetics of TRIMCyp restriction very clearly: it begins within 15 minutes of entry and half the infectious units in a sample are restricted within roughly an hour[71]. The problem with these data is that it fits very poorly with the kinetics of reverse-transcription. It is extremely hard to reconcile a model in which the CA coat serves to protect the reverse transcription process, with the evidence that the uncoating process is 50% complete at 1h post-infection but reverse-transcription is not 50% complete until at least 6h post-infection[70,71]. One explanation is that the structure of the CA coat is in fact necessary

to protect the RT process — but only during the first stage of it, up until the point at which the early RT products are complete. The generation of early RT products actually does take place with very similar kinetics to CsA-washout defined uncoating kinetics[42]. It is possible that generation of late RT products is distinct and self-sufficient. After that point there may no longer be any requirement for the CA coat to remain intact. On the other hand, the CsA washout assays may not reflect the kinetics of uncoating at all. They may simply reflect the kinetics of restriction. The observation that an intact core is required for restriction does not necessarily imply that failure to restrict at later time points is due to uncoating. It is possible that uncoating does not take place until just prior to nuclear entry, and that TRIM5α can only act within a window of time that is closed by an unknown event an hour or two post-infection.

Nuclear import

As early as 1959, it was recognized that retroviruses depended on cell proliferation for infection[125]. It was not until the early 1990s that it became clear that HIV-1, in contrast, was able to infect both terminally differentiated macrophages and growth-arrested Hela cells[126]. Infection by Moloney murine leukemia virus (MLV) was found to specifically require the passage of cells through mitosis[127,128], when the nuclear

envelope is broken down. It is now known that gammaretroviruses as a whole are restricted to dividing cells, while lentiviruses can infect non-dividing cells[126]. Research aimed at understanding this difference has thus focused on the identification of the determinants that allow HIV-1 to be actively transported through the nuclear pore of intact interphase nuclei.

HIV-1 enters the nucleus through energy-requiring active transport[129]. Active nuclear import in cells is mediated by import receptors (known as importins or karyopherins) that bind to nuclear localization signals (NLS) on import substrates, and to proteins of the nuclear pore (nucleoporins)[130-135]. Correspondingly, requirements during HIVHIV-1clear entry have been described for the nucleoporins NUP98[136], RanBP2[137,138], and NUP153[137,139,140], karyopherinα[141,142], importin 7[143], and transportin SR-2(TNPO3)[137,140,144]. But for HIV-1 to be actively imported into nuclei, the PIC would be expected to contain components with one or more NLS, and this NLS should be able to be shown to be necessary and sufficient for nuclear transport of the PIC. Indeed many different PIC components do carry NLS, or interact with host proteins that do[145,146]. However, after many years of work, none of these determinants has ever turned out to be responsible for nuclear entry. Every putative nuclear entry determinant has been shown to be dispensable for the infection of non-dividing cells, or to have equal effects in both dividing and non-dividing cells. It is very possible that the various NLS are highly redundant or interrelated, or play different roles in different settings. The field has had a suprising

density of published work in contradiction with other published work, and to this

day it remains unclear how HIV-1 enters the nucleus.

The viral proteins matrix (MA), Vpr, integrase (IN), and a DNA structure known as

the central DNA flap have all been implicated in the nuclear import of HIV-1 PICs.

MA was claimed to mediate nuclear import via its N-terminal basic patch[142,147,148], or

by a putative NLS[145]. Further experiments found no differential effects on dividing

and non-dividing cells cells, no compelling NLS activity, and generally pleiotropic

effects of the basic region[149-152]. The Vpr protein is a nuclear shuttling protein with

non-canonical NLSs[153] that appears to interact directly with karyopherins, and was

thought to increase the activity of the NLS on MA[154-157]. In addition, Vpr enhances

infection of the canonical HIV-1 non-dividing target cell, macrophages[158,159].

However, there is no absolute requirement for Vpr in the infection of non-dividing

cells[126,152,160,161]

Various putative NLS have been found in the HIV-1 integrase (IN) protein. Because

of its role in the nucleus IN is required to remain with the PIC into the nucleus, and

is a good candidate for mediating nuclear import. Indeed, HIV-1 IN localizes to the

nuclei of cells, can localize other proteins there when fused to them, and may play a

role in nuclear localization of the PIC[141,162]. Also, a host factor, LEDGF, binds to IN

and has been shown to contain an NLS that was thought at first to play a role in PIC

nuclear transport[163,164]. However, mutations in IN, as in MA, are often pleotropic,

and some of the residues thought to play a role in nuclear import have been shown to play roles in the integration process itself[165]. In any case, as with every other putative entry determinant, IN has no effect on the relative efficiency of infection in dividing or non-dividing cells[160,161].

A structural DNA feature of the PIC has also been proposed to facilitate nuclear entry. During reverse transcription, the plus strand of the proviral DNA is synthesized in two discontinuous sections. When synthesis of the upstream half reaches the central polypurine tract (cPPT), it displaces a segment of the downstream half, resulting in a short triple-stranded region known as the central DNA flap[166]. This region has been proposed to play some structural or host-factor recruitment role that allows the PIC to translocate through the nuclear pore[167,168]. Mutants without this structure were shown to have a defect in nuclear accumulation of LTR-circles, viral genomes, and replication[166,169,170]. These results have been contradicted by other studies[171,172]. However, it has been shown in some strains and cell types[160,172], and especially in HIV-1-based vectors[169], to enhance transduction efficiency, and vector constructs with the sequence encoding the central DNA flap are now in wide use.

In recent years, attention has begun to focus on a viral component of the PIC, the CA protein, that in fact has no NLS at all. The CA protein forms a shell around the PIC that is lost in a regulated fashion during or after reverse-transcription, and has been

linked to nuclear entry through several lines of research. A chimera that replaced

HIV-1 MA and CA with MLV MA, p12, and CA was, for the first time, successfully able

to transfer the phenotype of a block to infection of non-dividing cells between these

viruses[170]. This chimeric virus was able to very efficiently infect non-dividing cells,

but cells that had been growth-arrested by a number of methods were unable to be

infected. Chimeras including only MLV MA or p12 did not show this effect, arguing

that the CA domain was responsible for the phenotype. The same group later

isolated point mutations in CA that specifically impaired the ability to infect non-

dividing cells[173]. Soon after, CA mutants were isolated that were impaired for a stage

of the life-cycle after reverse-transcription, and seemed to link the process of

uncoating with that of nuclear entry[174]. These were able to reverse-transcribe

normally, yet they were mostly unable to integrate or to form LTR circles. Consistent

with the notion that they had some kind of uncoating deficit as well, isolation of PICs

from cells infected with this virus showed that they had about 7-fold higher CA

content than wild type PICs. It was then shown that mutants that alter the the

interaction between cellular Cyclophilin A (CypA) and CA also alter the ability of

HIV-1 to infect non-dividing cells[175]. Most importantly, a somewhat artificial

restriction factor identified in a screen, CPSF6-358, was shown to block infection

much more severely in non-dividing cells than dividing cells, although it appeared to

act at the same stage as TRIM5α[176]. A mutation in CA that relieved this block

appeared to alter the nuclear entry pathway by largely removing dependence on

TNPO3 and several nucleoporins, while generating dependence on a different set of

nucleoporins[176].

Taken together, these results seem to point toward a picture in which CA plays a major role in how the HIV-1 core gains access to the nucleus. This may simply signal the importance of the uncoating process to the nuclear entry process. This would not be surprising, as the coated core is thought to be on the order of 56nm in diameter[177], which should be too large to pass through the nuclear pore channel[178]. The PIC of MLV, which cannot infect non-dividing cells, does not shed its CA coat so extensively[179]. Indeed, there are reports that HIV-1 uncoating does not actually take place until the PIC is close to, or even docked at, the nuclear pore itself[58,95]. These studies also indicate that the final stages of reverse-transcription trigger events that lead to uncoating and simultaneously allow nuclear import. Interpretation of results in this field may therefore have been enormously complicated by the extensive linkage between the process of reverse-transcription, uncoating, and nuclear entry.

They may have also been complicated by the equation of the nuclear entry capability of HIV-1 with its ability to infect non-dividing cells. There is evidence that HIV-1 does not take advantage of the dissolution of the nuclear membrane at mitosis to gain access to cellular chromatin[39,180]. Many mutations that affect nuclear entry do so in both dividing and non-dividing cell types. It is possible that HIV-1 uses the nuclear pore for entry even in dividing cells, or at least remains dependent upon pore components to complete the next stages of the lifecycle.

Integration

After entering the nucleus, the viral nucleoprotein complex moves to the cellular chromatin where the IN protein catalyzes the integration of the viral DNA into the host genome. This process may not be entirely separable from nuclear entry itself, as several nuclear pore proteins have been shown to modulate the integration process and have an impact on integration site selection[176,181,182]. Integration is also not assured once nuclear entry has been navigated. Non-productive end products for the viral DNA are found at high levels in infected cell cultures, and in fact have been generally used as the most convenient marker for successful nuclear entry[183]. These include 2-LTR circles, in which the proviral DNA is joined end to end; 1-LTR circles, formed by recombination between the LTRs; and various less common autointegration products. Inhibiting the integration process increases the levels of these non-productive replication products[182,183]. There are some reports, however, that these are not altogether silent. Low levels of transcription may be generated from some of these non-integrated products, and it has been claimed that in the presence of an integrated provirus expressing large amounts of Tat entire RNA genomes can be produced from unintegrated DNA[2,3,184-186]. If true, this would lead to a potentially expanded source of sequence diversity, as divergent genomes in co-infected cells can be co-packaged and generate recombinant viruses through template-swapping during reverse-transcription in target cells.

When productive integration is achieved, it can be essentially anywhere in the genome, but it is much more commonly found in regions with specific characteristics. HIV-1 most often integrates within active transcriptional units, whereas other retroviruses have integration site preferences distinct from this*. This integration site is determined by IN itself, and is transferable in chimeras in which the HIV-1 IN is replaced with the MLV IN. It is not, however, IN itself that directly targets the PIC to host chromatin. A host protein, LEDGF, binds tightly to both IN and DNA, and has been shown to be responsible for integration site choice[187,188]. LEDGF binds to chromatin at the same sites in which HIV-1 integration is typically found. Fusing LEDGF with DNA binding domains with alternate specificity retargets both LEDGF and HIV-1 integration[189]. The interaction between LEDGF and IN is also highly important for infection; blocking this interaction leads to both large reductions in infection and increases in the levels of 2-LTR circles[1].

Knowledge of this targeting mechanism has spurred attempts to modify either LEDGF or IN itself in ways that will generate more specific targeting to defined loci in the genome[7,9-11]. This is a critical research goal, as lentiviral vectors are a promising tool for gene therapy, and solving the problem of targeting to safe sites in the genome is the primary bottleneck this technology now faces. Polydactyl zinc-finger proteins can now be programmed with specificity for almost any DNA sequence, and fusions of either LEDGF or IN with these constructs, or ones like

them, holds the potential for both safe gene therapy applications, and widely applicable gene-targeting applications for research[10].

Once the viral DNA is tethered to the host genome via LEDGF, integration proceeds in the immediately adjacent DNA[190]. The mechanistic details of the integration reaction itself are well understood. IN forms a tetramer with a central channel that is formed around the free ends of the viral DNA[188,191-193]. The nuclease capability of IN removes the 3' dinucleotides from the viral DNA and the resulting 3' ends attack two phosphodiester bonds in the genomic target DNA[194,195]. The target DNA is held in position across one face of the central channel of IN, inducing a bend in the DNA at the point of attack. The bonds targeted by the ends of the viral DNA are separated by 5 nucleotides that then become single-stranded sections on either end of the inserted viral DNA. Cellular proteins repair this section, leaving a duplication on either side of the viral genome, trim the 5' overhanging dinucleotide on the viral RNA, and ligate the resulting 5' end to the target DNA[196,197]. The proviral genome is now part of the host genome and will be duplicated during cell division just as would any endogenous gene.

After integration, viral genes are transcribed and translated, and the structural genes drive the assembly of virions. Release of virions into the supernatant

completes the intracellular lifecycle, and, after an extracellular maturation step,

these virions are ready to re-infect new cells. Gene expression will be covered in

Chapter. 3. Assembly will be covered in Chapter 5.

References, Chapter 2

1.   De Rijck, J. *et al.* Overexpression of the lens epithelium-derived growth factor/p75 integrase binding domain inhibits human immunodeficiency virus replication. *J. Virol.* **80**, 11498–11509 (2006).

2.   Sloan, R. D. & Wainberg, M. A. The role of unintegrated DNA in HIV infection. *Retrovirology* **8**, 52 (2011).

3.   Kelly, J. *et al.* Human macrophages support persistent transcription from unintegrated HIV-1 DNA. *Virology* **372**, 300–312 (2008).

4.   Poon, B., Chang, M. A. & Chen, I. S. Y. Vpr is required for efficient Nef expression from unintegrated human immunodeficiency virus type 1 DNA. *J. Virol.* **81**, 10515–10523 (2007).

5.   Brussel, A. & Sonigo, P. Evidence for gene expression by unintegrated human immunodeficiency virus type 1 DNA species. *J. Virol.* **78**, 11263–11271 (2004).

6.   Saenz, D. T. *et al.* Unintegrated lentivirus DNA persistence and accessibility to expression in nondividing cells: analysis with class I integrase mutants. *J. Virol.* **78**, 2906–2920 (2004).

7.   Bushman, F. D. & Miller, M. D. Tethering human immunodeficiency virus type 1 preintegration complexes to target DNA promotes integration at nearby sites. *J. Virol.* **71**, 458–464 (1997).

8.   Yadav, S. S., Wilson, S. J. & Bieniasz, P. D. A facile quantitative assay for viral particle genesis reveals cooperativity in virion assembly and saturation of an antiviral protein. *Virology* (2012).doi:10.1016/j.virol.2012.04.008

9.   Bushman, F. D. Tethering human immunodeficiency virus 1 integrase to a DNA site directs integration to nearby sequences. *Proc. Natl. Acad. Sci. U.S.A.* **91**, 9233–9237 (1994).

10.   Su, K., Wang, D., Ye, J., Kim, Y. C. & Chow, S. A. Site-specific integration of retroviral DNA in human cells using fusion proteins consisting of human

immunodeficiency virus type 1 integrase and the designed polydactyl zinc-finger protein E2C. *Methods* **47**, 269–276 (2009).

11. McNeely, M. *et al.* In vitro DNA tethering of HIV-1 integrase by the transcriptional coactivator LEDGF/p75. *J. Mol. Biol.* **410**, 811–830 (2011).

12. Weiss, C. D., Levy, J. A. & White, J. M. Oligomeric organization of gp120 on infectious human immunodeficiency virus type 1 particles. *J. Virol.* **64**, 5674–5677 (1990).

13. Liu, J., Bartesaghi, A., Borgnia, M. J., Sapiro, G. & Subramaniam, S. Molecular architecture of native HIV-1 gp120 trimers. *Nature* **455**, 109–113 (2008).

14. Mizuochi, T. *et al.* Diversity of oligosaccharide structures on the envelope glycoprotein gp 120 of human immunodeficiency virus 1 from the lymphoblastoid cell line H9. Presence of complex-type oligosaccharides with bisecting N-acetylglucosamine residues. *J. Biol. Chem.* **265**, 8519–8524 (1990).

15. Wolk, T. & Schreiber, M. N-Glycans in the gp120 V1/V2 domain of the HIV-1 strain NL4-3 are indispensable for viral infectivity and resistance against antibody neutralization. *Med. Microbiol. Immunol.* **195**, 165–172 (2006).

16. Pottathil, R. Constant and variable antigenic regions of the HIV. *Transfus Med Rev* **3**, 17–22 (1989).

17. Cheng-Mayer, C., Homsy, J., Evans, L. A. & Levy, J. A. Identification of human immunodeficiency virus subtypes with distinct patterns of sensitivity to serum neutralization. *Proc. Natl. Acad. Sci. U.S.A.* **85**, 2815–2819 (1988).

18. Neurath, A. R. & Strick, N. Confronting the hypervariability of an immunodominant epitope eliciting virus neutralizing antibodies from the envelope glycoprotein of the human immunodeficiency virus type 1 (HIV-1). *Mol. Immunol.* **27**, 539–549 (1990).

19. Le, S. Y., Chen, J. H., Chatterjee, D. & Maizel, J. V. Sequence divergence and open regions of RNA secondary structures in the envelope regions of the 17 human immunodeficiency virus isolates. *Nucleic Acids Res.* **17**, 3275–3288 (1989).

20. Scheid, J. F. *et al.* Broad diversity of neutralizing antibodies isolated from memory B cells in HIV-infected individuals. *Nature* **458**, 636–640 (2009).

21. Dacheux, L. *et al.* Evolutionary dynamics of the glycan shield of the human immunodeficiency virus envelope during natural infection and implications

for exposure of the 2G12 epitope. *J. Virol.* **78**, 12625–12637 (2004).

22.   Weiss, C. D. *et al.* Studies of HIV-1 envelope glycoprotein-mediated fusion using a simple fluorescence assay. *AIDS* **10**, 241–246 (1996).

23.   Hart, T. K., Truneh, A. & Bugelski, P. J. Characterization of CD4-gp120 activation intermediates during human immunodeficiency virus type 1 syncytium formation. *AIDS Res. Hum. Retroviruses* **12**, 1305–1313 (1996).

24.   Frey, S. *et al.* Temperature dependence of cell-cell fusion induced by the envelope glycoprotein of human immunodeficiency virus type 1. *J. Virol.* **69**, 1462–1472 (1995).

25.   Melikyan, G. B. *et al.* Evidence that the transition of HIV-1 gp41 into a six-helix bundle, not the bundle configuration, induces membrane fusion. *J. Cell Biol.* **151**, 413–423 (2000).

26.   Hsu, S.-T. D. & Bonvin, A. M. J. J. Atomic insight into the CD4 binding-induced conformational changes in HIV-1 gp120. *Proteins* **55**, 582–593 (2004).

27.   Zhang, W. *et al.* Conformational changes of gp120 in epitopes near the CCR5 binding site are induced by CD4 and a CD4 miniprotein mimetic. *Biochemistry* **38**, 9405–9416 (1999).

28.   Choe, H. *et al.* The beta-chemokine receptors CCR3 and CCR5 facilitate infection by primary HIV-1 isolates. *Cell* **85**, 1135–1148 (1996).

29.   Balter, M. A second coreceptor for HIV in early stages of infection. *Science* **272**, 1740 (1996).

30.   Dragic, T. *et al.* HIV-1 entry into CD4+ cells is mediated by the chemokine receptor CC-CKR-5. *Nature* **381**, 667–673 (1996).

31.   Deng, H. *et al.* Identification of a major co-receptor for primary isolates of HIV-1. *Nature* **381**, 661–666 (1996).

32.   Chan, D. C., Fass, D., Berger, J. M. & Kim, P. S. Core structure of gp41 from the HIV envelope glycoprotein. *Cell* **89**, 263–273 (1997).

33.   Weissenhorn, W., Dessen, A., Harrison, S. C., Skehel, J. J. & Wiley, D. C. Atomic structure of the ectodomain from HIV-1 gp41. *Nature* **387**, 426–430 (1997).

34.   Gallo, S. A., Puri, A. & Blumenthal, R. HIV-1 gp41 six-helix bundle formation occurs rapidly after the engagement of gp120 by CXCR4 in the HIV-1 Env-mediated fusion process. *Biochemistry* **40**, 12231–12236 (2001).

35.   Platt, E. J., Durnin, J. P. & Kabat, D. Kinetic factors control efficiencies of cell entry, efficacies of entry inhibitors, and mechanisms of adaptation of human immunodeficiency virus. *J. Virol.* **79**, 4347–4356 (2005).

36.   Peng, C., Ho, B. K., Chang, T. W. & Chang, N. T. Role of human immunodeficiency virus type 1-specific protease in core protein maturation and viral infectivity. *J. Virol.* **63**, 2550–2556 (1989).

37.   Ross, E. K. *et al.* Maturation of human immunodeficiency virus particles assembled from the gag precursor protein requires in situ processing by gag-pol protease. *AIDS Res. Hum. Retroviruses* **7**, 475–483 (1991).

38.   Fassati, A. & Goff, S. P. Characterization of intracellular reverse transcription complexes of human immunodeficiency virus type 1. *J. Virol.* **75**, 3626–3635 (2001).

39.   Iordanskiy, S., Berro, R., Altieri, M., Kashanchi, F. & Bukrinsky, M. Intracytoplasmic maturation of the human immunodeficiency virus type 1 reverse transcription complexes determines their capacity to integrate into chromatin. *Retrovirology* **3**, 4 (2006).

40.   Farnet, C. M. & Haseltine, W. A. Integration of human immunodeficiency virus type 1 DNA in vitro. *Proc. Natl. Acad. Sci. U.S.A.* **87**, 4164–4168 (1990).

41.   Kim, J., Tipper, C. & Sodroski, J. Role of TRIM5α RING domain E3 ubiquitin ligase activity in capsid disassembly, reverse transcription blockade, and restriction of simian immunodeficiency virus. *J. Virol.* **85**, 8116–8132 (2011).

42.   Hulme, A. E., Perez, O. & Hope, T. J. Complementary assays reveal a relationship between HIV-1 uncoating and reverse transcription. *Proceedings of the National Academy of Sciences* **108**, 9975–9980 (2011).

43.   Shi, J. & Aiken, C. Saturation of TRIM5 alpha-mediated restriction of HIV-1 infection depends on the stability of the incoming viral capsid. *Virology* **350**, 493–500 (2006).

44.   Forshey, B. M. & Aiken, C. Disassembly of human immunodeficiency virus type 1 cores in vitro reveals association of Nef with the subviral ribonucleoprotein complex. *J. Virol.* **77**, 4409–4414 (2003).

45.   Forshey, B. M., Schwedler, von, U., Sundquist, W. I. & Aiken, C. Formation of a human immunodeficiency virus type 1 core of optimal stability is crucial for viral replication. *J. Virol.* **76**, 5667–5677 (2002).

46.   Naghavi, M. H. & Goff, S. P. Retroviral proteins that interact with the host cell cytoskeleton. *Curr. Opin. Immunol.* **19**, 402–407 (2007).

47.   Naghavi, M. H., Hatziioannou, T., Gao, G. & Goff, S. P. Overexpression of fasciculation and elongation protein zeta-1 (FEZ1) induces a post-entry block to retroviruses in cultured cells. *Genes Dev.* **19**, 1105–1115 (2005).

48.   McDonald, D. *et al.* Visualization of the intracellular behavior of HIV in living cells. *J. Cell Biol.* **159**, 441–452 (2002).

49.   Bukrinskaya, A., Brichacek, B., Mann, A. & Stevenson, M. Establishment of a functional human immunodeficiency virus type 1 (HIV-1) reverse transcription complex involves the cytoskeleton. *J. Exp. Med.* **188**, 2113–2125 (1998).

50.   Karczewski, M. K. & Strebel, K. Cytoskeleton association and virion incorporation of the human immunodeficiency virus type 1 Vif protein. *J. Virol.* **70**, 494–507 (1996).

51.   Iyengar, S., Hildreth, J. E. & Schwartz, D. H. Actin-dependent receptor colocalization required for human immunodeficiency virus entry into host cells. *J. Virol.* **72**, 5251–5255 (1998).

52.   Barrero-Villar, M. *et al.* Moesin is required for HIV-1-induced CD4-CXCR4 interaction, F-actin redistribution, membrane fusion and viral infection in lymphocytes. *J. Cell. Sci.* **122**, 103–113 (2009).

53.   Vorster, P. J. *et al.* LIM kinase 1 modulates cortical actin and CXCR4 cycling and is activated by HIV-1 to initiate viral infection. *J. Biol. Chem.* **286**, 12554–12564 (2011).

54.   Yoder, A. *et al.* HIV envelope-CXCR4 signaling activates cofilin to overcome cortical actin restriction in resting CD4 T cells. *Cell* **134**, 782–792 (2008).

55.   Campbell, E. M., Nunez, R. & Hope, T. J. Disruption of the actin cytoskeleton can complement the ability of Nef to enhance human immunodeficiency virus type 1 infectivity. *J. Virol.* **78**, 5745–5755 (2004).

56.   Schwartz, O., Maréchal, V., Danos, O. & Heard, J. M. Human immunodeficiency virus type 1 Nef increases the efficiency of reverse transcription in the infected cell. *J. Virol.* **69**, 4053–4059 (1995).

57.   Aiken, C. Pseudotyping human immunodeficiency virus type 1 (HIV-1) by the glycoprotein of vesicular stomatitis virus targets HIV-1 entry to an endocytic pathway and suppresses both the requirement for Nef and the

sensitivity to cyclosporin A. *J. Virol.* **71**, 5871–5877 (1997).

58. Arhel, N. *et al.* Quantitative four-dimensional tracking of cytoplasmic and nuclear HIV-1 complexes. *Nat. Methods* **3**, 817–824 (2006).

59. Fontenot, D. R. *et al.* Dynein light chain 1 peptide inhibits human immunodeficiency virus infection in eukaryotic cells. *Biochem. Biophys. Res. Commun.* **363**, 901–907 (2007).

60. Komano, J., Miyauchi, K., Matsuda, Z. & Yamamoto, N. Inhibiting the Arp2/3 complex limits infection of both intracellular mature vaccinia virus and primate lentiviruses. *Mol. Biol. Cell* **15**, 5197–5207 (2004).

61. Yu, D., Wang, W., Yoder, A., Spear, M. & Wu, Y. The HIV envelope but not VSV glycoprotein is capable of mediating HIV latent infection of resting CD4 T cells. *PLoS Pathog.* **5**, e1000633 (2009).

62. Fackler, O. T. *et al.* Association of human immunodeficiency virus Nef protein with actin is myristoylation dependent and influences its subcellular localization. *Eur. J. Biochem.* **247**, 843–851 (1997).

63. Hottiger, M. *et al.* The large subunit of HIV-1 reverse transcriptase interacts with beta-actin. *Nucleic Acids Res.* **23**, 736–741 (1995).

64. Wilk, T., Gowen, B. & Fuller, S. D. Actin associates with the nucleocapsid domain of the human immunodeficiency virus Gag polyprotein. *J. Virol.* **73**, 1931–1940 (1999).

65. Kubo, Y. *et al.* Ezrin, Radixin, and Moesin (ERM) proteins function as pleiotropic regulators of human immunodeficiency virus type 1 infection. *Virology* **375**, 130–140 (2008).

66. Haedicke, J., de Los Santos, K., Goff, S. P. & Naghavi, M. H. The Ezrin-radixin-moesin family member ezrin regulates stable microtubule formation and retroviral infection. *J. Virol.* **82**, 4665–4670 (2008).

67. Naghavi, M. H. *et al.* Moesin regulates stable microtubule formation and limits retroviral infection in cultured cells. *EMBO J.* **26**, 41–52 (2007).

68. Gallo, D. E. & Hope, T. J. Knockdown of MAP4 and DNAL1 produces a post-fusion and pre-nuclear translocation impairment in HIV-1 replication. *Virology* **422**, 13–21 (2012).

69. Apodaca, G. Endocytic traffic in polarized epithelial cells: role of the actin and microtubule cytoskeleton. *Traffic* **2**, 149–159 (2001).

70. Kim, S. Y., Byrn, R., Groopman, J. & Baltimore, D. Temporal aspects of DNA and RNA synthesis during human immunodeficiency virus infection: evidence for differential gene expression. *J. Virol.* **63**, 3708–3713 (1989).

71. Perez-Caballero, D., Hatziioannou, T., Zhang, F., Cowan, S. & Bieniasz, P. D. Restriction of human immunodeficiency virus type 1 by TRIM-CypA occurs with rapid kinetics and independently of cytoplasmic bodies, ubiquitin, and proteasome activity. *J. Virol.* **79**, 15567–15572 (2005).

72. Zhang, H. *et al.* Reverse transcription takes place within extracellular HIV-1 virions: potential biological significance. *AIDS Res. Hum. Retroviruses* **9**, 1287–1296 (1993).

73. Lori, F. *et al.* Viral DNA carried by human immunodeficiency virus type 1 virions. *J. Virol.* **66**, 5067–5074 (1992).

74. Trono, D. Partial reverse transcripts in virions from human immunodeficiency and murine leukemia viruses. *J. Virol.* **66**, 4893–4900 (1992).

75. Kim, B., Nguyen, L. A., Daddacha, W. & Hollenbaugh, J. A. Tight Interplay Among SAMHD1 Level, Cellular dNTP Levels and HIV-1 Proviral DNA Synthesis Kinetics in Human Primary Monocyte-Derived Macrophages. *J. Biol. Chem.* (2012).doi:10.1074/jbc.C112.374843

76. Goldstone, D. C. *et al.* HIV-1 restriction factor SAMHD1 is a deoxynucleoside triphosphate triphosphohydrolase. *Nature* **480**, 379–382 (2011).

77. Johns, D. G. & Gao, W. Y. Selective depletion of DNA precursors: an evolving strategy for potentiation of dideoxynucleoside activity against human immunodeficiency virus. *Biochem. Pharmacol.* **55**, 1551–1556 (1998).

78. Hooker, C. W. & Harrich, D. The first strand transfer reaction of HIV-1 reverse transcription is more efficient in infected cells than in cell-free natural endogenous reverse transcription reactions. *J. Clin. Virol.* **26**, 229–238 (2003).

79. Gilboa, E., Mitra, S. W., Goff, S. & Baltimore, D. A detailed model of reverse transcription and tests of crucial aspects. *Cell* **18**, 93–100 (1979).

80. Peliska, J. A. & Benkovic, S. J. Mechanism of DNA strand transfer reactions catalyzed by HIV-1 reverse transcriptase. *Science* **258**, 1112–1118 (1992).

81. DeStefano, J. J., Mallaber, L. M., Rodriguez-Rodriguez, L., Fay, P. J. & Bambara, R. A. Requirements for strand transfer between internal regions of

heteropolymer templates by human immunodeficiency virus reverse transcriptase. *J. Virol.* **66**, 6370–6378 (1992).

82. Huber, H. E., McCoy, J. M., Seehra, J. S. & Richardson, C. C. Human immunodeficiency virus 1 reverse transcriptase. Template binding, processivity, strand displacement synthesis, and template switching. *J. Biol. Chem.* **264**, 4669–4678 (1989).

83. Buiser, R. G., Bambara, R. A. & Fay, P. J. Pausing by retroviral DNA polymerases promotes strand transfer from internal regions of RNA donor templates to homopolymeric acceptor templates. *Biochim. Biophys. Acta* **1216**, 20–30 (1993).

84. Roberts, J. D., Bebenek, K. & Kunkel, T. A. The accuracy of reverse transcriptase from HIV-1. *Science* **242**, 1171–1173 (1988).

85. Hübner, A., Kruhoffer, M., Grosse, F. & Krauss, G. Fidelity of human immunodeficiency virus type I reverse transcriptase in copying natural RNA. *J. Mol. Biol.* **223**, 595–600 (1992).

86. Ji, J. P. & Loeb, L. A. Fidelity of HIV-1 reverse transcriptase copying RNA in vitro. *Biochemistry* **31**, 954–958 (1992).

87. Bebenek, K., Abbotts, J., Roberts, J. D., Wilson, S. H. & Kunkel, T. A. Specificity and mechanism of error-prone replication by human immunodeficiency virus-1 reverse transcriptase. *J. Biol. Chem.* **264**, 16948–16956 (1989).

88. Fisher, A. G. *et al.* Biologically diverse molecular variants within a single HIV-1 isolate. *Nature* **334**, 444–447 (1988).

89. Howell, R. M. *et al.* In vivo sequence variation of the human immunodeficiency virus type 1 env gene: evidence for recombination among variants found in a single individual. *AIDS Res. Hum. Retroviruses* **7**, 869–876 (1991).

90. Robertson, D. L., Sharp, P. M., McCutchan, F. E. & Hahn, B. H. Recombination in HIV-1. *Nature* **374**, 124–126 (1995).

91. Stremlau, M. *et al.* The cytoplasmic body component TRIM5alpha restricts HIV-1 infection in Old World monkeys. *Nature* **427**, 848–853 (2004).

92. Karageorgos, L., Li, P. & Burrell, C. Characterization of HIV replication complexes early after cell-to-cell infection. *AIDS Res. Hum. Retroviruses* **9**, 817–823 (1993).

93. Bukrinsky, M. I. *et al.* Association of integrase, matrix, and reverse transcriptase antigens of human immunodeficiency virus type 1 with viral nucleic acids following acute infection. *Proc. Natl. Acad. Sci. U.S.A.* **90**, 6125–6129 (1993).

94. Grewe, C., Beck, A. & Gelderblom, H. R. HIV: early virus-cell interactions. *J. Acquir. Immune Defic. Syndr.* **3**, 965–974 (1990).

95. Arhel, N. J. *et al.* HIV-1 DNA Flap formation promotes uncoating of the pre-integration complex at the nuclear pore. *EMBO J.* **26**, 3025–3037 (2007).

96. Lelek, M. *et al.* Superresolution imaging of HIV in infected cells with FlAsH-PALM. *Proceedings of the National Academy of Sciences* **109**, 8564–8569 (2012).

97. Kratovac, Z. *et al.* Primate lentivirus capsid sensitivity to TRIM5 proteins. *J. Virol.* **82**, 6772–6777 (2008).

98. Perez-Caballero, D., Hatziioannou, T., Yang, A., Cowan, S. & Bieniasz, P. D. Human tripartite motif 5alpha domains responsible for retrovirus restriction activity and specificity. *J. Virol.* **79**, 8969–8978 (2005).

99. Hatziioannou, T., Perez-Caballero, D., Yang, A., Cowan, S. & Bieniasz, P. D. Retrovirus resistance factors Ref1 and Lv1 are species-specific variants of TRIM5alpha. *Proc. Natl. Acad. Sci. U.S.A.* **101**, 10774–10779 (2004).

100. Virgen, C. A., Kratovac, Z., Bieniasz, P. D. & Hatziioannou, T. Independent genesis of chimeric TRIM5-cyclophilin proteins in two primate species. *Proc. Natl. Acad. Sci. U.S.A.* **105**, 3563–3568 (2008).

101. Liao, C.-H., Kuang, Y.-Q., Liu, H.-L., Zheng, Y.-T. & Su, B. A novel fusion gene, TRIM5-Cyclophilin A in the pig-tailed macaque determines its susceptibility to HIV-1 infection. *AIDS* **21 Suppl 8**, S19–26 (2007).

102. Sayah, D. M., Sokolskaja, E., Berthoux, L. & Luban, J. Cyclophilin A retrotransposition into TRIM5 explains owl monkey resistance to HIV-1. *Nature* **430**, 569–573 (2004).

103. Wilson, S. J. *et al.* Independent evolution of an antiviral TRIMCyp in rhesus macaques. *Proceedings of the National Academy of Sciences* **105**, 3557–3562 (2008).

104. Towers, G. J. *et al.* Cyclophilin A modulates the sensitivity of HIV-1 to host restriction factors. *Nat. Med.* **9**, 1138–1143 (2003).

105.	Yap, M. W., Dodding, M. P. & Stoye, J. P. Trim-cyclophilin A fusion proteins can restrict human immunodeficiency virus type 1 infection at two distinct phases in the viral life cycle. *J. Virol.* **80**, 4061–4067 (2006).

106.	Yap, M. W., Nisole, S. & Stoye, J. P. A single amino acid change in the SPRY domain of human Trim5alpha leads to HIV-1 restriction. *Curr. Biol.* **15**, 73–78 (2005).

107.	Sebastian, S. & Luban, J. TRIM5alpha selectively binds a restriction-sensitive retroviral capsid. *Retrovirology* **2**, 40 (2005).

108.	Song, B. *et al.* The B30.2(SPRY) domain of the retroviral restriction factor TRIM5alpha exhibits lineage-specific length and sequence variation in primates. *J. Virol.* **79**, 6111–6121 (2005).

109.	Sawyer, S. L., Wu, L. I., Emerman, M. & Malik, H. S. Positive selection of primate TRIM5alpha identifies a critical species-specific retroviral restriction domain. *Proc. Natl. Acad. Sci. U.S.A.* **102**, 2832–2837 (2005).

110.	Stremlau, M. *et al.* Specific recognition and accelerated uncoating of retroviral capsids by the TRIM5alpha restriction factor. *Proc. Natl. Acad. Sci. U.S.A.* **103**, 5514–5519 (2006).

111.	Forshey, B. M., Shi, J. & Aiken, C. Structural requirements for recognition of the human immunodeficiency virus type 1 core during host restriction in owl monkey cells. *J. Virol.* **79**, 869–875 (2005).

112.	Hatziioannou, T., Cowan, S. & Bieniasz, P. D. Capsid-dependent and -independent postentry restriction of primate lentivirus tropism in rodent cells. *J. Virol.* **78**, 1006–1011 (2004).

113.	Hatziioannou, T., Cowan, S., Goff, S. P., Bieniasz, P. D. & Towers, G. J. Restriction of multiple divergent retroviruses by Lv1 and Ref1. *EMBO J.* **22**, 385–394 (2003).

114.	Ganser-Pornillos, B. K. *et al.* Hexagonal assembly of a restricting TRIM5alpha protein. *Proceedings of the National Academy of Sciences* **108**, 534–539 (2011).

115.	Li, X., Yeung, D. F., Fiegen, A. M. & Sodroski, J. Determinants of the higher order association of the restriction factor TRIM5alpha and other tripartite motif (TRIM) proteins. *J. Biol. Chem.* **286**, 27959–27970 (2011).

116.	Zhao, G. *et al.* Rhesus TRIM5α disrupts the HIV-1 capsid at the inter-hexamer interfaces. *PLoS Pathog.* **7**, e1002009 (2011).

117. Danielson, C. M., Cianci, G. C. & Hope, T. J. Recruitment and dynamics of proteasome association with rhTRIM5α cytoplasmic complexes during HIV-1 infection. *Traffic* **9999**, (2012).

118. Diaz-Griffero, F. *et al.* Modulation of retroviral restriction and proteasome inhibitor-resistant turnover by changes in the TRIM5alpha B-box 2 domain. *J. Virol.* **81**, 10362–10378 (2007).

119. Campbell, E. M., Perez, O., Anderson, J. L. & Hope, T. J. Visualization of a proteasome-independent intermediate during restriction of HIV-1 by rhesus TRIM5alpha. *J. Cell Biol.* **180**, 549–561 (2008).

120. Wu, X., Anderson, J. L., Campbell, E. M., Joseph, A. M. & Hope, T. J. Proteasome inhibitors uncouple rhesus TRIM5alpha restriction of HIV-1 reverse transcription and infection. *Proc. Natl. Acad. Sci. U.S.A.* **103**, 7465–7470 (2006).

121. Roa, A. *et al.* RING domain mutations uncouple TRIM5α restriction of HIV-1 from inhibition of reverse transcription and acceleration of uncoating. *J. Virol.* **86**, 1717–1727 (2012).

122. Anderson, J. L. *et al.* Proteasome inhibition reveals that a functional preintegration complex intermediate can be generated during restriction by diverse TRIM5 proteins. *J. Virol.* **80**, 9754–9760 (2006).

123. Klarmann, G. J., Schauber, C. A. & Preston, B. D. Template-directed pausing of DNA synthesis by HIV-1 reverse transcriptase during polymerization of HIV-1 sequences in vitro. *J. Biol. Chem.* **268**, 9793–9802 (1993).

124. Li, S., Hill, C. P., Sundquist, W. I. & Finch, J. T. Image reconstructions of helical assemblies of the HIV-1 CA protein. *Nature* **407**, 409–413 (2000).

125. Rubin, H. & Temin, H. M. A radiological study of cell-virus interaction in the Rous sarcoma. *Virology* **7**, 75–91 (1959).

126. Lewis, P., Hensel, M. & Emerman, M. Human immunodeficiency virus infection of cells arrested in the cell cycle. *EMBO J.* **11**, 3053–3058 (1992).

127. Roe, T., Reynolds, T. C., Yu, G. & Brown, P. O. Integration of murine leukemia virus DNA depends on mitosis. *EMBO J.* **12**, 2099–2108 (1993).

128. Lewis, P. F. & Emerman, M. Passage through mitosis is required for oncoretroviruses but not for the human immunodeficiency virus. *J. Virol.* **68**, 510–516 (1994).

129. Bukrinsky, M. I. *et al.* Active nuclear import of human immunodeficiency virus type 1 preintegration complexes. *Proc. Natl. Acad. Sci. U.S.A.* **89**, 6580–6584 (1992).

130. Görlich, D., Prehn, S., Laskey, R. A. & Hartmann, E. Isolation of a protein that is essential for the first step of nuclear protein import. *Cell* **79**, 767–778 (1994).

131. Murphy, R., Watkins, J. L. & Wente, S. R. GLE2, a Saccharomyces cerevisiae homologue of the Schizosaccharomyces pombe export factor RAE1, is required for nuclear pore complex structure and function. *Mol. Biol. Cell* **7**, 1921–1937 (1996).

132. Rexach, M. & Blobel, G. Protein import into nuclei: association and dissociation reactions involving transport substrate, transport factors, and nucleoporins. *Cell* **83**, 683–692 (1995).

133. Görlich, D. *et al.* Two different subunits of importin cooperate to recognize nuclear localization signals and bind them to the nuclear envelope. *Curr. Biol.* **5**, 383–392 (1995).

134. Moroianu, J., Blobel, G. & Radu, A. Previously identified protein of uncertain function is karyopherin alpha and together with karyopherin beta docks import substrate at nuclear pore complexes. *Proc. Natl. Acad. Sci. U.S.A.* **92**, 2008–2011 (1995).

135. Belanger, K. D., Kenna, M. A., Wei, S. & Davis, L. I. Genetic and physical interactions between Srp1p and nuclear pore complex proteins Nup1p and Nup2p. *J. Cell Biol.* **126**, 619–630 (1994).

136. Ebina, H., Aoki, J., Hatta, S., Yoshida, T. & Koyanagi, Y. Role of Nup98 in nuclear entry of human immunodeficiency virus type 1 cDNA. *Microbes Infect.* **6**, 715–724 (2004).

137. König, R. *et al.* Global analysis of host-pathogen interactions that regulate early-stage HIV-1 replication. *Cell* **135**, 49–60 (2008).

138. Hutten, S., Wälde, S., Spillner, C., Hauber, J. & Kehlenbach, R. H. The nuclear pore component Nup358 promotes transportin-dependent nuclear import. *J. Cell. Sci.* **122**, 1100–1110 (2009).

139. Woodward, C. L., Prakobwanakit, S., Mosessian, S. & Chow, S. A. Integrase interacts with nucleoporin NUP153 to mediate the nuclear import of human immunodeficiency virus type 1. *J. Virol.* **83**, 6522–6533 (2009).

140.   Brass, A. L. *et al.* Identification of host proteins required for HIV infection through a functional genomic screen. *Science* **319**, 921–926 (2008).

141.   Gallay, P., Hope, T., Chin, D. & Trono, D. HIV-1 infection of nondividing cells through the recognition of integrase by the importin/karyopherin pathway. *Proc. Natl. Acad. Sci. U.S.A.* **94**, 9825–9830 (1997).

142.   Gallay, P., Stitt, V., Mundy, C., Oettinger, M. & Trono, D. Role of the karyopherin pathway in human immunodeficiency virus type 1 nuclear import. *J. Virol.* **70**, 1027–1032 (1996).

143.   Zaitseva, L. *et al.* HIV-1 exploits importin 7 to maximize nuclear import of its DNA genome. *Retrovirology* **6**, 11 (2009).

144.   Christ, F. *et al.* Transportin-SR2 imports HIV into the nucleus. *Curr. Biol.* **18**, 1192–1202 (2008).

145.   Haffar, O. K. *et al.* Two nuclear localization signals in the HIV-1 matrix protein regulate nuclear import of the HIV-1 pre-integration complex. *J. Mol. Biol.* **299**, 359–368 (2000).

146.   Bukrinsky, M. I. & Haffar, O. K. HIV-1 nuclear import: in search of a leader. *Front. Biosci.* **2**, d578–87 (1997).

147.   Schwedler, von, U., Kornbluth, R. S. & Trono, D. The nuclear localization signal of the matrix protein of human immunodeficiency virus type 1 allows the establishment of infection in macrophages and quiescent T lymphocytes. *Proc. Natl. Acad. Sci. U.S.A.* **91**, 6992–6996 (1994).

148.   Bukrinsky, M. I. *et al.* A nuclear localization signal within HIV-1 matrix protein that governs infection of non-dividing cells. *Nature* **365**, 666–669 (1993).

149.   Reil, H., Bukovsky, A. A., Gelderblom, H. R. & Göttlinger, H. G. Efficient HIV-1 replication can occur in the absence of the viral matrix protein. *EMBO J.* **17**, 2699–2708 (1998).

150.   Lee, P. P. & Linial, M. L. Efficient particle formation can occur if the matrix domain of human immunodeficiency virus type 1 Gag is substituted by a myristylation signal. *J. Virol.* **68**, 6644–6654 (1994).

151.   Zhou, W., Parent, L. J., Wills, J. W. & Resh, M. D. Identification of a membrane-binding domain within the amino-terminal region of human immunodeficiency virus type 1 Gag protein which interacts with acidic phospholipids. *J. Virol.* **68**, 2556–2569 (1994).

152.	Kootstra, N. A. & Schuitemaker, H. Phenotype of HIV-1 lacking a functional nuclear localization signal in matrix protein of gag and Vpr is comparable to wild-type HIV-1 in primary macrophages. *Virology* **253**, 170–180 (1999).

153.	Jenkins, Y., McEntee, M., Weis, K. & Greene, W. C. Characterization of HIV-1 vpr nuclear import: analysis of signals and pathways. *J. Cell Biol.* **143**, 875–885 (1998).

154.	Fouchier, R. A. *et al.* Interaction of the human immunodeficiency virus type 1 Vpr protein with the nuclear pore complex. *J. Virol.* **72**, 6004–6013 (1998).

155.	Vodicka, M. A., Koepp, D. M., Silver, P. A. & Emerman, M. HIV-1 Vpr interacts with the nuclear transport pathway to promote macrophage infection. *Genes Dev.* **12**, 175–185 (1998).

156.	Mahalingam, S., Ayyavoo, V., Patel, M., Kieber-Emmons, T. & Weiner, D. B. Nuclear import, virion incorporation, and cell cycle arrest/differentiation are mediated by distinct functional domains of human immunodeficiency virus type 1 Vpr. *J. Virol.* **71**, 6339–6347 (1997).

157.	Connor, R. I., Chen, B. K., Choe, S. & Landau, N. R. Vpr is required for efficient replication of human immunodeficiency virus type-1 in mononuclear phagocytes. *Virology* **206**, 935–944 (1995).

158.	Subbramanian, R. A. *et al.* Human immunodeficiency virus type 1 Vpr localization: nuclear transport of a viral protein modulated by a putative amphipathic helical structure and its relevance to biological activity. *J. Mol. Biol.* **278**, 13–30 (1998).

159.	Popov, S. *et al.* Viral protein R regulates nuclear import of the HIV-1 pre-integration complex. *EMBO J.* **17**, 909–917 (1998).

160.	Rivière, L., Darlix, J.-L. & Cimarelli, A. Analysis of the viral elements required in the nuclear import of HIV-1 DNA. *J. Virol.* **84**, 729–739 (2010).

161.	Yamashita, M. & Emerman, M. The cell cycle independence of HIV infections is not determined by known karyophilic viral elements. *PLoS Pathog.* **1**, e18 (2005).

162.	Bouyac-Bertoia, M. *et al.* HIV-1 infection requires a functional integrase NLS. *Mol. Cell* **7**, 1025–1035 (2001).

163.	llano, M. *et al.* LEDGF/p75 determines cellular trafficking of diverse lentiviral but not murine oncoretroviral integrase proteins and is a component of functional lentiviral preintegration complexes. *J. Virol.* **78**,

9524–9537 (2004).

164. Maertens, G. *et al.* LEDGF/p75 is essential for nuclear and chromosomal targeting of HIV-1 integrase in human cells. *J. Biol. Chem.* **278**, 33528–33539 (2003).

165. Limón, A. *et al.* Nuclear localization of human immunodeficiency virus type 1 preintegration complexes (PICs): V165A and R166A are pleiotropic integrase mutants primarily defective for integration, not PIC nuclear import. *J. Virol.* **76**, 10598–10607 (2002).

166. Zennou, V. *et al.* HIV-1 genome nuclear import is mediated by a central DNA flap. *Cell* **101**, 173–185 (2000).

167. Arhel, N., Munier, S., Souque, P., Mollier, K. & Charneau, P. Nuclear import defect of human immunodeficiency virus type 1 DNA flap mutants is not dependent on the viral strain or target cell type. *J. Virol.* **80**, 10262–10269 (2006).

168. Ao, Z., Yao, X. & Cohen, E. A. Assessment of the role of the central DNA flap in human immunodeficiency virus type 1 replication by using a single-cycle replication system. *J. Virol.* **78**, 3170–3177 (2004).

169. Dardalhon, V. *et al.* Lentivirus-mediated gene transfer in primary T cells is enhanced by a central DNA flap. *Gene Ther.* **8**, 190–198 (2001).

170. Sirven, A. *et al.* The human immunodeficiency virus type-1 central DNA flap is a crucial determinant for lentiviral vector nuclear import and gene transduction of human hematopoietic stem cells. *Blood* **96**, 4103–4110 (2000).

171. Dvorin, J. D. *et al.* Reassessment of the roles of integrase and the central DNA flap in human immunodeficiency virus type 1 nuclear import. *J. Virol.* **76**, 12087–12096 (2002).

172. Limón, A., Nakajima, N., Lu, R., Ghory, H. Z. & Engelman, A. Wild-type levels of nuclear localization and human immunodeficiency virus type 1 replication in the absence of the central DNA flap. *J. Virol.* **76**, 12078–12086 (2002).

173. Yamashita, M., Perez, O., Hope, T. J. & Emerman, M. Evidence for direct involvement of the capsid protein in HIV infection of nondividing cells. *PLoS Pathog.* **3**, 1502–1510 (2007).

174. Dismuke, D. J. & Aiken, C. Evidence for a functional link between uncoating

of the human immunodeficiency virus type 1 core and nuclear import of the viral preintegration complex. *J. Virol.* **80**, 3712–3720 (2006).

175. Qi, M., Yang, R. & Aiken, C. Cyclophilin A-dependent restriction of human immunodeficiency virus type 1 capsid mutants for infection of nondividing cells. *J. Virol.* **82**, 12001–12008 (2008).

176. Lee, K. *et al.* Flexible use of nuclear import pathways by HIV-1. *Cell Host Microbe* **7**, 221–233 (2010).

177. Miller, M. D., Farnet, C. M. & Bushman, F. D. Human immunodeficiency virus type 1 preintegration complexes: studies of organization and composition. *J. Virol.* **71**, 5382–5390 (1997).

178. Pante, N. & Kann, M. Nuclear pore complex is able to transport macromolecules with diameters of about 39 nm. *Mol. Biol. Cell* **13**, 425–434 (2002).

179. Fassati, A. & Goff, S. P. Characterization of intracellular reverse transcription complexes of Moloney murine leukemia virus. *J. Virol.* **73**, 8919–8925 (1999).

180. Katz, R. A., Greger, J. G., Boimel, P. & Skalka, A. M. Human immunodeficiency virus type 1 DNA nuclear import and integration are mitosis independent in cycling cells. *J. Virol.* **77**, 13412–13417 (2003).

181. Valle-Casuso, J. C. *et al.* TNPO3 is required for HIV-1 replication after nuclear import but prior to integration and binds the HIV-1 core. *J. Virol.* **86**, 5931–5936 (2012).

182. Cribier, A. *et al.* Mutations affecting interaction of integrase with TNPO3 do not prevent HIV-1 cDNA nuclear import. *Retrovirology* **8**, 104 (2011).

183. Farnet, C. M. & Haseltine, W. A. Circularization of human immunodeficiency virus type 1 DNA in vitro. *J. Virol.* **65**, 6942–6952 (1991).

184. Gelderblom, H. C. *et al.* Viral complementation allows HIV-1 replication without integration. *Retrovirology* **5**, 60 (2008).

185. Cara, A., Cereseto, A., Lori, F. & Reitz, M. S. HIV-1 protein expression from synthetic circles of DNA mimicking the extrachromosomal forms of viral DNA. *J. Biol. Chem.* **271**, 5393–5397 (1996).

186. Stevenson, M. *et al.* Integration is not necessary for expression of human immunodeficiency virus type 1 protein products. *J. Virol.* **64**, 2421–2425

(1990).

187.   Emiliani, S. *et al.* Integrase mutants defective for interaction with LEDGF/p75 are impaired in chromosome tethering and HIV-1 replication. *J. Biol. Chem.* **280**, 25517–25523 (2005).

188.   Cherepanov, P. *et al.* HIV-1 integrase forms stable tetramers and associates with LEDGF/p75 protein in human cells. *J. Biol. Chem.* **278**, 372–381 (2003).

189.   Meehan, A. M. *et al.* LEDGF/p75 proteins with alternative chromatin tethers are functional HIV-1 cofactors. *PLoS Pathog.* **5**, e1000522 (2009).

190.   Ciuffi, A. *et al.* A role for LEDGF/p75 in targeting HIV DNA integration. *Nat. Med.* **11**, 1287–1289 (2005).

191.   Wang, L.-D., Liu, C.-L., Chen, W.-Z. & Wang, C.-X. Constructing HIV-1 integrase tetramer and exploring influences of metal ions on forming integrase-DNA complex. *Biochem. Biophys. Res. Commun.* **337**, 313–319 (2005).

192.   Wang, J. Y., Ling, H., Yang, W. & Craigie, R. Structure of a two-domain fragment of HIV-1 integrase: implications for domain organization in the intact protein. *EMBO J.* **20**, 7333–7343 (2001).

193.   Deprez, E. *et al.* Oligomeric states of the HIV-1 integrase as measured by time-resolved fluorescence anisotropy. *Biochemistry* **39**, 9275–9284 (2000).

194.   Fujiwara, T. & Mizuuchi, K. Retroviral DNA integration: structure of an integration intermediate. *Cell* **54**, 497–504 (1988).

195.   Brown, P. O., Bowerman, B., Varmus, H. E. & Bishop, J. M. Retroviral integration: structure of the initial covalent product and its precursor, and a role for the viral IN protein. *Proc. Natl. Acad. Sci. U.S.A.* **86**, 2525–2529 (1989).

196.   Hare, S., Gupta, S. S., Valkov, E., Engelman, A. & Cherepanov, P. Retroviral intasome assembly and inhibition of DNA strand transfer. *Nature* **464**, 232–236 (2010).

197.   Maertens, G. N., Hare, S. & Cherepanov, P. The mechanism of retroviral integration from X-ray structures of its key intermediates. *Nature* **468**, 326–329 (2010).

Chapter 3. Gene expression.

Transcriptional and post-transcriptional regulation

After integrating into the genome of the host cell, HIV-1 transcription is driven from the viral Long Terminal Repeat (LTR), a promoter with a unique mode of activation. After integration, the LTR alone is not capable of driving replication. However, it contains binding sites for multiple cellular transcription factors, including NF-κβ and SP1[1], and these can drive a low basal level of activity capable of producing small amounts of the viral Tat protein. Tat then transactivates the LTR, and vigorous transcription of the viral genome begins[2,3]. The mechanism used for this transactivation is unusual, and not found in mammalian cells. Tat binds the cellular protein CyclinT1[4-8] and recruits it to the LTR via interaction, not with DNA, but with a short region of RNA just 3' of the initiation site known as the Tat Activation Region (TAR)[9,10,11-16]. The TAR RNA is present at the LTR because, although the LTR is not activated it is in fact strongly active for transcription *initiation*[11,17]. RNA Pol II binds the LTR and generates multiple short transcripts[18,19]. These transcripts are abortive and generally do not lead to the production of gene products. However they do cause the TAR RNA to be present near the transcription start site. Cyclin T1 is a component of the positive transcription elongation factor b (p-TEFb) complex[6,20].

Recruitment of this complex to the nascent viral transcript by Tat allows another p-TEFb component, CDK9, to phosphorylate RNA Pol II[21,22], strongly increasing its processivity and enhancing the apparent activity of the LTR by as much as 1000 fold[10,17,23-25].

Once the LTR is activated, it drives high-level transcription from the integrated viral genome. The mechanisms used to produce the nine major gene products of HIV-1 from this single transcript also serve to allow separate quantitative and temporal regulation of these genes. Multiple splice sites throughout the genome result in the production of over 30 unique transcripts[26-28]. These can be grouped into three size classes that undergo differing degrees of splicing[29,30]. Fully spliced transcripts are in the 2kb size class, and encode the regulatory gene products Tat, Rev, and Nef[29,31]. Singly-spliced transcripts make up the 4kb size class and encode Vif, Vpr, Vpu and Env[29,32,33]. Full-length, unspliced transcripts are also produced, and these serve a dual purpose. They function as packageable RNA genomes, and also as templates for translation of the structural proteins Gag and GagPol[31,34].
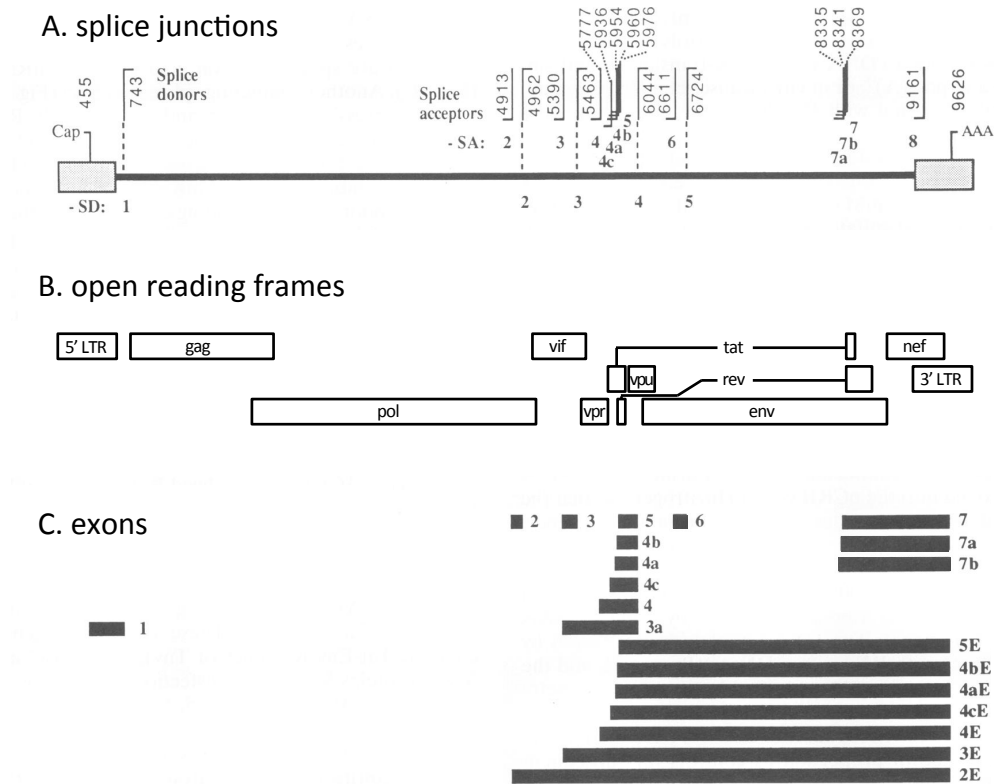
Fig. 3.1. The genomic and mRNA structure of HIV-1 (clone NL4-3). **A.** The positions of the splice donor and splice acceptor sites, with positions numbered from the first nucleotide of the 5' long terminal repeat (LTR). **B.** The organization of the HIV-1 genome. The open reading frames are shown as open rectangular boxes; the LTRs are shown as shaded boxes. **C.** The various exons generated by the use of the different splice donor and acceptor sites.

HIV-1 requires a mechanism for arranging the expression of many genes from a highly compact genome with only a single promoter (Fig.3.1). It utilizes a complex alternative splicing method to solve this problem, one that relies upon regulated avoidance of the cellular splicing machinery. Transcripts of various sizes need to be produced, as well as a full-length genomic transcript that remains entirely unspliced. HIV-1 therefore utilizes a method which allows variable inhibition of splicing – but over time, rather than simultaneously. The HIV-1 genome contains introns that are recognized by the cellular splicing machinery, and intron-containing messages are not normally able to exit the nucleus. Thus, at first, all transcripts of the viral genome reach the cytoplasm fully spliced, and no structural genes are produced.

A region within the intron that spans the env gene forms an RNA stem-loop structure known as the Rev Response Element (RRE)[35,36]. The viral Rev protein, produced from fully spliced mRNA, specifically binds this structure and escorts any messenger RNAs (mRNAs) containing it out of the nucleus[37-40]. Rev is a nuclear shuttling protein with both nuclear export and import signals[41-43], and it utilizes the cellular CRM1 nuclear export pathway to export the viral messages[44-46]. Rev therefore serves to protect these messages from splicing by removing them from the nucleus before the splicing machinery can act upon them. So although Rev is not thought to specifically inhibit splicing, it causes a regulated avoidance of splicing, by

allowing the export of full genomes and the production of viral proteins from regions identified by the cell as introns.

Rev itself is produced, as must be the case, from a fully spliced transcript, as are Tat and Nef. Tat, rev, and nef are the viral "early genes[47]." They are Rev-independent and may be produced in the absence of Rev. Once Rev accumulates sufficiently, both partially spliced and entirely unspliced messages begin to accumulate in the cytoplasm, and the "late", or Rev-dependent, gene products can produced[31,37,48] .

Rev solves a problem inherent in the need to produce multiple proteins from a single highly compact expression unit. The way that it does this results in temporal separation of the phases of gene expression. There is no known reason for HIV-1 to to delay the production of the structural genes. It may be a pleiotropic side effect of the mechanism that evolution hit upon for the efficient production of both spliced and unspliced transcripts. However, the same problem has been solved by other viruses in other ways[49-51]. It is also possible that the delay in the production of the structural genes serves a necessary downstream function. As we will also show in Chapter 4, the Rev-dependence of the late genes is not the only factor that leads to a delay in completion of the viral replication cycle. We suggest that HIV-1 replication requires the host cell to be prepared for the viral assembly process in ways that will allow it to be maximally productive of new infectious virions, and that this requires one or more regulated delays.

Reporter viruses

Despite the fact that so much is known about the mechanics of HIV-1 gene

expression, there is very little published work on the kinetics of gene expression.

The distinction between early and late genes is primarily logical, based on the Rev-

dependence of the late genes that guarantees that they cannot be expressed until

Rev itself (an early gene product) has been made. Until now it has not been known

how much of a delay actually exists between 'early' and 'late' gene expression.

In order to define this timing precisely, and also to have a very clear point of

reference for the timing of later events, we constructed a series of reporter viruses

that would provide a fluorescent read-out of both early- and late-gene expression

(Fig. 3.2). The early-gene reporter in these constructs is either GFP or mCherry

inserted into the viral genome in place of the accessory gene nef. The Nef protein

plays several roles but is not required for replication in cell culture. It is also known

to be expressed at high levels relative to the other early genes[31,34]. For the late gene

reporter we took advantage of the fact that the Gag polyprotein tolerates insertions

of GFP between the MA and CA subdomains[52]. We cloned either mCherry or GFP

into this position, duplicating the normal protease site found between MA and CA to

allow cleavage to take place on both sides of the inserted fluorophore. All of these

viruses additionally carry mutations in env, integrase and reverse-transcriptase,

rendering them replication-defective. The experiments these constructs were

designed for require only a single cycle of replication. Viral stocks are made by co-transfection of 293T cells with the viral reporter genome, a VSV-G envelope plasmid, and a GagPol expression plasmid. This is a standard method for the production of reporter viruses that are capable of only single-cycle infections. Providing an envelope in trans allows "pseudotyping" – production of virions carrying heterologous envelopes. Pseudotyping can allow both alteration of native target-cell tropism, and the use of viral genomes lacking the envelope gene. Inclusion of a WT HIV-1 Gag-Pol-expressing plasmid provides the IN and RT enzymes in trans, and also provides WT Gag which is necessary for the production of highly infectious virions with normal morphology when internal fluorophore insertions are present in the genomic Gag sequence.

To follow the kinetics of gene expression we primarily used the dual reporter NL4.MA-cherry.Nef:GFP, which expresses GFP from the early-gene position and mCherry fused to Gag as the late gene reporter. As a control we also constructed NL4.MA-GFP.Nef:cherry which carries the reporters in exchanged positions, to ensure that expression kinetics from these constructs are not fluorophore-specific in any way.
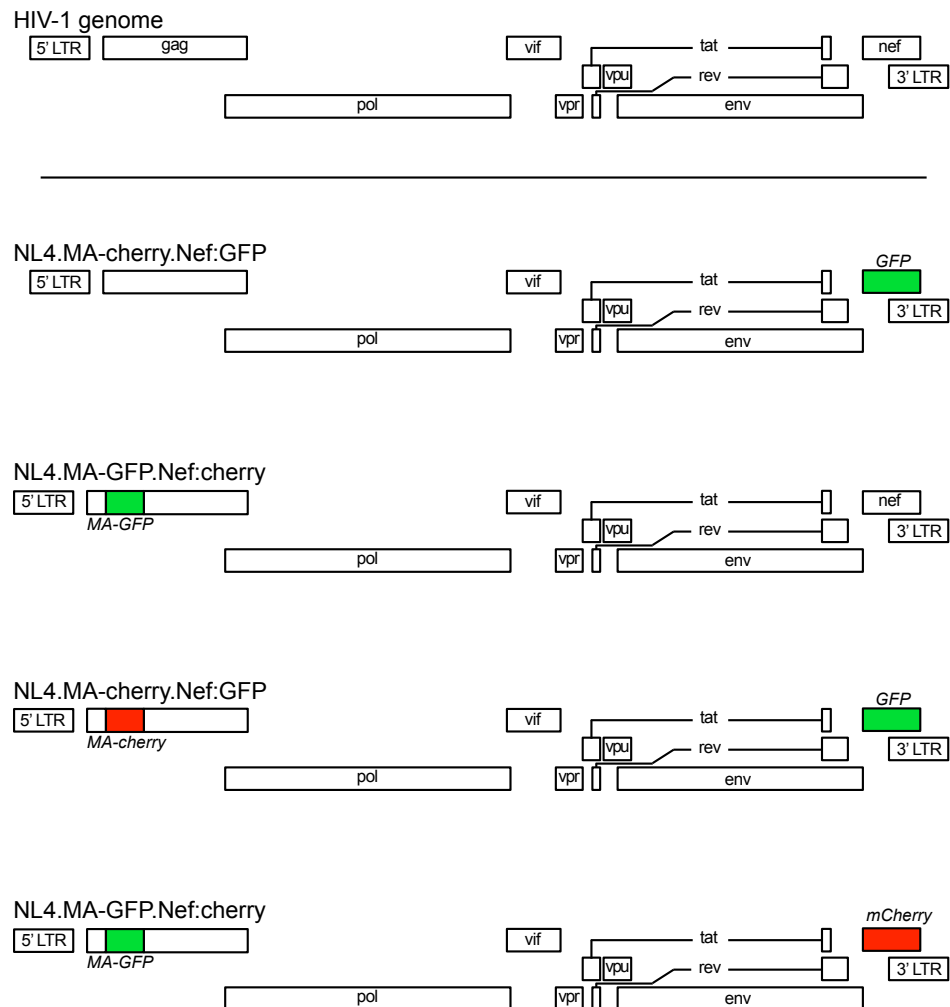
Fig. 3.2. Reporter viruses constructed and used in this study to follow gene expression from early-gene and late-gene positions in the HIV-1 genome. The WT genome is shown above. Fluorophores in the early-gene position replace the accessory gene nef. Fluorophores in the late-gene position are inserted within the gag coding region and cleaved post-translationally by the viral protease.

The delay between early and late gene expression

To track the kinetics of early and late gene expression we infected cells with dual-reporter viruses and measured the fluorescence of infected cells over time. Infections were synchronized by spinoculating (spin infecting)[53] cells at 15°C for 40 minutes, transferring them to 37°C for 90 minutes to allow fusion, and then washing. Mixing virus and cells at a lower temperature allows adherence to take place, but not entry. Once they are transferred to 37°C entry can proceed in a way that bypasses any asynchrony introduced in the course of the pre-fusion stages of entry. In our protocol this adherence stage takes place during the spinoculation step. Spinoculation of cells involves centrifugation of culture plates with added virus, and is known to increase infection efficiency. It therefore allows the attainment of high titer infections even though cells are washed after only a brief time at 37°C. For time course experiments based on flow cytometry analysis of fluorescent signals at intervals, large cultures were infected, washed, and split into smaller dishes. The cells were then collected at various time points thereafter, fixed in paraformaldehyde (PFA), and analyzed. In most experiments the T-cell line MT-4 was used, but we also performed experiments using the human osteosarcoma cell line HOS, and human peripheral blood mononuclear cells (PBMCs).

Flow cytometry data from these time course experiments using dual reporter viruses to infect MT-4 cells, HOS cells, and human PBMC

are shown in Fig. 3.3. In Fig. 3.3B the GFP v mCherry scatterplots are shown for each time point. Fig. 3.3A shows the data for each of these time points plotted as the percentage of cells positive for each fluorophore, over time. The first panels in Fig.s 3.3A and 3.3B show MT-4 cells infected with NL4.MA-GFP.Nef:cherry, the dual reporter expressing mCherry as an early gene and GFP as a late gene. In the graph it can be seen that at each time point the percentage of red cells expressing the early gene product is larger than the green cells expressing the late gene product. From the scatterplot it can be seen that the intensity in the green late gene channel increases only at later time points. The remaining panels of Fig. 3.3 show cells infected with the dual reporter carrying fluorophores in swapped positions, so that GFP is expressed early and mCherry is expressed late. For each of these cells types it can be seen quite clearly that GFP expression is apparent before mCherry expression and remains detectable in a higher percentage of cells throughout the experiment. On the other hand, the intensity of fluorescence, as can been seen in the scatterplots, increases over time in the red channel, ultimately leading to much higher intensities from the late gene reporter than from the early gene reporter.

At later time points, all of these cell types display two infected populations when transduced with this virus: a single-positive population expressing GFP from the early-gene position, and a double positive population expressing both GFP and the MA-mCherry fusion from the late-gene position (Fig. 3.3B). Until hr. 24 (hr. 36 in the case of the PBMCs) the majority of fluorescent cells are single-positive. After this

point the majority of cells are double-positive. At all time points the double-positive population shows a wider range of mCherry (late-gene) intensity, and a more restricted range of intensity in the GFP (early-gene) channel. Thus, flow cytometry of dual-reporter-transduced cells fixed at time points indicates that early genes do indeed become detectable prior to late genes, and that there is both more variation in the intensity range and more total intensity from the late gene reporter.

Flow cytometry is often referred to as a single-cell analysis method. However, when used to analyze cells in this type of time course experiment, flow cytometry effectively becomes a bulk-cell analysis method. It allows quantitation of the overall fluorescence levels, and their distribution, but it cannot provide information about how the fluorescence of individual cells changes from one time point to the next. For this reason we established a microscopy method to follow reporter gene expression in individual cells over time. Both adherent cell lines and suspension cells such as MT-4 are highly mobile and difficult to image. However, using a protein-based adherence reagent we were able to immobilize MT-4 cells for as long as 60 hours. This reagent, Cell-Tak, was adsorbed onto the surface of glass-bottom dishes, and infected cells were washed and then briefly spun onto the glass surface. The majority of cells were then unable to migrate around the dish, but were nonetheless healthy, still displayed the same expression levels when infected with reporter viruses, and still appeared to mobilize membrane projections constantly and energetically in all directions, as do untethered MT-4 cells.

We infected MT-4 cells with dual-reporter viruses, and using an Olympus VivaView

microscope we collected images of numerous cells at intervals of 4-8 min. The

intensity of each cell in both red (mCherry) and green (GFP) channels was

quantified over the duration of the experiment. Thus for each cell two traces were

generated, demonstrating the change in fluorescence intensity over time for both

early- and late-gene reporters. In Fig. 3.4 stills of representative cells at 4hr

intervals post-infection are shown, as well as intensity traces for the same cells. Fig.

3.4A shows a cell infected with NL4.MA-GFP.Nef:cherry and Fig. 3.4B shows a cell

infected with NL5.MA-cherry.Nef:GFP. MT-4 cells infected with these dual-reporter

viruses showed a stereotyped expression pattern. The late reporter became visible

several hours after the early reporter did. Both early and late reporters show a rapid

increase in intensity for the first several hours after they become detectable. During

this first phase both reporters increase smoothly and with rates of increase that are

approximately identical. At about four hours past the point at which the early-gene

reporter becomes detectable, there is a marked shoulder in the intensity trace for

this reporter, and although the fluorescence signal continues to increase, it does so

very gradually. The Gag-fused late-gene reporter does not show this inflection point,

and continues to increase in intensity for the duration of the experiment. This

finding is concordant with the behavior of populations of cells analyzed by flow

cytometry, in which the mean fluorescence intensity of the late reporter rises over

time to higher levels than the early reporter. See Fig. 3.3B, and in Fig. 3.5 compare

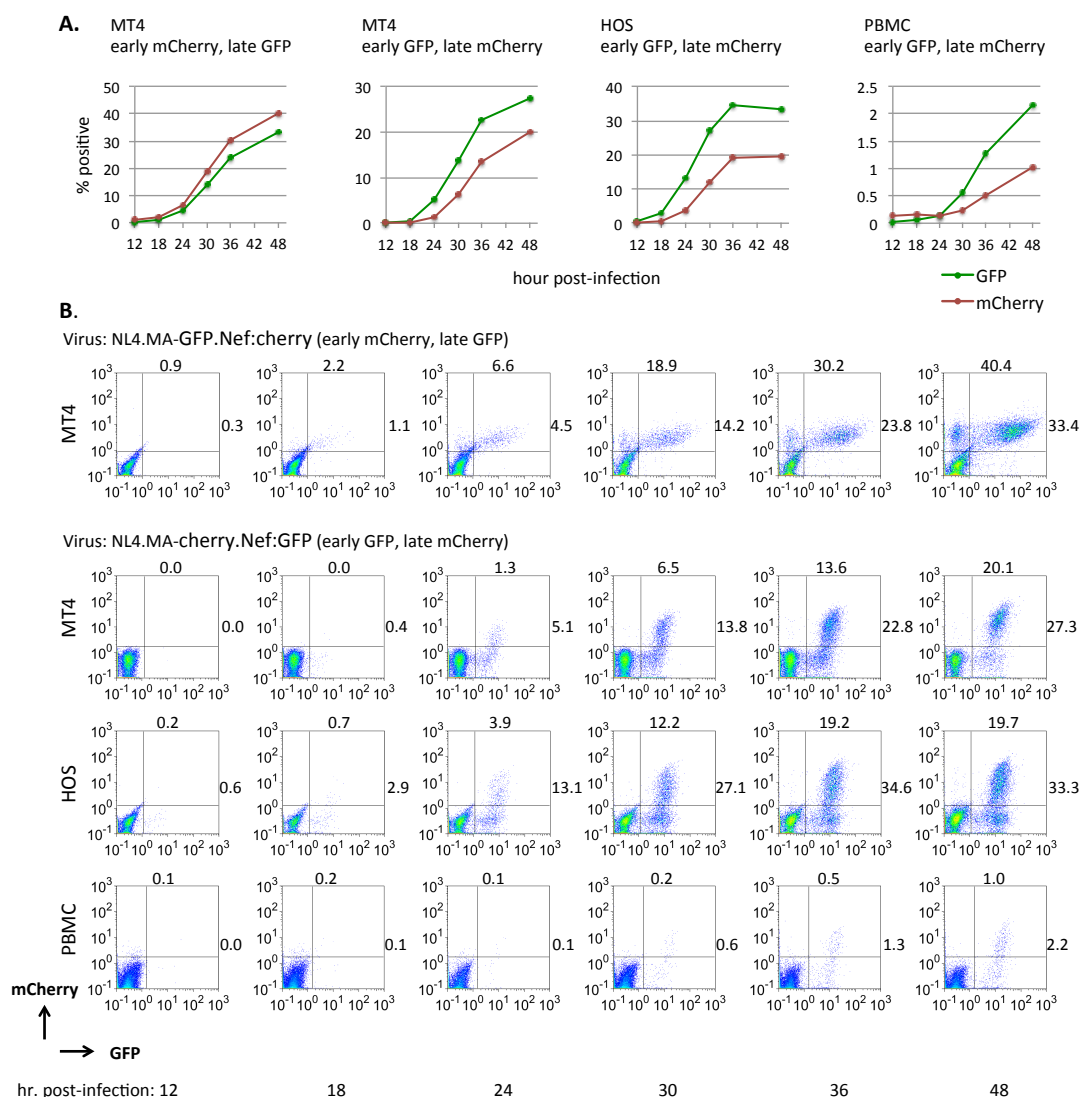the bottom panel of Fig. 3.5B with the top right panel of Fig. 3.5A.

Fig. 3.3. Dual reporter viruses were used to infect MT-4, HOS, or human PBMC cells. Samples were collected at time points and analyzed by flow cytometry. **A.** The percentage of cells positive for red or green fluorescence over time. **B.** Flow cytometry scatterplots of the data in A. Two overlapping gates are shown in each plot. The numbers to the right of the plots indicate the percentage of cells in the GFP-positive gate. The numbers at the top of each plot indicate the percentage of cells in the mCherry-positive gate. Gates are set to include less than one percent of the negative population. PBMCs become infected at a very low rate, but follow the same scatterplot distribution.

We sought to use these data to more precisely quantitate the delay between early and late gene expression. To accomplish this in an unbiased manner we used a custom Matlab script to fit a 5-parameter logistic equation to the relevant regions of each of these intensity curves, and to identify the points at which they rose above background. Logistic equations of this type generate sigmoid curves with horizontal asymptotes and are frequently used to model change over time. Background intensities vary smoothly over the Vivaview field of view, and this was corrected for by subtracting an empty negative control region close to each cell. The resulting intensity data has background levels that are close to zero, and correspond to the horizontal lower bound of the best-fit curve. The Matlab script defined the points at which the intensity curves rose to detectability above background as the first point on the best-fit curve at least 7 intensity units above this noise floor. Fig. 3.4 shows these best-fit curves in the bottom right panels. Fig. 3.5C shows an example intensity graph displaying the best-fit curve, the identified initiation points, and the region used for measurement of the delay between early and late gene expression.

Using this approach we found that the mean delay between the initiation of HIV-1 early and late gene expression is 2.76 hr. (+/- 0.6). This result is not statistically different between the two dual-reporter constructs and is therefore unaffected by the identity of the fluorophore in each position. Although there is wide variation between cells, with a range of 1.6-4.4 hr, the average obtained in this way for the delay between early and late gene expression is in agreement with the average

value of 3.3 hr (+/- 0.6). obtained by flow cytometry (Fig. 3.9). Fig. 3.8 shows the

values obtained for this measurement from cells infected by each of two dual-

reporter viruses. The original microscopy data for each of these cells is shown in

Figs. 3.6 and 3.7.

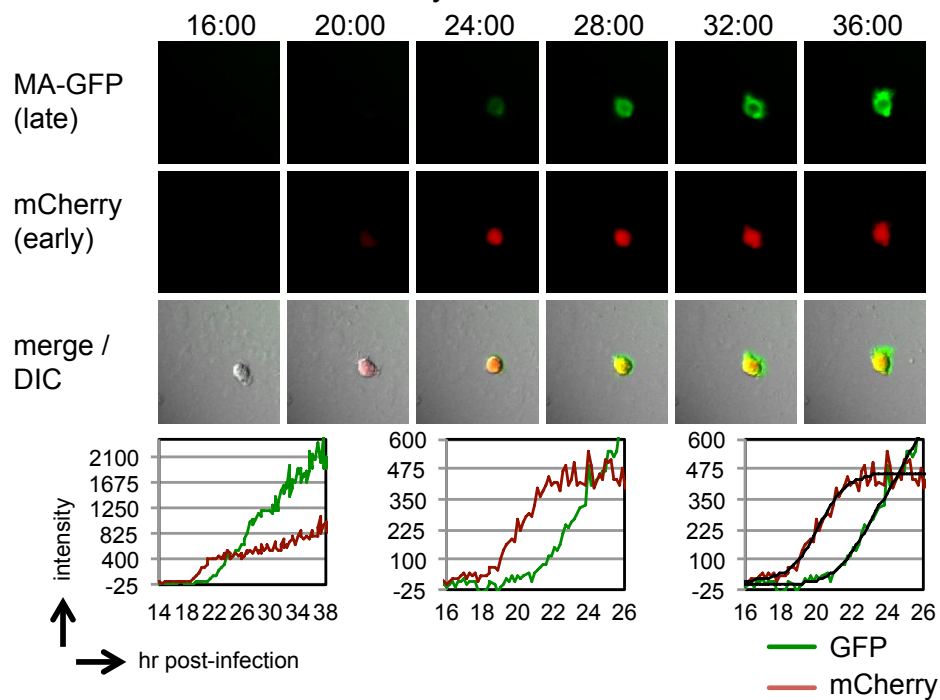## A. NL4.MA-cherry.Nef:GFP
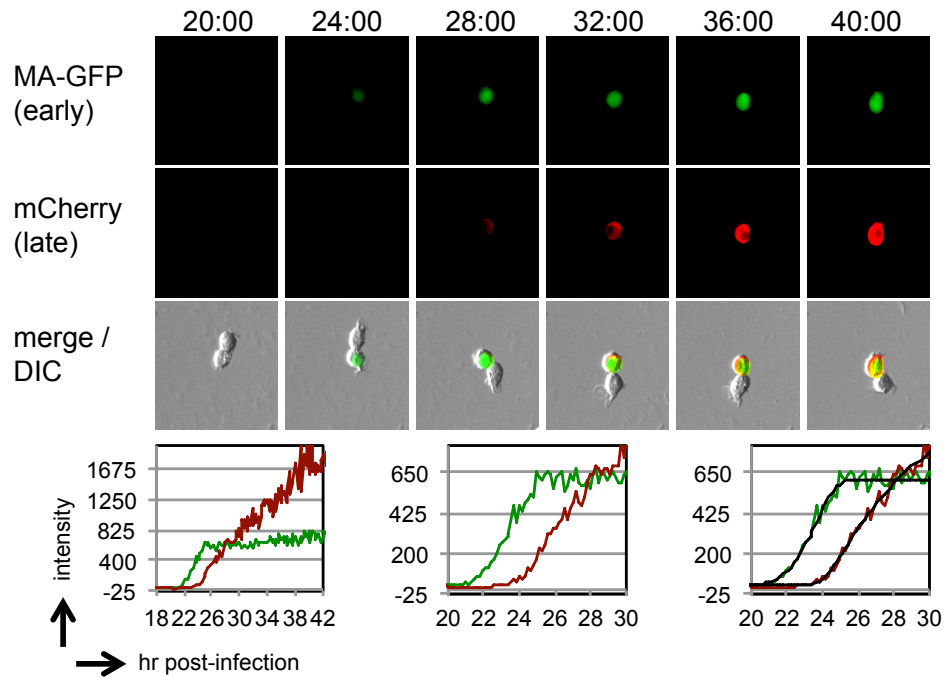
B. NL4.MA-GFP.Nef:cherry

Fig. 3.4. Stills from time-lapse movies of dual-reporter virus infections. A cell infected with NL4.MA-GFP.Nef:cherry, expressing the cherry reporter first, is

shown in panel **A**. An infection with NL4.MA-cherry.Nef:GFP, expressing the GFP reporter first, is shown in panel **B**. The time post-infection is indicated at the top. The charts below the images show the fluorescence intensity in each channel over time for the cell in the images. The raw intensity data is at the left, a close-up of the same data is in the center, and the 5-parameter logistic curve fit to the data is overlaid on the right. Intensity units are 12-bit grey-level values, from 0-4095.
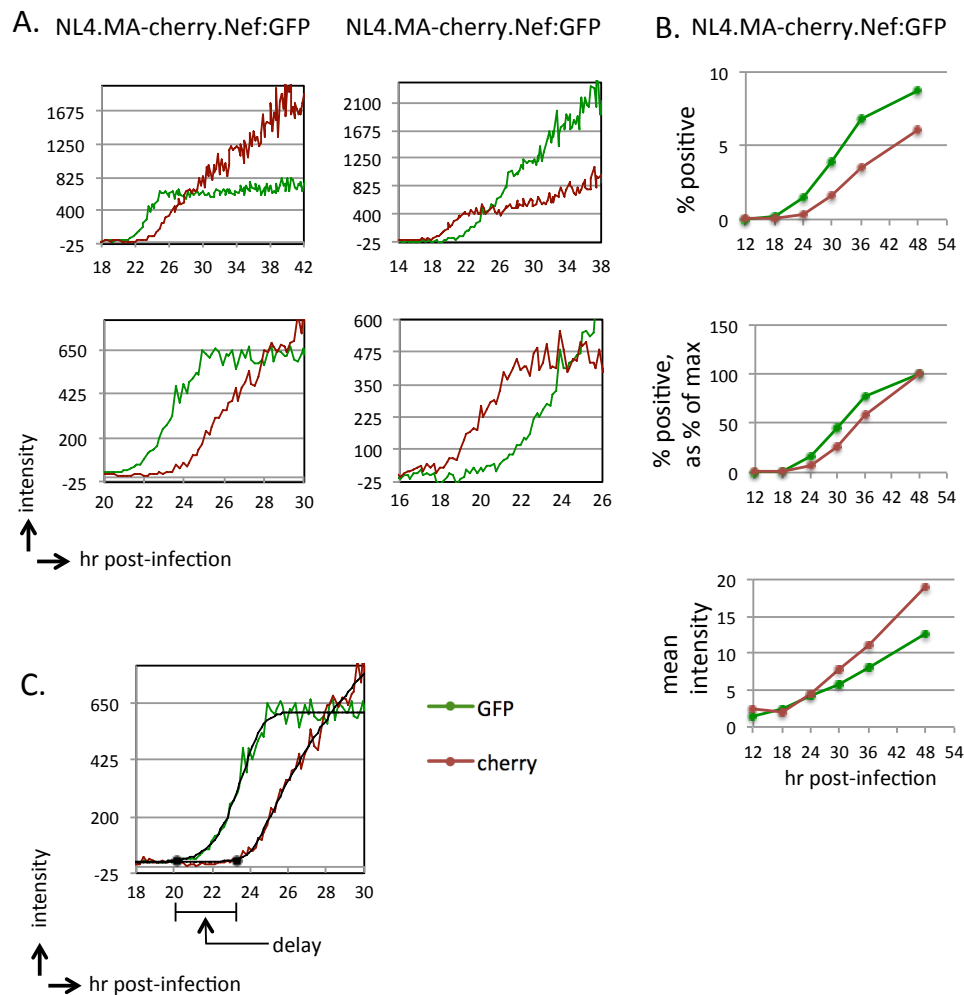
Fig. 3.5. Dual reporter viruses NL4.MA-cherry.Nef:GFP and NL4.MA-GFP.Nef:cherry were used to infect MT-4 cells. After washing, cultures were split into separate dishes. **A.** Samples for microscopy were adhered to glass bottom plates and single-cell quantitation was performed after time-lapse acquisition. The top panels show intensity traces in red and green channels from individual cells. The middle panels show the same traces as the top, scaled so as to make the initial intensity range more visible. The bottom panel is a diagram of the measurement method, as described in the text. Intensity units are 12-bit grey-level values, from 0-4095. **B.** Samples from an infection by NL4.MA-cherry.Nef:GFP were collected at time points and analyzed by flow cytometry. The top chart shows the change in the percentage of positive cells over time. The middle chart is the same data represented as percent of maximum to clarify the difference in expression timing. The bottom chart shows the mean fluorescence intensity of the samples over time.
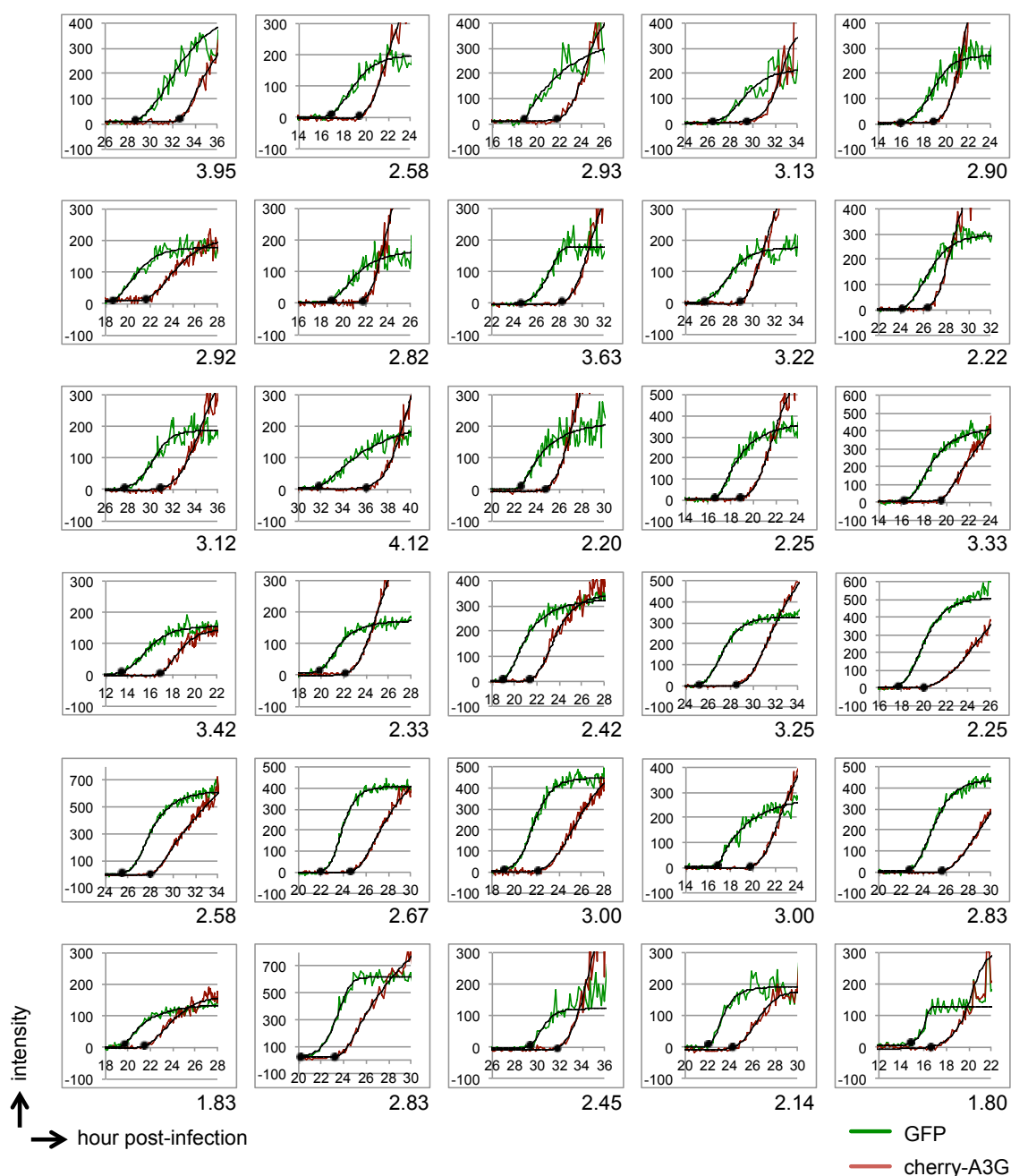
Fig. 3.6. NL4.MA-cherry.Nef:GFP infections used for quantitation in Fig. 3.8. The black lines are 5-parameter logistic curves fit to the data. The black dots represent the first points at which the fit curve rises seven intensity units above the background level corresponding to its lower bound. Intensity units are 12-bit grey-level values, from 0-4095.

Fig. 3.7. NL4.MA-GFP.Nef:cherry infections used for quantitation in Fig. 8. The black lines are 5-parameter logistic curves fit to the data. The black dots represent the first points at which the fit curve rises seven intensity units above the background level corresponding to its lower bound. Intensity units are 12-bit grey-level values, from 0-4095.
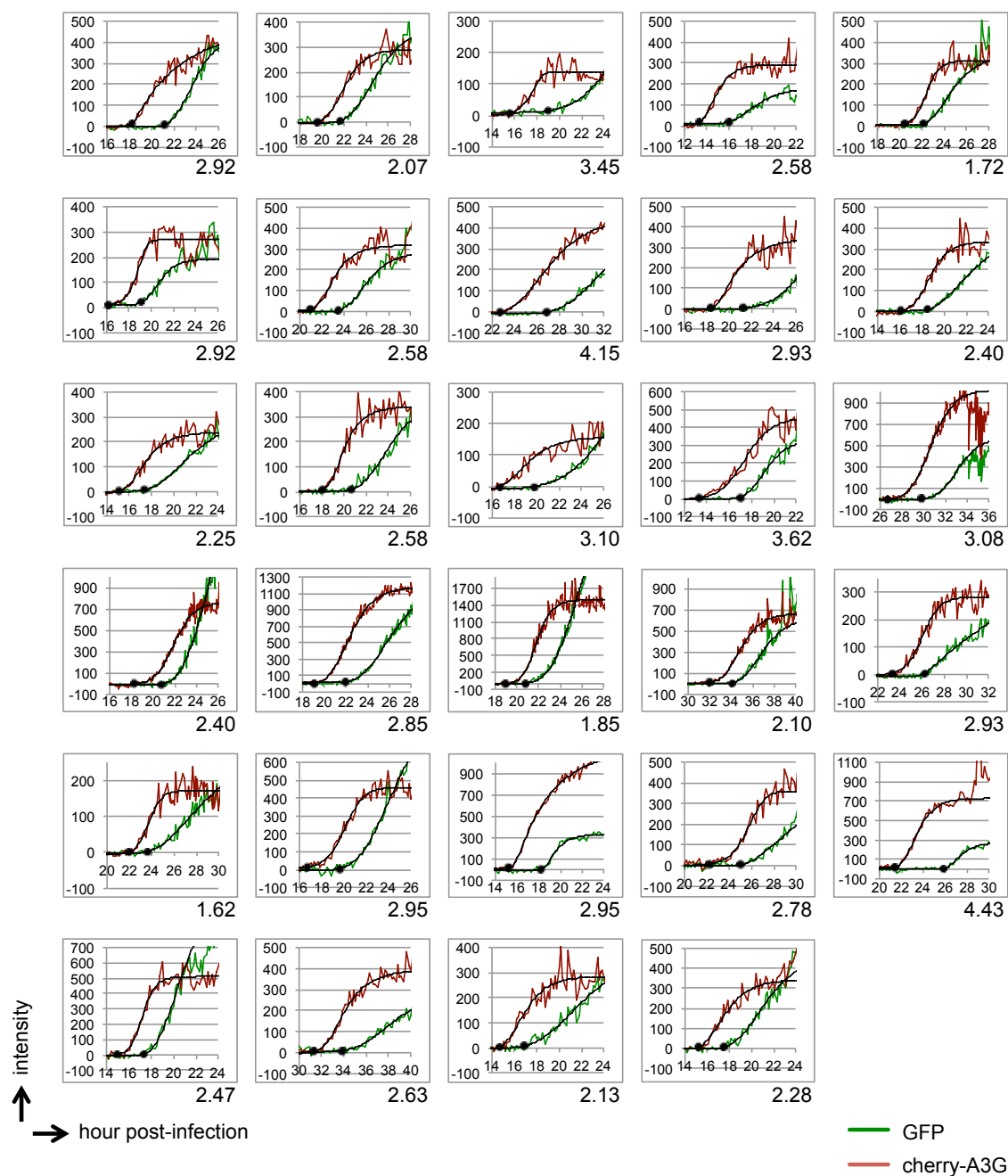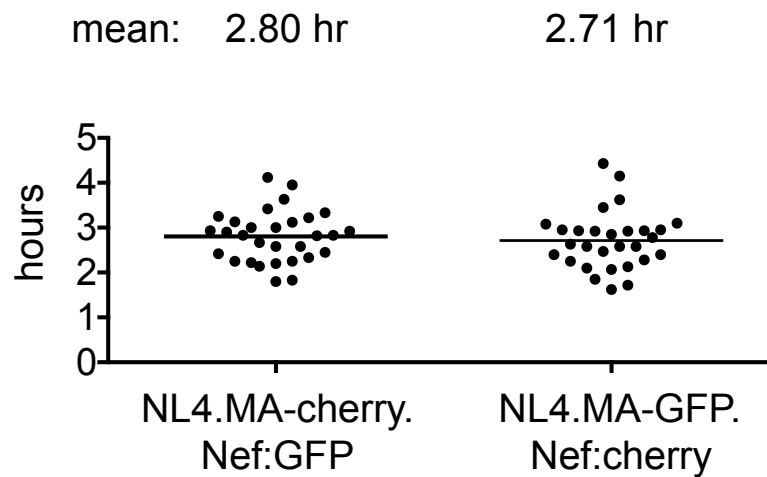
mean: 2.80 hr   2.71 hr

 Fig. 3.8. MT-4 cells were infected with dual-reporter viruses with fluorophores in swapped positions (NL4.MA-cherry.Nef:GFP and NL4.MA-GFP.Nef:cherry) and imaged by time-lapse live-cell microscopy. Quantitation of the time between initial detectability of early and late reporters, showing the delay between early and late gene expression for each cell, and the mean for each virus. The mean delay for NL4.MA-cherry.Nef:GFP is 2.80 (+/- 0.57; n=30). The mean delay for NL4.MA-GFP.Nef:cherry is 2.71 (+/- 0.65; n=29). The overall mean, combining the data from both viruses, is 2.76 hr (+/- 0.61). The raw intensity data for each of these cells is shown in Figs. 3.6 and 3.7.

A 2.8 hr delay for late-gene expression is somewhat less than might be expected

from early work using northern blot analysis to follow the appearance of

transcripts[31]. That study found that early-gene transcripts had reached significant

concentrations by 16 hr, and had reached close to their maximum levels by 24h

post-infection, whereas late-gene transcripts were barely detectable at 24h.

However, this is not incompatible with our data, given that our measurements are of

protein expression. This same study also showed much higher levels of late gene transcripts relative to early gene transcripts, and indicates that the much greater intensity we see for late gene expression is likely to reflect transcription rather than solely translation or protein stability.

The values we obtained from single-cell microscopy also match well with the data we generated by flow cytometry. The average delay between early and late gene expression calculated from our flow cytometry experiments is 3.3 hr (+/- 0.6 h) (See Fig. 3.9). This correspondence is reassuring, given the averaging effects of following the bulk population. Because there is wide variation in the time that each cell begins to express viral genes, the flow cytometry data include a great deal of asynchrony that is not visible when following a single cell expressing both early and late gene markers. This asynchrony, however, means that the single-cell quantitation approach is most useful for quantifying the relationship between two reporters in the same cell; it is not as useful for identifying the overall lag time between infection and gene expression. After infection of a cell, each successful virion has to navigate uncoating, transport, reverse transcription, nuclear entry, integration, Tat transactivation of transcription, Rev-dependent nuclear export of mRNAs, and cytoplasmic translation. Only then will the reporter fluorophores encoded by those mRNAs become visible, and over the course of all these steps the progress of infection in a cell culture becomes widely spread out over time. Despite the initial synchronization of infection, this asynchrony is such that individual cells first begin

to show reporter gene expression over a range of many hours. The first fluorescent cells are detected at about 12 hours post-infection, but some cells do not become fluorescent until as late as 40 hours post-infection. For quantifying the delay between infection and gene expression, the numerical power of flow cytometry is superior to single-cell techniques.

Our flow cytometry time course data indicates that the earliest point of detectable early gene expression is 12 hr. post-infection. It does not begin in a substantial percentage of cells until 24 hr. post- infection, and only by 30 hr. post-infection do half of the infected cells in a culture show detectable early gene expression. However, late-gene expression, though also showing a broad range of initiation times, follows closely behind early gene expression. In Fig 3.9 an experiment is shown in which cells were infected with a dual reporter virus at four different titers, and the fraction of red and green cells at each time point is expressed as a percentage of maximum. This experiment is described in more detail below. The delay between early and late gene expression was determined by calculating the average time difference between the points at which both reporters reached half of their maximal value. The average delay between early and late gene expression calculated in this manner is 3.3 hr. (+/- 0.6 h). Taken together with the microscopy data and calculations, this provides strong evidence that the actual average delay between early and late gene expression, at least at the level of protein production, is very close to 3 hr.

The early stages of the viral life cycle.

In order to define the temporal relationship between HIV-1 gene expression and the preceeding phases of the viral lifecycle we performed time course experiments to determine when reverse transcription and integration occur. These experiments employed a single-reporter virus, carrying GFP in the early-gene Nef position (See Fig. 3.2). After synchronized infection, inhibitors of reverse transcription or integration were added to cells at time points, and the cells were collected at 48 hr post-infection for flow cytometry. As the infection proceeds, an increasing number of infectious particles have passed the stage that is inhibited by the drug and are no longer sensitive to it.

Fig. 3.9A shows the kinetics of reverse transcription and integration. The chart in Fig. 3.9B shows the data from a single experiment with MT-4 cells, using three identical cultures. One was infected with single-reporter virus, and reverse transcriptase inhibitor was added at defined time points; one was infected with the same virus and integrase inhibitor was added at time points; and the third was infected with a dual-reporter virus and samples were collected and fixed at time points. The samples to which inhibitors were added were collected and fixed at 48 hours. Each arm of the experiment was performed at 4 different MOIs. All 12 parallel time courses are shown here, each expressed as a percentage of its maximum value. A Matlab script was used to fit 5-parameter sigmoid functions to

each of these 4 data sets and calculate the times at which each curve reached 50% of its maximum value. We found that 50% of incoming virions have completed reverse transcription at about 14.4 hr (+/- 0.4 hr) post-infection in MT-4 cells. This is in agreement with other work[54], though some studies find that reverse transcription is completed earlier in other cell types[55,56]. These parameters may be strongly cell-type dependent; because of low intracellular dNTP concentrations reverse transcription can take several days to complete in macrophages[55,57]. We find that 50% of incoming virions have completed integration at 19.3 hr (+/- 1.1 hr), a delay of about 5 hr after reverse transcription. This is consistent with another recent study that found a 4.6 hour delay between these stages[58]. The delay between early and late gene expression was determined by calculating the time difference between these half-maximal points. Using this approach we determined that there is an average delay of 10.8 hours (+/- 1.2 h) between integration and detection of early-gene expression.

During the period between integration and protein production there are chromatin modifications that need to take place; the initial, basal, Tat-independent transcription from the LTR is inefficient; viral mRNA needs to be exported from the nucleus; and translation has to take place. Our data shows that, in all, these processes appear take close to 11 hr on average. The Vpr protein of HIV-1 arrests the cell cycle at G2[59], and this appears to enhance transcription[60,61]. If transcription was delayed until the infected cell reaches G2, this would lead to a delay in an

infected culture. However, it would be a variable delay and would increase the asynchrony that we observe in each of the events of the life-cycle after after reverse transcription. As mentioned earlier, we do not see this; therefore any events causing this delay are likely to take place in a mostly stereotyped time frame.

Although several studies have provided estimates for the timing of HIV-1 reverse transcription or integration[54,57,58], the kinetics of these stages of the viral life cycle have never been been measured together and related to the timing of the phases of gene expression. The relative timing of early and late gene expression, aside from early studies of transcription[31], has never been determined. The work presented here provides the first thorough characterization of these parameters of HIV-1 replication, and will prove useful both as a context for understanding viral replication mechanisms and constraints, and as necessary information for the design of any experiments related to the timing of retroviral replication. We acknowledge that the estimates for the midpoints of the reverse transcription and integration processes (14.4 and 19.3 hrs post-infection) are contingent on several factors. As mentioned above, the timing of reverse-transcription varies widely between cell-types. In addition, all of these parameters can be strongly affected by the activation status of cells in general. It is also worth noting that the experiments performed here use viral stocks pseudotyped with a non-retroviral envelope (VSV-G) that leads to an endocytic route of entry that may proceed with different kinetics than normal plasma membrane fusion does. However, the delay calculated here

between reverse transcription and integration - 4.9 hr - is likely to be broadly accurate, as it is in very close agreement with data generated by antiretroviral treatment-interruption experiments in patients[58]. It is also in close agreement with a study in PM1 cells using the same type of drug-addition time course experiment as we utilized[54]. This study found that reverse transcription is complete in half the infected cells in a culture at about ten hours, and integration at about 16 hours. Importantly, this same study used a native HIV-1 envelope, ADA, for these infections, indicating that our use of the VSV-G envelope did not have very large effects on the overall timing of the life cycle stages.

There is no work that we are aware of that has quantified the delay between early and late gene expression at the protein production level. Our microscopy data show that late gene proteins appear between 1.6 and 4.4 hr after early gene proteins, with an average of 2.8 hr. Our flow cytometry data indicates an average delay of 3.3 hr, and, taken together with the microscopy data, we are confident that an average value of three hours is accurate. The process of Rev-induced export of unspliced viral proteins is well understood mechanistically. The data here provides an important temporal context for these processes, as well as a first step toward understanding the kinetics of the downstream viral stages and the assembly process itself. It is also the first report of the relative abundance of protein production from the viral Nef and Gag gene positions.
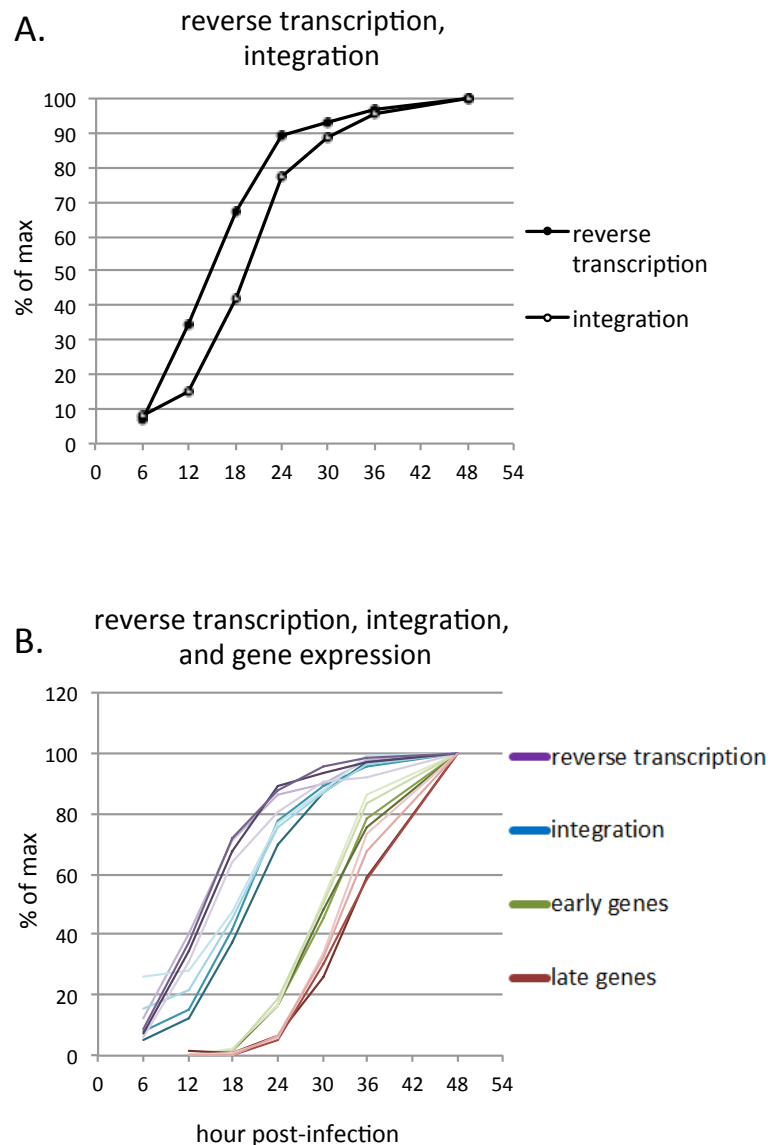
Fig.3.9. A. MT-4 cells were infected with a reporter virus carrying GFP in place of Nef. At regular time points inhibitors of reverse transcription (Efavirenz) or integration (Elvitegravir) were added. The cells were fixed at 48h post-infection and analyzed by flow cytometry. A representative experiment is shown, with the percentage of infection events that are resistant to drug inhibition following application of drug at the times indicated on the X-axis. **B.** The drug inhibition time course experiment in A. was performed in parallel with infections with the dual reporter NL4.MA-cherry.Nef:GFP at four different multiplicities of infection (MOIs) (0.1, 0.2, 0.4, and 0.8). Samples from the dual-reporter infections were collected at time points and analyzed by flow cytometry. Samples from the drug-inhibition time courses were collected and analyzed at hour 48. All four MOIs for each time course were expressed as a percentage of maximum on the same chart, to illustrate the relationship between the timing of reverse transcription, integration and early- and late-gene expression, as well as the fact that these events take place with kinetics that are relatively insensitive to MOI. Each arm of the experiment is illustrated with a single color in 4 different shadings representing the different MOIs. MOI 0.1 is represented by the darkest shading, MOI 0.2 by the next second darkest, and so on.

References, Chapter 3

1.   Nabel, G. & Baltimore, D. An inducible transcription factor activates expression of human immunodeficiency virus in T cells. *Nature* **326**, 711–713 (1987).

2.   Arya, S. K., Guo, C., Josephs, S. F. & Wong-Staal, F. Trans-activator gene of human T-lymphotropic virus type III (HTLV-III). *Science* **229**, 69–73 (1985).

3.   Muesing, M. A., Smith, D. H. & Capon, D. J. Regulation of mRNA accumulation by a human immunodeficiency virus trans-activator protein. *Cell* **48**, 691–701 (1987).

4.   Bieniasz, P. D., Grdina, T. A., Bogerd, H. P. & Cullen, B. R. Recruitment of a protein complex containing Tat and cyclin T1 to TAR governs the species specificity of HIV-1 Tat. *EMBO J.* **17**, 7056–7065 (1998).

5.   Fujinaga, K. *et al.* The ability of positive transcription elongation factor B to transactivate human immunodeficiency virus transcription depends on a functional kinase domain, cyclin T1, and Tat. *J. Virol.* **72**, 7154–7159 (1998).

6.   Wei, P., Garber, M. E., Fang, S. M., Fischer, W. H. & Jones, K. A. A novel CDK9-associated C-type cyclin interacts directly with HIV-1 Tat and mediates its high-affinity, loop-specific binding to TAR RNA. *Cell* **92**, 451–462 (1998).

7.   Garber, M. E., Wei, P. & Jones, K. A. HIV-1 Tat interacts with cyclin T1 to direct the P-TEFb CTD kinase complex to TAR RNA. *Cold Spring Harbor Symposia on Quantitative Biology* **63**, 371–380 (1998).

8.   Bieniasz, P. D., Grdina, T. A., Bogerd, H. P. & Cullen, B. R. Recruitment of cyclin T1/P-TEFb to an HIV type 1 long terminal repeat promoter proximal RNA target is both necessary and sufficient for full activation of transcription. *Proc. Natl. Acad. Sci. U.S.A.* **96**, 7791–7796 (1999).

9.   Rosen, C. A., Sodroski, J. G. & Haseltine, W. A. The location of cis-acting regulatory sequences in the human T cell lymphotropic virus type III (HTLV-III/LAV) long terminal repeat. *Cell* **41**, 813–823 (1985).

10.   Feng, S. & Holland, E. C. HIV-1 tat trans-activation requires the loop sequence

within tar. *Nature* **334**, 165–167 (1988).

11. Feinberg, M. B., Baltimore, D. & Frankel, A. D. The role of Tat in the human immunodeficiency virus life cycle indicates a primary effect on transcriptional elongation. *Proc. Natl. Acad. Sci. U.S.A.* **88**, 4045–4049 (1991).

12. Cullen, B. R. Regulation of HIV-1 gene expression. *FASEB J.* **5**, 2361–2368 (1991).

13. Selby, M. J., Bain, E. S., Luciw, P. A. & Peterlin, B. M. Structure, sequence, and position of the stem-loop in tar determine transcriptional elongation by tat through the HIV-1 long terminal repeat. *Genes Dev.* **3**, 547–558 (1989).

14. Dingwall, C. *et al.* HIV-1 tat protein stimulates transcription by binding to a U-rich bulge in the stem of the TAR RNA structure. *EMBO J.* **9**, 4145–4153 (1990).

15. Southgate, C., Zapp, M. L. & Green, M. R. Activation of transcription by HIV-1 Tat protein tethered to nascent RNA through another protein. *Nature* **345**, 640–642 (1990).

16. Berkhout, B., Silverman, R. H. & Jeang, K. T. Tat trans-activates the human immunodeficiency virus through a nascent RNA target. *Cell* **59**, 273–282 (1989).

17. Kao, S. Y., Calman, A. F., Luciw, P. A. & Peterlin, B. M. Anti-termination of transcription within the long terminal repeat of HIV-1 by tat gene product. *Nature* **330**, 489–493 (1987).

18. Bengal, E. & Aloni, Y. Transcriptional elongation by purified RNA polymerase II is blocked at the trans-activation-responsive region of human immunodeficiency virus type 1 in vitro. *J. Virol.* **65**, 4910–4918 (1991).

19. Ratnasabapathy, R., Sheldon, M., Johal, L. & Hernandez, N. The HIV-1 long terminal repeat contains an unusual element that induces the synthesis of short RNAs from various mRNA and snRNA promoters. *Genes Dev.* **4**, 2061–2074 (1990).

20. Zhou, Q., Chen, D., Pierstorff, E. & Luo, K. Transcription elongation factor P-TEFb mediates Tat activation of HIV-1 transcription at multiple stages. *EMBO J.* **17**, 3681–3691 (1998).

21. Transcription elongation factor P-TEFb is required for HIV-1 tat transactivation in vitro. **11**, 2622–2632 (1997).

22. Enhanced processivity of RNA polymerase II triggered by Tat-induced phosphorylation of its carboxy-terminal domain. **384**, 375–378 (1996).

23. Felber, B. K. & Pavlakis, G. N. A quantitative bioassay for HIV-1 based on trans-activation. *Science* **239**, 184–187 (1988).

24. Hauber, J. & Cullen, B. R. Mutational analysis of the trans-activation-responsive region of the human immunodeficiency virus type I long terminal repeat. *J. Virol.* **62**, 673–679 (1988).

25. Kato, H. *et al.* HIV-1 Tat acts as a processivity factor in vitro in conjunction with cellular elongation factors. *Genes Dev.* **6**, 655–666 (1992).

26. Purcell, D. F. & Martin, M. A. Alternative splicing of human immunodeficiency virus type 1 mRNA modulates viral protein expression, replication, and infectivity. *J. Virol.* **67**, 6365–6378 (1993).

27. Felber, B. K., Drysdale, C. M. & Pavlakis, G. N. Feedback regulation of human immunodeficiency virus type 1 expression by the Rev protein. *J. Virol.* **64**, 3734–3741 (1990).

28. Guatelli, J. C., Gingeras, T. R. & Richman, D. D. Alternative splice acceptor utilization during human immunodeficiency virus type 1 infection of cultured cells. *J. Virol.* **64**, 4093–4098 (1990).

29. Feinberg, M. B., Jarrett, R. F., Aldovini, A., Gallo, R. C. & Wong-Staal, F. HTLV-III expression and production involve complex regulation at the levels of splicing and translation of viral RNA. *Cell* **46**, 807–817 (1986).

30. Malim, M. H., Hauber, J., Fenrick, R. & Cullen, B. R. Immunodeficiency virus rev trans-activator modulates the expression of the viral regulatory genes. *Nature* **335**, 181–183 (1988).

31. Kim, S. Y., Byrn, R., Groopman, J. & Baltimore, D. Temporal aspects of DNA and RNA synthesis during human immunodeficiency virus infection: evidence for differential gene expression. *J. Virol.* **63**, 3708–3713 (1989).

32. Garrett, E. D., Tiley, L. S. & Cullen, B. R. Rev activates expression of the human immunodeficiency virus type 1 vif and vpr gene products. *J. Virol.* **65**, 1653–1657 (1991).

33. Schwartz, S., Felber, B. K. & Pavlakis, G. N. Expression of human immunodeficiency virus type 1 vif and vpr mRNAs is Rev-dependent and regulated by splicing. *Virology* **183**, 677–686 (1991).

34. Klotman, M. E. *et al.* Kinetics of expression of multiply spliced RNA in early human immunodeficiency virus type 1 infection of lymphocytes and monocytes. *Proc. Natl. Acad. Sci. U.S.A.* **88**, 5011–5015 (1991).

35. Rosen, C. A., Terwilliger, E., Dayton, A., Sodroski, J. G. & Haseltine, W. A. Intragenic cis-acting art gene-responsive sequences of the human immunodeficiency virus. *Proc. Natl. Acad. Sci. U.S.A.* **85**, 2071–2075 (1988).

36. Heaphy, S. *et al.* HIV-1 regulator of virion expression (Rev) protein binds to an RNA stem-loop structure located within the Rev response element region. *Cell* **60**, 685–693 (1990).

37. Malim, M. H., Hauber, J., Le, S. Y., Maizel, J. V. & Cullen, B. R. The HIV-1 rev trans-activator acts through a structured target sequence to activate nuclear export of unspliced viral mRNA. *Nature* **338**, 254–257 (1989).

38. Hadzopoulou-Cladaras, M. *et al.* The rev (trs/art) protein of human immunodeficiency virus type 1 affects viral mRNA and protein expression via a cis-acting sequence in the env region. *J. Virol.* **63**, 1265–1274 (1989).

39. Zapp, M. L. & Green, M. R. Sequence-specific RNA binding by the HIV-1 Rev protein. *Nature* **342**, 714–716 (1989).

40. Dayton, A. I. *et al.* Cis-acting sequences responsive to the rev gene product of the human immunodeficiency virus. *J. Acquir. Immune Defic. Syndr.* **1**, 441–452 (1988).

41. Meyer, B. E. & Malim, M. H. The HIV-1 Rev trans-activator shuttles between the nucleus and the cytoplasm. *Genes Dev.* **8**, 1538–1547 (1994).

42. Love, D. C., Sweitzer, T. D. & Hanover, J. A. Reconstitution of HIV-1 rev nuclear export: independent requirements for nuclear import and export. *Proc. Natl. Acad. Sci. U.S.A.* **95**, 10608–10613 (1998).

43. Kubota, S. *et al.* Functional similarity of HIV-I rev and HTLV-I rex proteins: identification of a new nucleolar-targeting signal in rev protein. *Biochem. Biophys. Res. Commun.* **162**, 963–970 (1989).

44. Bogerd, H. P., Echarri, A., Ross, T. M. & Cullen, B. R. Inhibition of human immunodeficiency virus Rev and human T-cell leukemia virus Rex function, but not Mason-Pfizer monkey virus constitutive transport element activity, by a mutant human nucleoporin targeted to Crm1. *J. Virol.* **72**, 8627–8635 (1998).

45. Fukuda, M. *et al.* CRM1 is responsible for intracellular transport mediated by

the nuclear export signal. *Nature* **390**, 308–311 (1997).

46. Neville, M., Stutz, F., Lee, L., Davis, L. I. & Rosbash, M. The importin-beta family member Crm1p bridges the interaction between Rev and the nuclear pore complex during nuclear export. *Curr. Biol.* **7**, 767–775 (1997).

47. Schwartz, S., Felber, B. K., Benko, D. M., Fenyo, E. M. & Pavlakis, G. N. Cloning and functional analysis of multiply spliced mRNA species of human immunodeficiency virus type 1. *J. Virol.* **64**, 2519–2529 (1990).

48. Sodroski, J. *et al.* A second post-transcriptional trans-activator gene required for HTLV-III replication. *Nature* **321**, 412–417 (1986).

49. Vassilaki, N. & Mavromara, P. Two alternative translation mechanisms are responsible for the expression of the HCV ARFP/F/core+1 coding open reading frame. *J. Biol. Chem.* **278**, 40503–40513 (2003).

50. Mattion, N. M., Mitchell, D. B., Both, G. W. & Estes, M. K. Expression of rotavirus proteins encoded by alternative open reading frames of genome segment 11. *Virology* **181**, 295–304 (1991).

51. Becerra, S. P., Koczot, F., Fabisch, P. & Rose, J. A. Synthesis of adeno-associated virus structural proteins requires both alternative mRNA splicing and alternative initiations from a single transcript. *J. Virol.* **62**, 2745–2754 (1988).

52. Müller, B. *et al.* Construction and characterization of a fluorescently labeled infectious human immunodeficiency virus type 1 derivative. *J. Virol.* **78**, 10803–10813 (2004).

53. Forestell, S. P., Dando, J. S., Böhnlein, E. & Rigg, R. J. Improved detection of replication-competent retrovirus. *J. Virol. Methods* **60**, 171–178 (1996).

54. Donahue, D. A. *et al.* Stage-dependent inhibition of HIV-1 replication by antiretroviral drugs in cell culture. *Antimicrob. Agents Chemother.* **54**, 1047–1054 (2010).

55. Collin, M. & Gordon, S. The kinetics of human immunodeficiency virus reverse transcription are slower in primary human macrophages than in a lymphoid cell line. *Virology* **200**, 114–120 (1994).

56. Perez-Caballero, D., Hatziioannou, T., Zhang, F., Cowan, S. & Bieniasz, P. D. Restriction of human immunodeficiency virus type 1 by TRIM-CypA occurs with rapid kinetics and independently of cytoplasmic bodies, ubiquitin, and proteasome activity. *J. Virol.* **79**, 15567–15572 (2005).

57. O'Brien, W. A. *et al.* Kinetics of human immunodeficiency virus type 1 reverse transcription in blood mononuclear phagocytes are slowed by limitations of nucleotide precursors. *J. Virol.* **68**, 1258–1263 (1994).

58. Murray, J. M., Kelleher, A. D. & Cooper, D. A. Timing of the components of the HIV life cycle in productively infected CD4+ T cells in a population of HIV-infected individuals. *J. Virol.* **85**, 10798–10805 (2011).

59. Jowett, J. B. *et al.* The human immunodeficiency virus type 1 vpr gene arrests infected T cells in the G2 + M phase of the cell cycle. *J. Virol.* **69**, 6304–6313 (1995).

60. Felzien, L. K. *et al.* HIV transcriptional activation by the accessory protein, VPR, is mediated by the p300 co-activator. *Proc. Natl. Acad. Sci. U.S.A.* **95**, 5281–5286 (1998).

61. Subbramanian, R. A. *et al.* Human immunodeficiency virus type 1 Vpr is a positive regulator of viral transcription and infectivity in primary human macrophages. *J. Exp. Med.* **187**, 1103–1111 (1998).

Chapter 4. Restriction factor counteraction

Antagonistic co-evolution

Retroviruses, like all viruses, are obligate parasites. They require the machinery of cells to reproduce themselves, and over the vast periods of time during which they have co-evolved with mammals they have developed and honed the numerous molecular interactions that allow them to interface with cellular components and pathways and redirect them in ways beneficial to themselves[1-6]. Mammals do not generally benefit from these interactions (the occasional re-purposing of ancient retroviral genes nothwithstanding[7,8]) and have been under selection pressure to avoid them. Human genes that code for proteins with host-virus interfaces show strong signals of positive selection[9]. Where these interactions are adaptive for the virus, they are maladaptive for the host, and the selection pressure on the host is toward residues that abrogate the interaction. This is not easily accomplished. Viruses are capable of much more rapid evolution than mammals, and the strongest signals of positive selection in the mammalian genome are usually found in regions involved in immunity or in proteins that interact directly with pathogens[9]. In addition, viral proteins have frequently evolved to bind to sites on cellular proteins that are identical to, or overlap with, the sites used for endogenous cellular interactions[10,11]. Thus, host cells are under selection pressure to adapt their proteins

in ways that minimize interactions with much faster-evolving viral proteins while at the same time preserving the endogenous interactions at the same sites that the virus uses.

Mammalian evolution has not confined itself to this type of passive evasion (ie, directional selection away from host-virus interactions) and has developed a number of active restriction factors that counteract infection by viruses[12-17]. These molecules also have long histories of genetic co-evolution with their viral targets, and they too show strong signals of positive selection[9,18-20]. They are often targeted to highly conserved[21-23] or non-protein viral components[16,24,25], or act in ways that do not require a specific molecular interaction with the virus[26-28]. This approach can be seen as successful in the sense that it is often a very strong determinant of host-range. For instance, restriction factors targeting primate retroviruses excel at blocking infection by the majority of primate retroviruses. But they are typically not successful against those viruses that are specifically adapted to the species expressing them. Human TRIM5α and Tetherin are proteins that serve to potently restrict a number of non-human retroviruses; however they are largely inactive against HIV-1, which is now highly adapted to its human hosts[13,14,29,30].

This adaptation often takes the form of viral accessory proteins that function specifically to counteract host restriction factors. It has been an effective strategy for viruses to acquire accessory proteins to target the restriction factors that were

acquired by the host to target the virus. In this this way the virus generates a new protein-protein interface in the antagonistic co-evolution process. It is not straightforward for the virus to escape an interaction with a host restriction factor that targets a conserved region of the virus, or an RNA domain, or a non-viral lipid target. But when the virus uses a viral accessory protein to in turn target the host restriction factor, now the co-evolutionary interface involves a viral protein with a dedicated purpose. A viral factor of this type is now are free to adapt to selection pressure, allowing it to maintain its interaction with the restriction factor it needs to inhibit. The Red Queen hypothesis argues that antagonistic co-evolution between pathogen and host will be characterized by ongoing directional selection in both, and will not settle into a stable equilibrium[31,32]. Because this form of directional selection will never reach an optimum, because changes on one side will usually be responded to by changes on the other. Both host and pathogen will keep running in place without getting anywhere—that is, they will continue to adapt with respect to each other, but because they are both doing so the interaction itself will supposedly remain largely stable.

This metaphor is useful in that it distinguishes this kind of directional selection from the kind that typically takes place in a species when, for instance, an environmental change leads to adaptation that moves toward a new optimum and then stabilizes. Antagonistic co-evolution is likely to lead to directional selection that never entirely ceases. But the Red Queen metaphor may be misleading insofar as it describes the

resulting molecular interactions as essentially stable, and the coevolutionary

process as one of constant or regular motion. The history of these types of molecular

interactions is beginning to be unearthed, revealing a much more complicated

picture. This picture appears to be marked less by stability than by sharp swings in

the rate of molecular adaptation, and many cases in which constraint and accident

play large roles.

In addition, the situation is inherently unequal because of the higher rate of

evolution of pathogens, especially retroviruses. Targeting viral processes indirectly

with restriction factors is one strategy against used by hosts to counter this fact. But

viral accessory proteins that target restriction factors can circumvent host targeting

of non-viral components. The notion of constant reciprocal change at co-

evolutionary interfaces does not fit easily with a scenario in which one side can

change at a rate many orders of magnitude faster than the other. The co-

evolutionary arms race is being run at vastly different timescales—and it favors the

pathogen, once they have committed to a specific host.

APOBEC3G

APOBEC3G (A3G) is a potent HIV-1 restriction factor that is packaged into virions in

producer cells and mediates destructive mutation of newly produced viral DNA in

target cells[25]. It is a member of a large family of vertebrate cytidine deaminases, and is capable of editing cytidines in ssDNA to uridines. When delivered to target cells in virions it associates with the RTC and edits nascent negative-stranded ssDNA produced by reverse transcriptase. This results in G➔A mutations in the proviral DNA at a level high enough to manifest as a drastic loss of infectivity.

APOBEC3G packaging into virions is dependent on interactions with the viral NC protein and RNA[33,34]. This mechanism is not entirely understood, but it is thought that initial RNA-A3G binding renders A3G competent for NC binding and packaging, presumably by forming a bridging interaction between them. Although it is probably the viral RNA genome that serves this role during infections, it is not specific or sequence-dependent. The use of this nonspecific interaction is likely to have made it quite difficult for HIV-1 to generate escape mutants. This notion is born out by the extremely broad range of targets that A3G is effective against: A3G restricts retroviruses from many species, and a range of endogenous retroelements as well.

However, wild-type HIV-1 is essentially unaffected by human A3G in cell culture (though this may not be the case in some patients[35]). This is the result of the expression of the viral accessory protein Vif, which recruits human A3G to a ubiquitin ligase complex, resulting in rapid and efficient proteasome-mediated degradation[36-40]. The Vif-A3G interaction is dependent in particular on a single amino acid in A3G, an aspartate at position 128. Several primate species that are

hosts to SIV strains carry a lysine at this position. Modifying the human A3G from

D128 to K128 blocks counteraction by HIV-1 Vif and allows degradation of A3G by

Vif from SIV strains that are otherwise restricted by human A3G[41-43]. In turn,

mutating the African green monkey or Rhesus macaque A3G to D128 renders them

sensitive to HIV-1 Vif. Thus, small changes in the interaction sites between

restriction factors and their viral targets or the viral genes that target *them*, can be

crucial determinants of the host-range and species-specifity of retroviruses. This

insight has been put to use in attempts to adapt HIV-1 to replicate in macaques,

where using SIV-derived Vif sequences has been an important step toward a

working animal model of HIV-1 infection[44,45].

The kinetics of APOBEC3G degradation

HIV-1 Vif is a Rev-dependent late gene, transcribed as part of the 4kb class of

transcripts that appear after the early regulatory genes, and together with the

structural genes that drive budding. Therefore Vif needs to effectively degrade A3G

before the point at which budding that packages A3G can take place. In order to

characterize the timing of these events, we constructed both MT-4 and HOS cell lines

stably expressing an N-terminal fusion of mCherry to APOBEC3G and infected them

with HIV-1 reporter viruses carrying GFP in either the early-gene Nef position or the

late-gene Gag position. These cells turn green as gene expression begins, and they

lose their red fluorescence as cherry-A3G is degraded by Vif. We characterized the kinetics of these infections using both flow cytometry of cells fixed at regular time points and single-cell quantitative time-lapse microscopy.

The flow cytometry data for cherry-A3G degradation in MT-4 cells is shown in Fig. 4.1; the corresponding data for HOS cells is shown in Fig. 4.2. GFP v mCherry scatterplots are shown for each time point, as well as histograms of the GFP-positive populations that illustrate more quantitatively the drop in cherry-A3G signal over time. Redistribution of cells to the GFP-high, mCherry-low gate is plotted in the charts to the right of the histograms. It can be seen from these charts that, for both cell types, the progress of GFP expression in infected cells (black circles) largely precedes cherry-A3G degradation (open circles) in the case of the early-gene reporter. In the case of the late gene reporter, the process of cherry-A3G degradation takes place much earlier with respect to GFP expression. In other words, early gene expression begins mostly before A3G is degraded, whereas late gene expression begins largely during or after A3G degradation.

In MT-4 cells (Fig. 4.1) infected with either early- or late-gene reporters, cells that have successfully down-regulated cherry-A3G begin to appear soon after GFP-positive cells do, and these GFP-positive, mCherry-negative cells predominate by hour 36 post-infection. In both cases a small population of double-positive cells remains at late time points. Because of the bulk nature of flow cytometry data it is

not possible to distinguish between the possibility that these cells are infected but failing to down-regulate cherry-A3G and the possibility that they represent late-starting infections in their initial hours of GFP expression. The infected population in scatterplots for the late-gene reporter show the characteristic spread of intensity typical of HIV-1 late-gene expression. The double-positive population shows this as well to some degree. However for the most part the double-positive cells show less GFP intensity than do the cells in GFP-positive, cherry-negative population, arguing that these are likely to be late-starting infections.

In HOS cells (Fig. 4.2), the pattern apparent in the scatterplots is somewhat different. The double-positive (infected but not down-regulated) population is large in the early-reporter infections, and essentially absent in the late-reporter infections. This may reflect both a greater delay between early and late gene expression in HOS cells and a greater level of infection asynchrony in the MT-4 cells. In both cell types it is clear that down-regulation begins soon after gene expression does, but the bulk nature of the data makes it quite difficult to calculate either the duration of the down-regulation process or the exact timing with respect to gene expression.
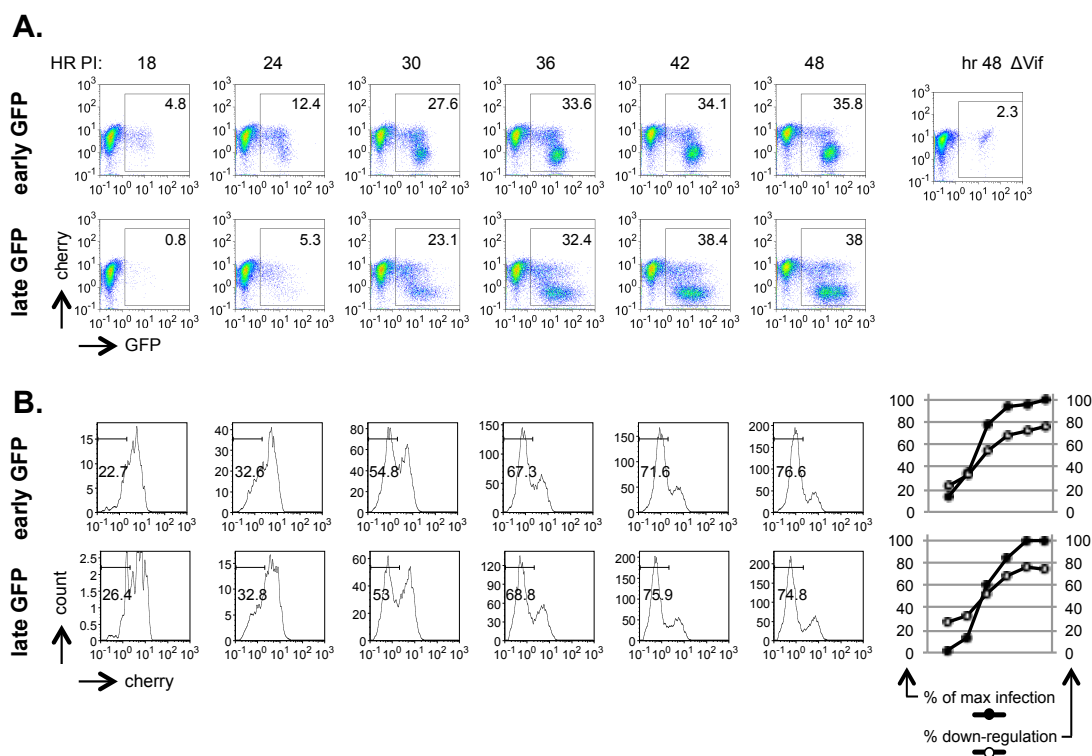
Fig. 4.1. APOBEC3G down-regulation in MT4 cells. MT-4 cells stably expressing an mCherry-A3G fusion were infected with an HIV-1 reporter virus construct carrying GFP in either early or late gene positions, collected and fixed at the indicated time points, and analyzed by flow cytometry. GFP v. mCherry scatterplots are shown in **A.** A sample infected with a ΔVif virus and collected at 48 hr post- infection is shown in the upper right. The histograms in **B.** are the GFP-positive populations gated in A., showing the progressive down-regulation of mCherry levels in infected cells. This is charted at the right of the row for each virus, with down-regulation plotted as the percentage shown in the cherry-low gates on the histograms, and the course of infection plotted as a percentage of maximum GFP expression.

Fig.4.2. APOBEC3G down-regulation in HOS cells. HOS cells stably expressing an mCherry-A3G fusion were infected with an HIV-1 reporter virus construct carrying GFP in either early or late gene positions, collected and fixed at the indicated time points, and analyzed by flow cytometry. GFP v. mCherry scatterplots are shown in **A.** A sample infected with a ΔVif virus and collected at 48 hr post- infection is shown in the upper right. The histograms in **B.** are the GFP-positive populations gated in A., showing the progressive down-regulation of mCherry levels in infected cells. This is charted at the right of the row for each virus, with down-regulation plotted as the percentage shown in the cherry-low gates on the histograms, and the course of infection plotted as a percentage of maximum GFP expression.
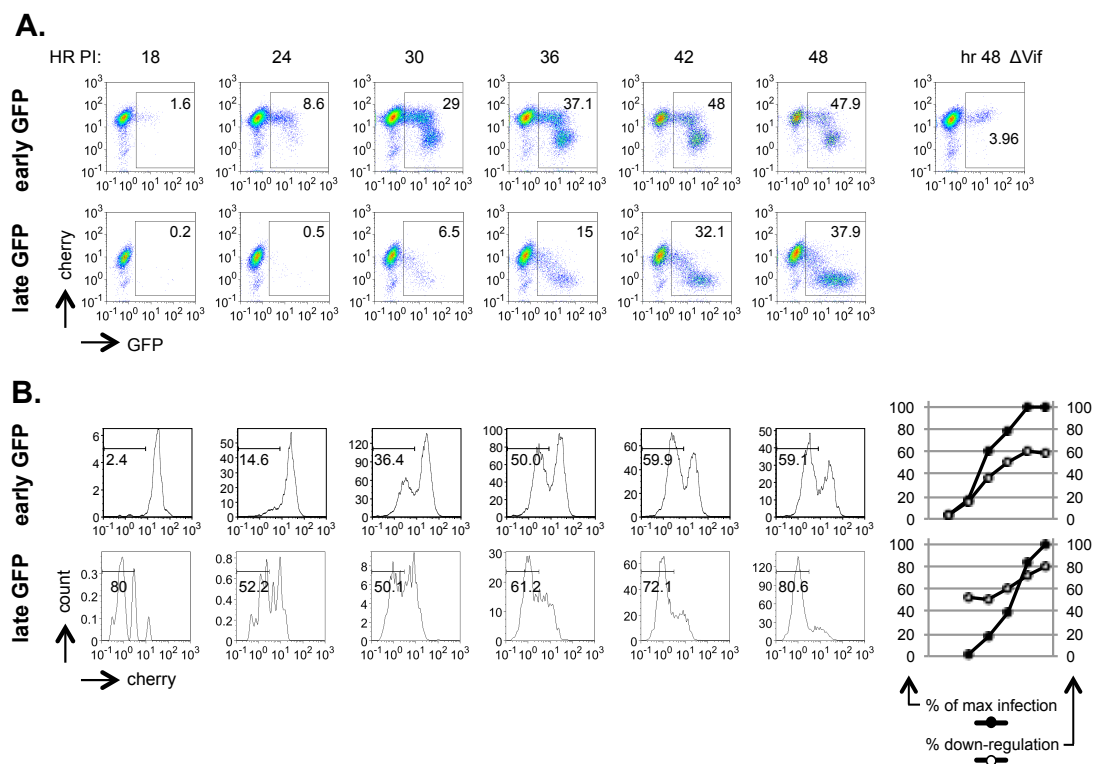
Single-cell microscopy has allowed us to determine the timing of these events with more precision. The high motility of HOS cells makes it impossible to use the technique with them, as cells need to remain both isolated and within the same field of view for up to 48 hours in order to be tracked and quantitated effectively. MT-4 cells proved amenable to an adherence technique (described in Materials and Methods) that allows them to be imaged in place over the entire course of infection. MT-4 cells are a T-cell line, and more likely to reflect the behavior of HIV-1 in its natural host cells. Using this approach we have been able to quantitate the kinetics of A3G down-regulation with some precision.

The microscopy approach also provides some evidence that the double-positive population seen in the flow cytometry scatterplots is unlikely to represent occasional failures of A3G down-regulation. In many hundreds of hours of time-lapse data, it was almost never possible to identify yellow double-positive cells by eye. All infected cells appeared to lose cherry expression as they gained GFP expression, with almost no detectable overlap. Quantitation of the intensity of these cells over time, in both channels, showed that there could in fact be periods of double-positive signal in early-gene reporter infections, but that these were extremely brief and apparent only in rare cells in which reporter gene expression was atypically early with respect to cherry-A3G down-regulation. All of these cells became GFP-positive and mCherry-negative within a period of several hours. In addition, the asynchrony of infection was such that it was frequently possible to

follow cells that did not show initial GFP expression until much later than others, in some cases as late as 40 hours post-infection. Although the possibility of failed A3G down-regulation in rare cells cannot be ruled out, the presence of delayed infections capable of brief periods of double-positive signal is likely to explain the presence of the double-positive population at late time points in the flow cytometry scatterplots.

We generated time course movies of cells infected with both early- and late-gene HIV-1 reporter viruses, and generated intensity traces over time for individual cells. Fig. 4.3A shows stills from a representative movie, and the cell in the images can be seen to lose its red signal at essentially the same time as it begins to turn green. Intensity traces for early, late, and ΔVif reporters are shown in Fig 4.3B. We used a Matlab script to fit 5-parameter logistic curves to the intensity data for each cell, to identify the points at which GFP expression rose above background levels and mCherry expression dropped to background levels, and to calculate the delay between these points for the GFP and mCherry curves for each cell. These turning points were defined as the lowest points on the curve at least 7 intensity units above the horizontal asymptote representing the threshold of fluorescence background noise.

A Vif $^+$ early GFP

B

Vif $^+$ early GFP

Vif $^+$ late GFP
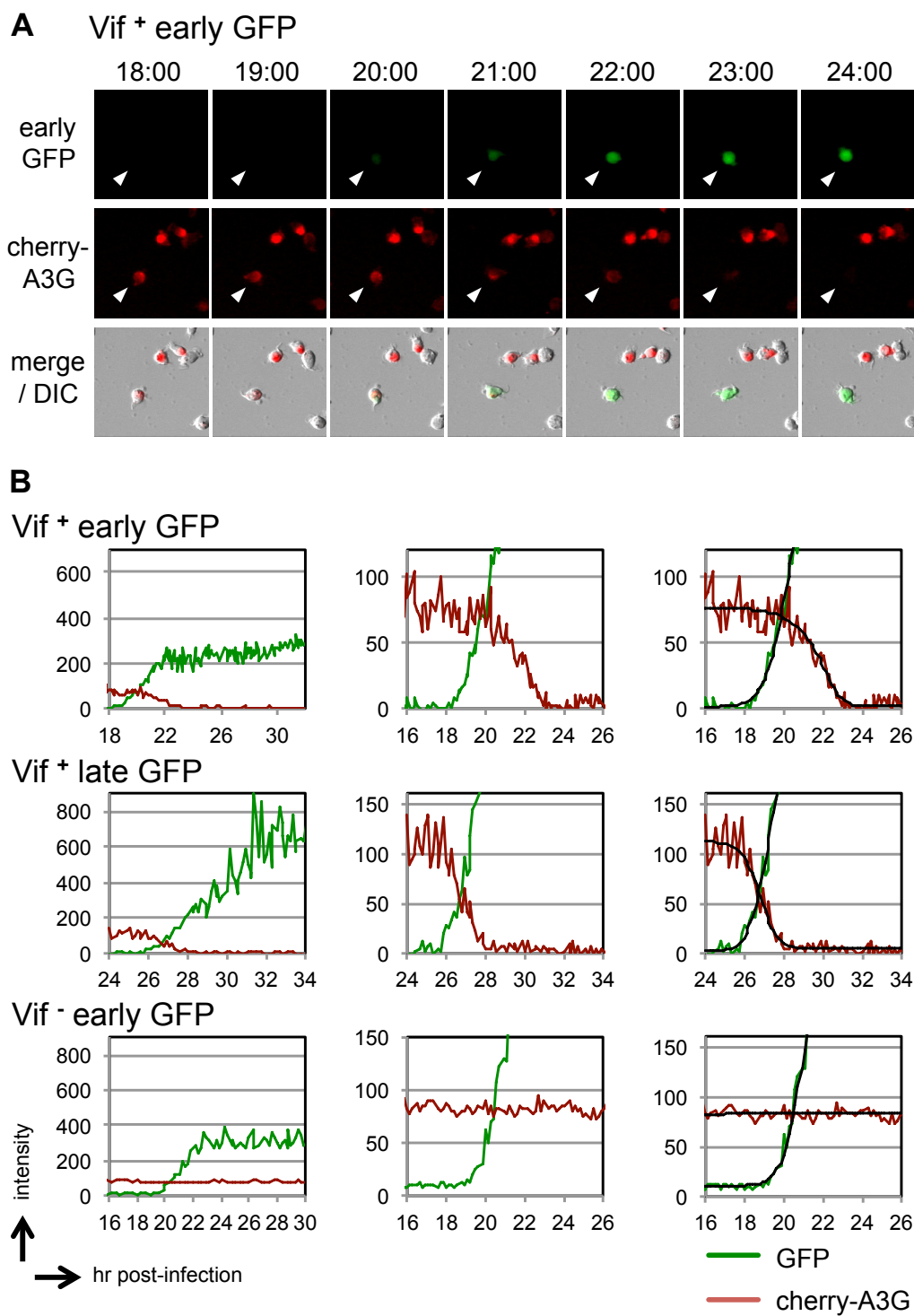
Vif $^-$ early GFP

Fig. 4.3. APOBEC3G down-regulation: single-cell microscopy. **A.** Stills from a time-lapse microscopy movie of MT-4 cells stably expressing an mCherry-A3G

fusion protein and infected with an HIV-1 reporter virus carrying GFP in the early gene Nef position. The infected cells were adhered to glass-bottom dishes after spinoculation, incubation, and washing, and imaged in an Olympus Vivaview microscope. The time post-infection is indicated above the images. (**B**) Quantitation of GFP and mCherry intensity from time-lapse movies. The top row of charts is intensity data from the cell indicated with the white arrowheads in A., and infected with an early-gene reporter virus. The middle row of charts is data from a cell infected with a late-gene reporter virus, and the bottom row of charts is data from a cell infected with an early-gene reporter virus lacking the Vif gene. The middle column shows close-ups of the data and the right column shows the 5-parameter logistic curve fit to the data. Intensity units are 12-bit grey-level values, from 0-4095.
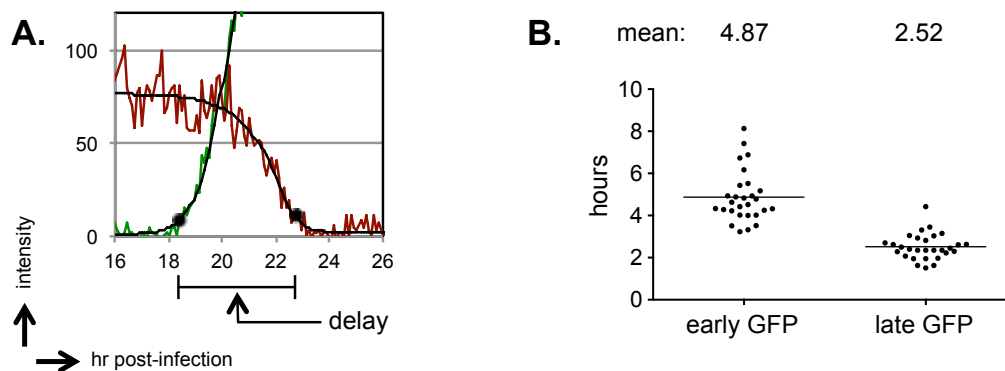
Fig. 4.4. Cherry-A3G degradation: microscopy quantitation. **A.** Intensity data from the cell shown in Fig. 4.3A, with the fit-curve overlaid. The black dots indicate the time points identified for the initiation or disappearance of fluorescence signal, defined as the first point at which the fit-curve rises or falls to 7 intensity units above its lower bound. The time difference between these points is the defined as the delay between detectable initiation of viral protein production and removal of detectable cherry-A3G. **B.** Cells infected with each reporter virus (carrying GFP in either early or late positions) were recorded and the delay between initiation of GFP expression and removal of cherry-A3G was calculated for each. For the early-reporter virus the mean delay is 4.87 hr (+/-1.22; n=28). For the late-reporter virus the mean delay is 2.52 hr (+/-0.61; n=29). The raw intensity data and best fit curves for each of these cells is shown in Figs. 4.5 and 4.6.

Fig. 4.4A shows an example of the intensity curves for a single cell, with the best fit

curve, the identified turning points, and the calculated delay period. Values for each

cell we quantitated, and means, are shown in Fig. 4.4B. The raw data for each cell

are shown in Fig.s 4.5 and 4.6. In this manner, we determined that the mean time

from the initiation of early gene expression to the completion of cherry-A3G down-

regulation was 4.9 hr. (+/- 1.2). The mean time from the initiation of late gene

expression to the completion of cherry-A3G down-regulation was 2.5 hr. (+/- 0.6).

The difference between these values, 2.4 hours, is broadly in agreement with the

value of 2.8 hr. calculated for the delay between early and late gene expression using

single-cell microscopy with dual-reporter viruses.

In the absence of Vif, cherry-A3G expression remained stable over the course of

infection. In the presence of Vif, the cherry signal was rapidly lost. Vif is produced

from Rev-dependent late-gene transcripts, and is therefore produced at roughly the

same time as the structural genes that drive HIV-1 assembly. For Vif to complete the

A3G degradation process in time for assembly to proceed, it therefore needs to

perform this job very rapidly. We find that it does so: the disappearance of cherry-

A3G signal is complete on average by 2.5 hr (Fig. 4.4B) after late-gene expression

becomes detectable. We estimate that the loss of cherry-A3G signal, from initiation

to completion, takes about 3 hours to complete, though we did not quantitate this

value as it was not possible to algorithmically identify the point at which cherry-A3G

signal begins to drop off. A lower bound for the speed of this process is the 4.9 hr

delay (Fig. 4.4B) between detectability of early gene expression and cherry-A3G

disappearance. An upper bound is the 2.5 hr delay between detectability of late gene

expression and cherry-A3G disappearance. Based on our visual estimate of the time course of cherry-A3G degradation in many cells, and the fact that Vif cannot be produced before Rev activity begins, we believe that 3 hours is an accurate average value for the length of the Vif-driven A3G degradation process in a given cell.

Earlier work has examined the timing of A3G degradation in the presence or absence of Vif in transfected cell lines. These studies have produced conflicting results. Several have used pulse-chase studies in cell lines to show that A3G is degraded by Vif in several hours[46-48], or even in minutes[36,38]. The use of fluorescence fusions has shown longer degradation times, even in the same studies[48]. The reasons for this are not clear, but A3G may be continuously produced in cells, and pulse-chase experiments will follow a recently produced burst of protein, whereas fluorescence experiments monitor the entire pool present in cells[48,49]. It has been suggested that recently produced A3G forms a functionally different pool than longer-lived A3G and may respond differently to Vif[49]. In any event, we believe that the approach we have taken bypasses many of the potential confounding factors in these studies. In our experiments, Vif is produced from a normally integrated post-infection provirus, in a T cell similar to to the natural target type of HIV-1. Presumably the transcription and translation kinetics will be more similar to those in patients. In addition, our analysis follows the total level of protein in single cells, and is thus not related to the average values produced in an entire culture. These results have bearing on the evolutionary relationship between

viruses and host restriction factors, and, in addition, may shed light on the processes which HIV-1 is required to perform in the hours just before the assembly process, if it is to generate a productive burst of new infectious virions.

Fig. 4.5. MT4.cherry-A3G cells infected with NL4.Nef:GFP early-gene reporter virus. Graphs show zoomed-in regions used for quantitation in Fig. 4.6. Numbers below panels indicate the calculated time in hours from initiation of GFP signal to disappearance of mCherry signal. Intensity units are 12-bit grey-level values, from 0-4095.
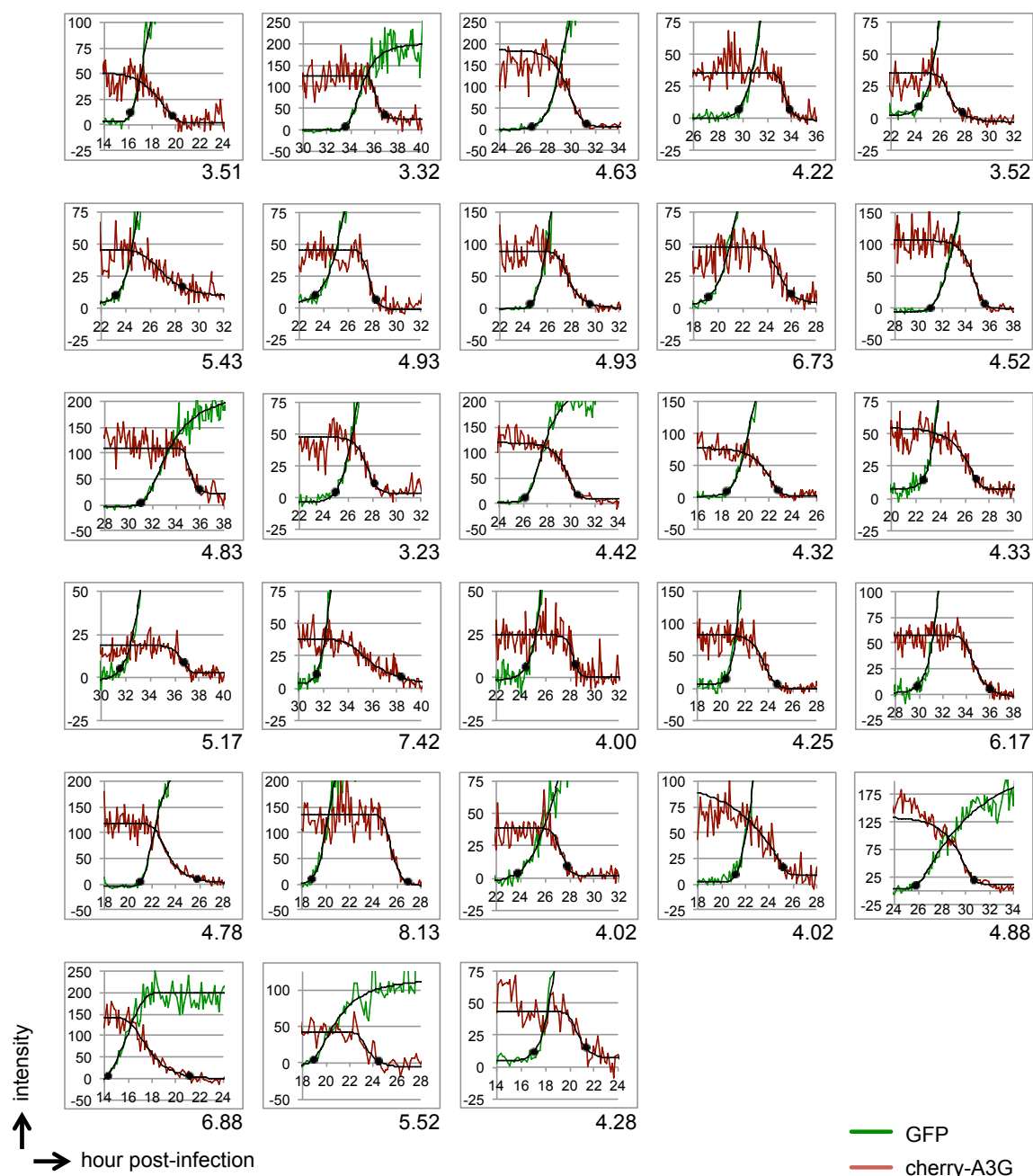
Fig. 4.6. MT4.cherry-A3G cells infected with NL4.MA-GFP late-gene reporter virus. Graphs show zoomed-in regions used for quantitation in Fig. 4.6. Numbers below panels indicate the calculated time in hours from initiation of GFP signal to disappearance of mCherry signal. Intensity units are 12-bit grey-level values, from 0-4095.
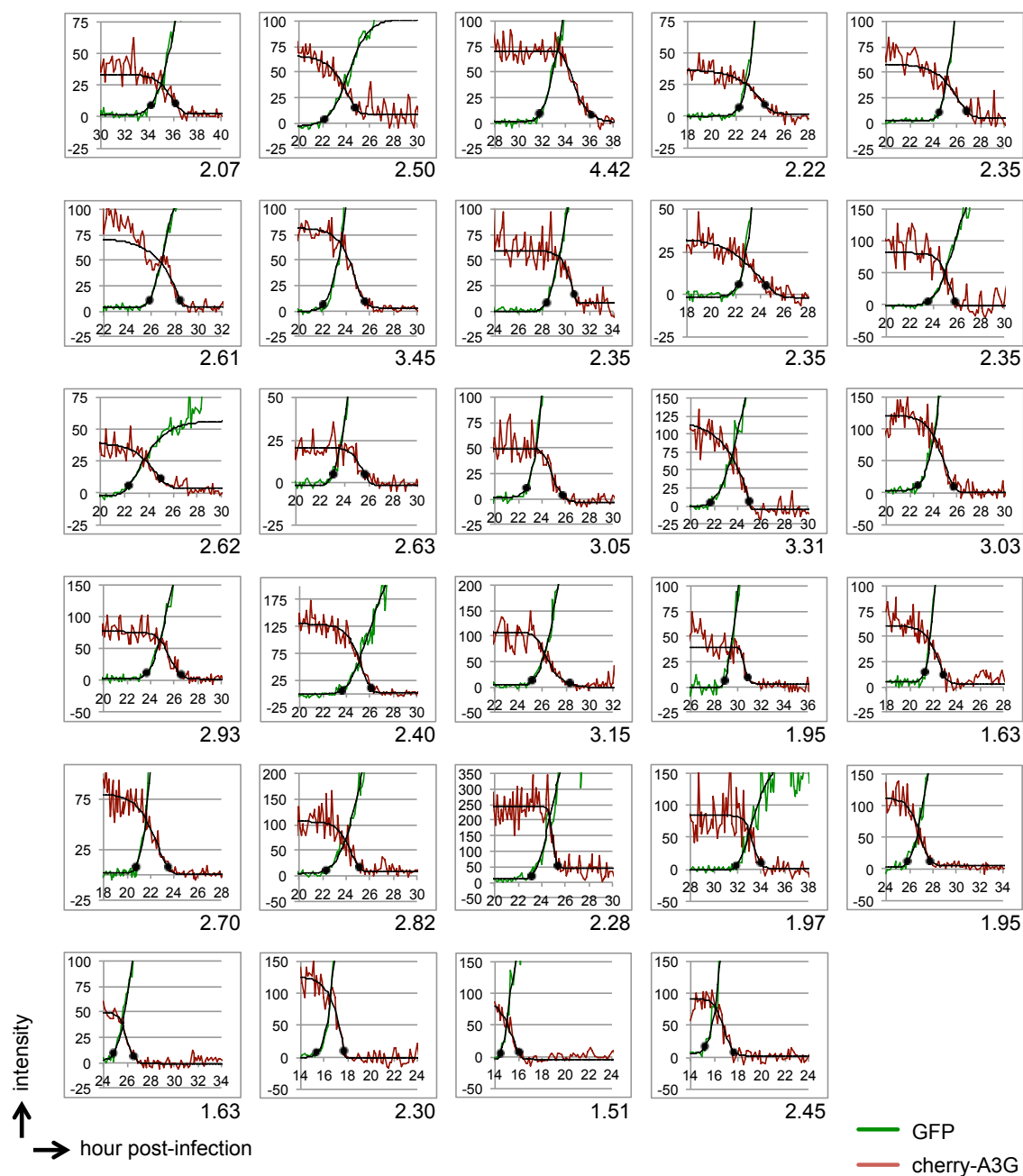
Tetherin

Tetherin is an interferon-induced mammalian antiviral restriction factor with an extraordinary co-evolutionary past and a uniquely non-specific mechanism of action. It forms an extracellular coiled-coil structure with membrane anchors at both ends capable of embedding themselves either in cellular membranes or the membranes of enveloped viruses[13,26,28]. In this way it functions as a physical tether linking budded virions to the cell that produced them and holding them in place until they can be internalized and degraded by the endolysosomal pathway[50,51]. This approach requires no direct interaction with viral proteins and therefore provides two large advantages to host cells: It provides no straightforward means for viruses to escape the interaction through adaptation, and it allows restriction of an extremely wide variety of viruses. In addition to retroviruses, tetherin has been shown to have activity against members of the herpesvirus, filovirus, arenavirus, paramyxovirus, and rhabdovirus families[52-58]. In order to replicate in cells expressing tetherin, many of these viruses have evolved methods of counteracting it. In the case of lentiviruses, research into the species-specificity of these countermeasures has provided a glimpse into the co-evolutionary past of these pathogens and their primate hosts.

Tetherin molecules consist of a cytoplasmic tail, a single transmembrane domain, an extended alpha-helical extracellular domain, and a C-terminal glycophosphatidylinositol (GPI) anchor. The functional form of the molecule is a dimer in which the ectodomains form a cysteine-bonded coiled-coil[27,59]. Structural studies have shown that pairs of these dimers can associate to form an antiparallel four-helix bundle in vitro, but this conformation is not required for activity[26]. It is unknown exactly what orientation active tetherin dimers adopt during the tethering process, although it is most likely to be an extended conformation with both amino-termini together in either the virion or cellular membrane[28,59]. A remarkable piece of evidence for the generality of this mechanism is that tetherin activity can be reproduced by an entirely artificial molecule designed from heterologous proteins with functionally analogous but unrelated domains[28]. Tetherin appears to operate by binding to viral and cellular membrane regions alone, without the need for any sequence-specified inter-molecular interactions.

Further evidence for this generality comes from experiments exploring the species-specificity of tetherin. It appears to be a crucial part of adaptation to many host species that viruses gain the ability to counteract or avoid the activity of the host-encoded tetherin. Tetherin from a given species can frequently serve as a powerful inhibitor of viruses found in *other* species. One result of this is that cells from one species can be supplied with tetherin from another species, and it will frequently serve to restrict the release of virus adapted to that cell type. This is largely because

of the sequence-independence of the interactions between tetherin and its viral

targets. It is a remarkably self-sufficient molecule, and it has been somewhat free

from the evolutionary pressures many other proteins face as their various binding

partners evolve. In fact, despite tetherin's role as a powerful effector of the innate

antiviral immune system, the majority of its coding sequence shows evidence of

having changed over time only as a result of neutral genetic drift. The exception to

this are several residues in the transmembrane domain and cytoplasmic tail. These

show strong signals of positive selection, and they are the sites of interaction with

viral proteins that counteract the effects of tetherin[60-62].

Primate lentiviruses have, at various points in their history, found ways to use three

separate virally-encoded proteins to counteract tetherin. Most SIV strains use

Nef[63,64]. HIV-1 uses Vpu[13], and HIV-2 uses Env[65]. Nef interacts with the cytoplasmic

domain of tetherin and induces its internalization[63,66,67]. The tetherin residues that

participate in this interaction are not present in human tetherin, due to a 5-residue

deletion that was present in the human lineage as long ago as the divergence

between humans and Neanderthals[63,64,68]. Accordingly, HIV-1 has developed the

capacity to use the accessory protein Vpu to counteract tetherin, and HIV-2 (which

lacks Vpu) has developed the capacity to use the Env protein for the same purpose.

The Vpu protein also serves to down-regulate the HIV-1 receptor, CD4[69,70], and this

function is important for effective viral replication[71]. Of the known types of HIV, only

HIV-1 Group M is pandemic. HIV-2, and HIV-1 groups O and N have all failed to

spread significantly in the human population. HIV-2 lacks Vpu altogether, whereas the Vpu of HIV-N does not downregulate CD4 and the the Vpu of HIV-O does not antagonize tetherin[72]. The rare Group P strain cannot antagonize tetherin with either Nef, Vpu, or Env[73]. Only HIV-M encodes a Vpu that efficiently performs both of these functions. One theory about the zoonotic transmission of SIV from chimpanzees to humans, and the resultant pandemic spread of HIV-1, is that the requirement for the down-regulation of these two host molecules, CD4 and tetherin, served as the critical barrier between humans and other primates that has both served to halt the spread of other lentiviral zoonoses and allowed the worldwide spread of HIV-1 Group M infection[72]. For HIV-1 to become established in humans it may have had to carry or develop the ability of Vpu to counteract tetherin, as the Nef-interacting domain was absent from human tetherin[63,64]. In addition it may have had to develop this capability while maintaining the separate ability to down-regulate CD4. On this theory, because only HIV-1 M successfully acquired both of these traits, it was the only group capable of fully transferring species and spreading throughout the human population.

One issue with this theory is that the SIVcpz strain that gave rise to HIV-1, and that utilizes Nef to counteract tetherin, is itself descended from Old World Monkey strains of SIV that carry Vpu proteins capable of counteracting tetherin[74]. So while this function is generally performed by Nef in most monkeys and in all great apes, it does not appear to be a function that was newly acquired by Vpu only in humans.

This observation serves to underline one important fact about genetic conflict between host and pathogens. The Red Queen Hypothesis posits a state of continual change at molecular interfaces that results in the maintenance of those interfaces. But the history of the conflict between tetherin and retroviruses does not fit with that kind of steady state. It does indeed seem to describe a great deal of change and responsive co-evolution over time, but it seems that there was rarely a balance, that there were frequent adaptative bursts, and that most of the time one side or the other had clear dominance.

HIV-1 Vpu blocks the ability of tetherin to restrict virus release, but how it does so is not entirely clear. A variety of mechanisms have been reported, and none have been shown to be absolutely essential. Vpu is thought to bind to the inner leaflet of the plasma membrane, and interact with tetherin via their respective transmembrane domains[50,75,76]. In general, Vpu efficiently reduces the amount of tetherin present at the cell surface[13,50,77]. It is not clear if the primary cause of this is active down-regulation[66,78], or a secretory pathway block, or both[79,80]. In some cases, Vpu appears to cause the degradation of tetherin as well, but this is not required for its activity[81,82], and it is not known whether this process utilizes proteasomal or lysosomal degradation[13,50,77]. Recent reports have indicated that an endocytosis motif in the cytoplasmic domain of Vpu leads to clathrin-dependent internalization of tetherin[83], and that Vpu interaction with the E3 ligase β-TrCP leads to the ubiquitination and ESCRT-dependent targeting of tetherin to lysosomes[51,84,85,80,86].

Because tetherin is constitutively recycled, active removal by Vpu is not required for down-regulation, and it has been reported that Vpu blocks both recycling and de novo surface-directed transport[79]. Whatever the central mechanism may be, Vpu counteraction of tetherin appears to correlate with the reduction of surface levels of tetherin. The requirement for this has been questioned[87], however the preponderance of evidence points to the functional relevance of down-regulation, as does the logic of the tethering mechanism itself.

The kinetics of tetherin down-regulation

In order to assess whether tetherin down-regulation takes place rapidly enough to account for the effect of Vpu on virus release, we followed the kinetics of tetherin removal from the surface of cells after infection with HIV-1 carrying a marker for early gene expression in place of the Nef gene.

MT-4 cells stably expressing tetherin were infected with this reporter virus and analyzed by flow cytometry at regular time points. The GFP v. tetherin-APC scatterplots are shown in Fig. 4.7A. Histograms of the GFP-positive population are shown in Fig. 4.7B, and the progress of GFP expression and APC reduction in GFP-positive cells is charted at the right. We found that soon after green cells appear, the levels of tetherin at the cell surface drop sharply. Substantial down-regulation is

present by 24 hours post-infection, and reaches close to its maximum level by 30 hours. When the same cells were infected with a reporter virus lacking Vpu, the cell-surface tetherin levels remain unchanged as the infection proceeds. An example is shown in the upper right panel of Fig. 4.7. This experiment was also performed in HOS cells stably expressing tetherin, (Fig. 4.8) and although these cells express higher levels of tetherin the overall kinetics of down-regulation are quite similar to those seen in MT-4 cells.

No fluorescently tagged version of tetherin has been constructed that maintains both virus release restriction and Vpu-counteraction phenoptypes. Therefore single cell microscopy analysis was not available to us as a means to quantify the kinetics of Vpu-induced tetherin downregulation. Therefore this data remains largely qualitative. What we can draw from it, however, is the evidence from the flow cytometry results indicating that when cells are infected with a Vpu+ virus, surface levels of tetherin appear to drop in the same manner, and with broadly similar timing, as intracellular levels of A3G do upon infection with Vif+ virus. The pattern of the scatterplots over time is markedly similar between the two types of experiment, and down-regulation of tetherin appear to be both rapid and efficient, supporting the idea that Vpu removes tetherin from the cell surface fast enough to for this to be the primary mechanism abrogating tetherin-induced restriction of viral release.
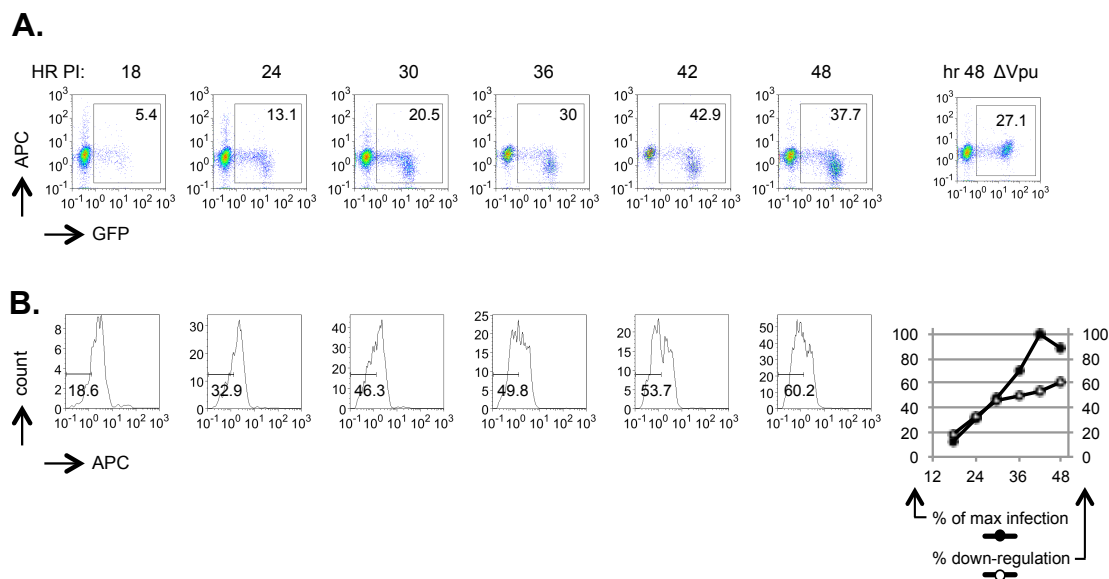
A.

HR PI: 18   24   30   36   42   48   hr 48 ΔVpu

APC ↑   5.4   13.1   20.5   30   42.9   37.7   27.1

→ GFP

B.

count ↑   18.6   32.9   46.3   49.8   53.7   60.2

→ APC

% of max infection ●
% down-regulation ○

Fig. 4.7. Tetherin down-regulation in MT4-Tetherin cells. MT-4 cells stably expressing tetherin were infected with an HIV-1 reporter virus construct carrying GFP in the early gene Nef position, collected and fixed at the indicated time points, stained for extracellular tetherin expression using an APC-conjugated secondary antibody, and analyzed by flow cytometry. GFP v. APC scatterplots are shown in **A.** A sample of cells infected with a ΔVpu virus and collected at 48 hr post-infection is shown in the upper right. The charts in **B.** are histograms of the GFP-positive populations shown in A., showing the progressive down-regulation of mCherry levels in infected cells. This is charted to the right of the histograms, with down-regulation plotted as the percentage shown in the APC-low gates on the histograms, and the course of infection plotted as a percentage of maximum.
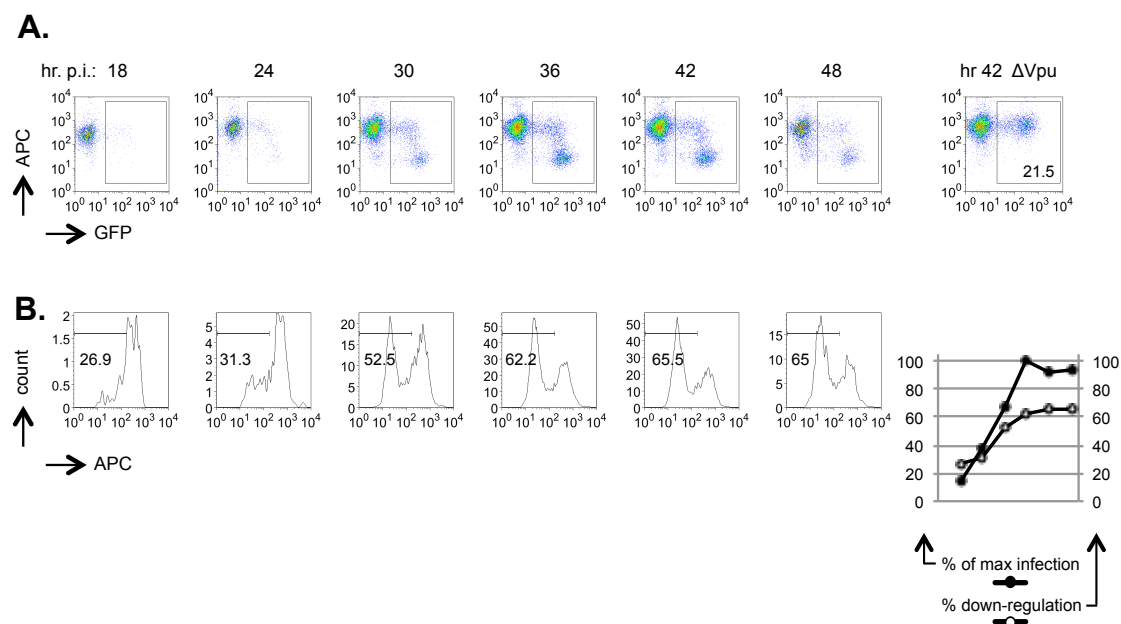
Fig. 4.8. Tetherin down-regulation in HOS-Tetherin cells. HOS cells stably expressing tetherin were infected with an HIV-1 reporter virus construct carrying GFP in the early gene Nef position, collected and fixed at the indicated time points, stained for extracellular tetherin expression using an APC-conjugated secondary antibody, and analyzed by flow cytometry. GFP v. APC scatterplots are shown in **A.** A sample of cells infected with a ΔVpu virus and collected at 42 hr post-infection is shown in the upper right. The charts in **B.** are histograms of the GFP-positive populations shown in A., showing the progressive down-regulation of mCherry levels in infected cells. This is charted to the right for each virus, with down-regulation plotted as the percentage shown in the APC-low gates on the histograms, and the course of infection plotted as a percentage of maximum.

References, Chapter 4

1. Fadel, H. J. & Poeschla, E. M. Retroviral restriction and dependency factors in primates and carnivores. *Vet. Immunol. Immunopathol.* **143**, 179–189 (2011).

2. Lehmann, M., Nikolic, D. S. & Piguet, V. How HIV-1 takes advantage of the cytoskeleton during replication and cell-to-cell transmission. *Viruses* **3**, 1757–1776 (2011).

3. Lehmann-Che, J. & Saïb, A. Early stages of HIV replication: how to hijack cellular functions for a successful infection. *AIDS Rev* **6**, 199–207 (2004).

4. Gifford, R. J. Viral evolution in deep time: lentiviruses and mammals. *Trends Genet.* **28**, 89–100 (2012).

5. Bozek, K. & Lengauer, T. Positive selection of HIV host factors and the evolution of lentivirus genes. *BMC Evol. Biol.* **10**, 186 (2010).

6. Daugherty, M. D. & Malik, H. S. Rules of engagement: molecular insights from host-virus arms races. *Annu. Rev. Genet.* **46**, 677–700 (2012).

7. Frendo, J. L. *et al.* Direct involvement of HERV-W Env glycoprotein in human trophoblast cell fusion and differentiation. *Mol. Cell. Biol.* **23**, 3566–3574 (2003).

8. Mi, S. *et al.* Syncytin is a captive retroviral envelope protein involved in human placental morphogenesis. *Nature* **403**, 785–789 (2000).

9. Sawyer, S. L., Emerman, M. & Malik, H. S. Ancient adaptive evolution of the primate antiviral DNA-editing enzyme APOBEC3G. *PLoS Biol.* **2**, E275 (2004).

10. Franzosa, E. A. & Xia, Y. Structural principles within the human-virus protein-protein interaction network. *Proc. Natl. Acad. Sci. U.S.A.* **108**, 10538–10543 (2011).

11. Elde, N. C., Child, S. J., Geballe, A. P. & Malik, H. S. Protein kinase R reveals an evolutionary model for defeating viral mimicry. *Nature* **457**, 485–489 (2009).

12. Hatziioannou, T., Cowan, S., Goff, S. P., Bieniasz, P. D. & Towers, G. J. Restriction of multiple divergent retroviruses by Lv1 and Ref1. *EMBO J.* **22**, 385–394 (2003).

13. Neil, S. J. D., Zang, T. & Bieniasz, P. D. Tetherin inhibits retrovirus release and is antagonized by HIV-1 Vpu. *Nature* **451**, 425–430 (2008).

14. Stremlau, M. *et al.* The cytoplasmic body component TRIM5alpha restricts HIV-1 infection in Old World monkeys. *Nature* **427**, 848–853 (2004).

15. Neil, S. J. D., Sandrin, V., Sundquist, W. I. & Bieniasz, P. D. An interferon-alpha-induced tethering mechanism inhibits HIV-1 and Ebola virus particle release but is counteracted by the HIV-1 Vpu protein. *Cell Host Microbe* **2**, 193–203 (2007).

16. Mangeat, B. *et al.* Broad antiretroviral defence by human APOBEC3G through lethal editing of nascent reverse transcripts. *Nature* **424**, 99–103 (2003).

17. Bieniasz, P. D. Restriction factors: a defense against retroviral infection. *Trends Microbiol.* **11**, 286–291 (2003).

18. Sawyer, S. L., Wu, L. I., Emerman, M. & Malik, H. S. Positive selection of primate TRIM5alpha identifies a critical species-specific retroviral restriction domain. *Proc. Natl. Acad. Sci. U.S.A.* **102**, 2832–2837 (2005).

19. Johnson, W. E. & Sawyer, S. L. Molecular evolution of the antiretroviral TRIM5 gene. *Immunogenetics* **61**, 163–176 (2009).

20. Zhang, J. & Webb, D. M. Rapid evolution of primate antiviral enzyme APOBEC3G. *Hum. Mol. Genet.* **13**, 1785–1791 (2004).

21. Ohkura, S. *et al.* Novel escape mutants suggest an extensive TRIM5α binding site spanning the entire outer surface of the murine leukemia virus capsid protein. *PLoS Pathog.* **7**, e1002011 (2011).

22. Stremlau, M. *et al.* Specific recognition and accelerated uncoating of retroviral capsids by the TRIM5alpha restriction factor. *Proc. Natl. Acad. Sci. U.S.A.* **103**, 5514–5519 (2006).

23. Sebastian, S. & Luban, J. TRIM5alpha selectively binds a restriction-sensitive retroviral capsid. *Retrovirology* **2**, 40 (2005).

24. Lecossier, D., Bouchonnet, F., Clavel, F. & Hance, A. J. Hypermutation of HIV-1 DNA in the absence of the Vif protein. *Science* **300**, 1112 (2003).

25. Sheehy, A. M., Gaddis, N. C., Choi, J. D. & Malim, M. H. Isolation of a human gene that inhibits HIV-1 infection and is suppressed by the viral Vif protein. *Nature* **418**, 646–650 (2002).

26. Yang, H. *et al.* Structural insight into the mechanisms of enveloped virus tethering by tetherin. *Proc. Natl. Acad. Sci. U.S.A.* **107**, 18428–18432 (2010).

27. Hinz, A. *et al.* Structural basis of HIV-1 tethering to membranes by the BST-2/tetherin ectodomain. *Cell Host Microbe* **7**, 314–323 (2010).

28. Perez-Caballero, D. *et al.* Tetherin inhibits HIV-1 release by directly tethering virions to cells. *Cell* **139**, 499–511 (2009).

29. Hatziioannou, T., Perez-Caballero, D., Yang, A., Cowan, S. & Bieniasz, P. D. Retrovirus resistance factors Ref1 and Lv1 are species-specific variants of TRIM5alpha. *Proc. Natl. Acad. Sci. U.S.A.* **101**, 10774–10779 (2004).

30. Yap, M. W., Nisole, S., Lynch, C. & Stoye, J. P. Trim5alpha protein restricts both HIV-1 and murine leukemia virus. *Proc. Natl. Acad. Sci. U.S.A.* **101**, 10786–10791 (2004).

31. Morran, L. T., Schmidt, O. G., Gelarden, I. A., Parrish, R. C. & Lively, C. M. Running with the Red Queen: host-parasite coevolution selects for biparental sex. *Science* **333**, 216–218 (2011).

32. Woolhouse, M. E. J., Webster, J. P., Domingo, E., Charlesworth, B. & Levin, B. R. Biological and biomedical implications of the co-evolution of pathogens and their hosts. *Nat. Genet.* **32**, 569–577 (2002).

33. Zennou, V., Perez-Caballero, D., Göttlinger, H. & Bieniasz, P. D. APOBEC3G incorporation into human immunodeficiency virus type 1 particles. *J. Virol.* **78**, 12058–12061 (2004).

34. Bogerd, H. P. & Cullen, B. R. Single-stranded RNA facilitates nucleocapsid: APOBEC3G complex formation. *RNA* **14**, 1228–1236 (2008).

35. Kourteva, Y., De Pasquale, M., Allos, T., McMunn, C. & D'Aquila, R. T. APOBEC3G expression and hypermutation are inversely associated with human immunodeficiency virus type 1 (HIV-1) burden in vivo. *Virology* (2012).doi:10.1016/j.virol.2012.03.018

36. Mehle, A. *et al.* Vif overcomes the innate antiviral activity of APOBEC3G by promoting its degradation in the ubiquitin-proteasome pathway. *J. Biol. Chem.* **279**, 7792–7798 (2004).

37. Yu, X. *et al.* Induction of APOBEC3G ubiquitination and degradation by an HIV-1 Vif-Cul5-SCF complex. *Science* **302**, 1056–1060 (2003).

38. Marin, M., Rose, K. M., Kozak, S. L. & Kabat, D. HIV-1 Vif protein binds the editing enzyme APOBEC3G and induces its degradation. *Nat. Med.* **9**, 1398–1403 (2003).

39. Sheehy, A. M., Gaddis, N. C. & Malim, M. H. The antiretroviral enzyme APOBEC3G is degraded by the proteasome in response to HIV-1 Vif. *Nat. Med.* **9**, 1404–1407 (2003).

40. Liu, B., Yu, X., Luo, K., Yu, Y. & Yu, X.-F. Influence of primate lentiviral Vif and proteasome inhibitors on human immunodeficiency virus type 1 virion packaging of APOBEC3G. *J. Virol.* **78**, 2072–2081 (2004).

41. Mangeat, B., Turelli, P., Liao, S. & Trono, D. A single amino acid determinant governs the species-specific sensitivity of APOBEC3G to Vif action. *J. Biol. Chem.* **279**, 14481–14483 (2004).

42. Bogerd, H. P., Doehle, B. P., Wiegand, H. L. & Cullen, B. R. A single amino acid difference in the host APOBEC3G protein controls the primate species specificity of HIV type 1 virion infectivity factor. *Proc. Natl. Acad. Sci. U.S.A.* **101**, 3770–3774 (2004).

43. Schröfelbauer, B., Chen, D. & Landau, N. R. A single amino acid of APOBEC3G controls its species-specific interaction with virion infectivity factor (Vif). *Proc. Natl. Acad. Sci. U.S.A.* **101**, 3927–3932 (2004).

44. Hatziioannou, T. *et al.* Generation of simian-tropic HIV-1 by restriction factor evasion. *Science* **314**, 95 (2006).

45. Hatziioannou, T. *et al.* A macaque model of HIV-1 infection. *Proc. Natl. Acad. Sci. U.S.A.* **106**, 4425–4429 (2009).

46. Dang, Y., Siew, L. M. & Zheng, Y.-H. APOBEC3G is degraded by the proteasomal pathway in a Vif-dependent manner without being polyubiquitylated. *J. Biol. Chem.* **283**, 13124–13131 (2008).

47. Stopak, K., de Noronha, C., Yonemoto, W. & Greene, W. C. HIV-1 Vif blocks the antiviral activity of APOBEC3G by impairing both its translation and intracellular stability. *Mol. Cell* **12**, 591–601 (2003).

48. Conticello, S. G., Harris, R. S. & Neuberger, M. S. The Vif protein of HIV triggers degradation of the human antiretroviral DNA deaminase APOBEC3G. *Curr. Biol.* **13**, 2009–2013 (2003).

49. Goila-Gaur, R., Khan, M. A., Miyagi, E. & Strebel, K. Differential sensitivity of "old" versus 'new' APOBEC3G to human immunodeficiency virus type 1 vif. *J. Virol.* **83**, 1156–1160 (2009).

50. Iwabu, Y. *et al.* HIV-1 accessory protein Vpu internalizes cell-surface BST-2/tetherin through transmembrane interactions leading to lysosomes. *J. Biol. Chem.* **284**, 35060–35072 (2009).

51. Mitchell, R. S. *et al.* Vpu antagonizes BST-2-mediated restriction of HIV-1 release via beta-TrCP and endo-lysosomal trafficking. *PLoS Pathog.* **5**, e1000450 (2009).

52. Kaletsky, R. L., Francica, J. R., Agrawal-Gamse, C. & Bates, P. Tetherin-mediated restriction of filovirus budding is antagonized by the Ebola glycoprotein. *Proceedings of the National Academy of Sciences* **106**, 2886–2891 (2009).

53. Jouvenet, N. *et al.* Broad-spectrum inhibition of retroviral and filoviral particle release by tetherin. *J. Virol.* **83**, 1837–1844 (2009).

54. Sarojini, S., Theofanis, T. & Reiss, C. S. Interferon-induced tetherin restricts vesicular stomatitis virus release in neurons. *DNA Cell Biol.* **30**, 965–974 (2011).

55. Pardieu, C. *et al.* The RING-CH ligase K5 antagonizes restriction of KSHV and HIV-1 particle release by mediating ubiquitin-dependent endosomal degradation of tetherin. *PLoS Pathog.* **6**, e1000843 (2010).

56. Mansouri, M. *et al.* Molecular mechanism of BST2/tetherin downregulation by K5/MIR2 of Kaposi's sarcoma-associated herpesvirus. *J. Virol.* **83**, 9672–9681 (2009).

57. Weidner, J. M. *et al.* Interferon-induced cell membrane proteins, IFITM3 and tetherin, inhibit vesicular stomatitis virus infection via distinct mechanisms. *J. Virol.* **84**, 12646–12657 (2010).

58. Radoshitzky, S. R. *et al.* Infectious Lassa virus, but not filoviruses, is restricted by BST-2/tetherin. *J. Virol.* **84**, 10569–10580 (2010).

59. Cole, G., Simonetti, K., Ademi, I. & Sharpe, S. Dimerization of the Transmembrane Domain of Human Tetherin in Membrane Mimetic Environments. *Biochemistry* (2012).doi:10.1021/bi201747t

60. Lim, E. S., Malik, H. S. & Emerman, M. Ancient adaptive evolution of tetherin shaped the functions of Vpu and Nef in human immunodeficiency virus and primate lentiviruses. *J. Virol.* **84**, 7124–7134 (2010).

61. Liu, J., Chen, K., Wang, J.-H. & Zhang, C. Molecular evolution of the primate antiviral restriction factor tetherin. *PLoS ONE* **5**, e11904 (2010).

62. McNatt, M. W. *et al.* Species-specific activity of HIV-1 Vpu and positive selection of tetherin transmembrane domain variants. *PLoS Pathog.* **5**, e1000300 (2009).

63. Zhang, F. *et al.* Nef proteins from simian immunodeficiency viruses are tetherin antagonists. *Cell Host Microbe* **6**, 54–67 (2009).

64. Jia, B. *et al.* Species-specific activity of SIV Nef and HIV-1 Vpu in overcoming restriction by tetherin/BST2. *PLoS Pathog.* **5**, e1000429 (2009).

65. Le Tortorec, A. & Neil, S. J. D. Antagonism to and intracellular sequestration of human tetherin by the human immunodeficiency virus type 2 envelope glycoprotein. *J. Virol.* **83**, 11966–11978 (2009).

66. Zhang, F. *et al.* SIV Nef proteins recruit the AP-2 complex to antagonize Tetherin and facilitate virion release. *PLoS Pathog.* **7**, e1002039 (2011).

67. Serra-Moreno, R., Jia, B., Breed, M., Alvarez, X. & Evans, D. T. Compensatory changes in the cytoplasmic tail of gp41 confer resistance to tetherin/BST-2 in a pathogenic nef-deleted SIV. *Cell Host Microbe* **9**, 46–57 (2011).

68. Sauter, D., Vogl, M. & Kirchhoff, F. Ancient origin of a deletion in human BST2/Tetherin that confers protection against viral zoonoses. *Hum. Mutat.* **32**, 1243–1245 (2011).

69. Chen, M. Y., Maldarelli, F., Karczewski, M. K., Willey, R. L. & Strebel, K. Human immunodeficiency virus type 1 Vpu protein induces degradation of CD4 in vitro: the cytoplasmic domain of CD4 contributes to Vpu sensitivity. *J. Virol.* **67**, 3877–3884 (1993).

70. Willey, R. L., Maldarelli, F., Martin, M. A. & Strebel, K. Human immunodeficiency virus type 1 Vpu protein induces rapid degradation of CD4. *J. Virol.* **66**, 7193–7200 (1992).

71. Bimodal down-regulation of CD4 in cells expressing human immunodeficiency virus type 1 Vpu and Env. **77 (Pt 10)**, 2393–2401 (1996).

72. Sauter, D. *et al.* Tetherin-driven adaptation of Vpu and Nef function and the evolution of pandemic and nonpandemic HIV-1 strains. *Cell Host Microbe* **6**, 409–421 (2009).

73. Sauter, D. *et al.* HIV-1 Group P is unable to antagonize human tetherin by Vpu,

Env or Nef. *Retrovirology* **8**, 103 (2011).

74. Nikovics, K. *et al.* Counteraction of tetherin antiviral activity by two closely related SIVs differing by the presence of a Vpu gene. *PLoS ONE* **7**, e35411 (2012).

75. Kobayashi, T. *et al.* Identification of amino acids in the human tetherin transmembrane domain responsible for HIV-1 Vpu interaction and susceptibility. *J. Virol.* **85**, 932–945 (2011).

76. Vigan, R. & Neil, S. J. D. Determinants of tetherin antagonism in the transmembrane domain of the human immunodeficiency virus type 1 Vpu protein. *J. Virol.* **84**, 12958–12970 (2010).

77. Iwabu, Y., Fujita, H., Tanaka, Y., Sata, T. & Tokunaga, K. Direct internalization of cell-surface BST-2/tetherin by the HIV-1 accessory protein Vpu. *Commun Integr Biol* **3**, 366–369 (2010).

78. Habermann, A. *et al.* CD317/tetherin is enriched in the HIV-1 envelope and downregulated from the plasma membrane upon virus infection. *J. Virol.* **84**, 4646–4658 (2010).

79. Schmidt, S., Fritz, J. V., Bitzegeio, J., Fackler, O. T. & Keppler, O. T. HIV-1 Vpu blocks recycling and biosynthetic transport of the intrinsic immunity factor CD317/tetherin to overcome the virion release restriction. *MBio* **2**, e00036–11 (2011).

80. Dubé, M. *et al.* Antagonism of tetherin restriction of HIV-1 release by Vpu involves binding and sequestration of the restriction factor in a perinuclear compartment. *PLoS Pathog.* **6**, e1000856 (2010).

81. Tervo, H.-M. *et al.* β-TrCP is dispensable for Vpu's ability to overcome the CD317/Tetherin-imposed restriction to HIV-1 release. *Retrovirology* **8**, 9 (2011).

82. Goffinet, C. *et al.* Antagonism of CD317 restriction of human immunodeficiency virus type 1 (HIV-1) particle release and depletion of CD317 are separable activities of HIV-1 Vpu. *J. Virol.* **84**, 4089–4094 (2010).

83. Kueck, T. & Neil, S. J. D. A cytoplasmic tail determinant in HIV-1 Vpu mediates targeting of tetherin for endosomal degradation and counteracts interferon-induced restriction. *PLoS Pathog.* **8**, e1002609 (2012).

84. Douglas, J. L. *et al.* Vpu directs the degradation of the human immunodeficiency virus restriction factor BST-2/Tetherin via a {beta}TrCP-

dependent mechanism. *J. Virol.* **83**, 7931–7947 (2009).

85. Tokarev, A. A., Munguia, J. & Guatelli, J. C. Serine-threonine ubiquitination mediates downregulation of BST-2/tetherin and relief of restricted virion release by HIV-1 Vpu. *J. Virol.* **85**, 51–63 (2011).

86. Dubé, M. *et al.* Suppression of Tetherin-restricting activity upon human immunodeficiency virus type 1 particle release correlates with localization of Vpu in the trans-Golgi network. *J. Virol.* **83**, 4574–4590 (2009).

87. Miyagi, E., Andrew, A. J., Kao, S. & Strebel, K. Vpu enhances HIV-1 virus release in the absence of Bst-2 cell surface down-modulation and intracellular depletion. *Proceedings of the National Academy of Sciences* **106**, 2868–2873 (2009).

Chapter 5. Assembly.

Critical Gag interactions

In the late phase of HIV-1 gene expression, transcripts of the full viral genome are produced and exported from the nucleus unspliced. These are the templates for translation of the viral Gag and GagPol gene products, and they themselves serve as packageable viral genomes. Gag proteins are translated in the cytosol and ultimately several thousand copies will multimerize at the plasma membrane and initiate the curvature that leads to the formation of the budding virion[1-7]. In the absence of any other viral proteins Gag alone is capable of driving the assembly and budding of empty virions or virus-like particles (VLPs)[2]. For the production of infectious virions, two copies of the RNA genome need to be packaged[8,9], envelope needs to be incorporated into the viral membrane[10], and small numbers of accessory proteins need to be packaged[11-13]. Many cellular molecules are also required for this complex process[14-19], and, in addition, there are cellular factors that must be evaded or destroyed[20,21]. Kinetic information about the intracellular assembly process has not been straightforward to obtain, as virus-producing cells are full of viral components that may or may not be actually involved in productive assembly or may be at very different stages in the assembly process[22-24].

The three central intracellular events of the assembly process are Gag-Gag multimerization, Gag-RNA binding, and Gag-membrane binding. By the end of the process, Gag has bound its RNA genome, translocated to the PM, and multimerized into a large and highly ordered structure[25]. These events are highly interrelated and it has proven difficult to separate the various stages biochemically or genetically. However, a model has emerged in recent years, and there is strong evidence that both RNA binding and early multimerization steps occur in the cytoplasm[23,26-29]. In this view, early Gag multimers form around a dimer of genomic RNA in the cytoplasm, and this leads to rearrangements that increase the membrane affinity of Gag and lead to specific targeting to the PM where higher-order multimerization occurs[30-32]. After this nucleation event, further Gag molecules may be added directly from the cytoplasm, or laterally by diffusion within the PM (See Fig. 5.2). The time between nucleation at the PM and egress is extremely short, on the order of 25 minutes[30,33]. The final scission of the virion bud from the cell is mediated by cellular ESCRT proteins that normally perform a similar topological role driving vesicle budding into multi-vesicular endosomes, and severing the membrane linkage between dividing cells[15,16,18,34].

The N-terminal MA domain of Gag is responsible for membrane binding, via a basic patch and a myristate group attached to the terminal glycine residue[35]. In monomeric Gag molecules this myristate is sequestered inside the globular head of MA, but initial multimerization steps lead to a conformational change that exposes

the myristate and targets Gag to the PM[36,37]. Non-myristoylated Gag molecules are not competent for membrane targeting and remain cytoplasmic. However, they can be rescued to the PM and incorporated into virions by co-expressed myristoylated Gag molecules[38]. On the other hand, blocking multimerization, by mutating key residues in CA and NC, can severely impair membrane binding, even when N-terminal myristoylation is intact[39-42]. These findings fit well with a model in which some degree of multimerization can take place in the cytoplasm, which then enhances the membrane-binding capability of the Gag molecules involved. Once at the PM, higher order multimerization is possible and presumably enhanced by the fact that only lateral diffusion is possible. This picture is also supported by the findings that membrane binding by Gag is highly sensitive to intracellular concentration[27], but that only once Gag is at the PM does multimerization proceed at the scale necessary to display a detectable FRET signal[43]. Finally, recent biochemical experiments have found that RNA forms stable complexes with myristoylated *or* non-myristoylated Gag in the cytoplasm of infected cells, and that myristoylated Gag was capable of relocating RNA from the cytoplasm to the PM[26].
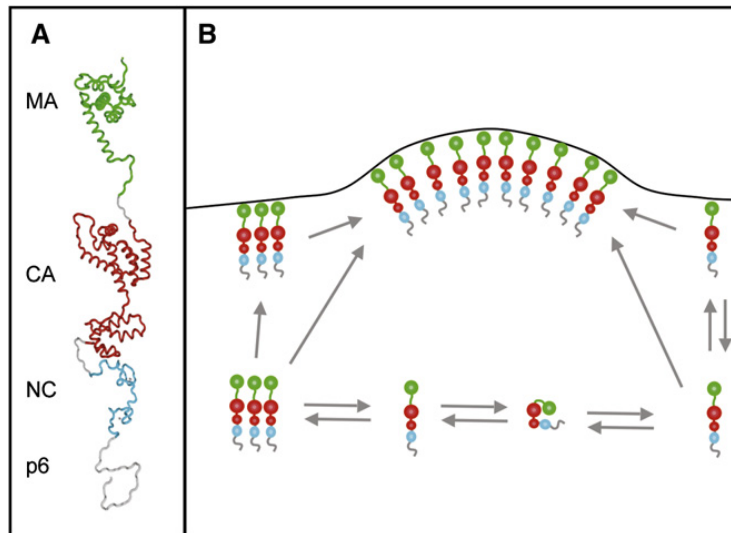
Fig. 5.1. Gag-driven virion assembly. A model for the Gag polyprotein in extended conformation is shown on the left. Several possible pathways for addition of Gag molecules to the growing virion shell are indicated, including the potential for a "folded" cytoplasmic conformation. Not shown are the possibilities that this folded conformation could exist as low-order oligomers, or could be maintained until it encounters the plasma membrane.

The initial multimerization steps that lead to myristate exposure are RNA dependent[44], and although these steps are thought to occur in the cytoplasm there is reason to believe that membrane interactions themselves can be involved in the exposure of the myristate group. The basic region of MA adjacent to the myristate group participates in membrane binding[45,46] and is also capable of binding RNA[47-50]. In vitro experiments have shown that lipid membranes, though only those containing phosphatidylinositol-4,5-bisphosphate (PIP2) can compete with RNA for

interaction with MA[4,51]. In addition, there is evidence that MA is involved in exclusion of spliced viral RNAs from virions[52]. Thus, although the nature and function of the RNA-binding capability of MA is still uncertain, evidence has begun to accumulate indicating that it does play a role of some kind in genome packaging, or perhaps that RNA binding by MA performs a regulatory function that modulates when and where Gag binds to the plasma membrane. Structural studies investigating the conformation of the entire extended Gag polyprotein have indicated that Gag may in fact be folded in such a way as to bring MA and NC near to each other in space[28,53-55]. This would enable both domains to participate in interactions with the genome, presumably until the presence of PIP2-containing PM domains led to a reconfiguration of Gag into the extended conformation it assumes in virions, with MA at the outside beneath the membrane, and NC at the center coating the dimeric genome.

The interaction between NC and RNA is required for virion assembly[56]. Initial Gag-Gag interactions are thought to be mediated partly by RNA itself[57]; and though cellular RNA or unspliced viral RNA can serve this purpose[44,58,59] the NC domain is capable of selectively incorporating the full-length genome[52]. The basis for this selectivity is not yet fully understood, but the interaction is primarily dependent upon structural features found in the 5' UTR of the genome. A number of stem-loop and more complicated RNA structures are found here that have been implicated in various ways in the genome packaging process (Fig. 5.1)[52,60]. From the 5' end, the

first of these are the TAR site, the poly A site, the primer binding site (PBS, responsible for the initiation of reverse-transcription) and stem-loops 1-4 (SL1-SL4). SL1 (also referred to as the dimer initiation site, DIS) and SL3 (also referred to as Psi) bind NC with high affinity[61,62], and because the major splice donor site (SD) lies within SL2, between these high-affinity loops, this is thought to account for much of the selectivity for full-length genome. Only unspliced transcripts contain both SL1 and SL3. SL4 contains the initiating AUG of Gag and extends 17 nucleotides into MA. Two other structures, immediately downstream of SL4 have also been described, and referred to as SL5 and SL6[63]. These are thought to participate in long-range interactions with the structures upstream in the 5' UTR[63,64]. SL4 itself does not bind NC with high affinity, but is required for efficient packaging, and is now believed to participate in precisely this kind of long-range interaction as well, serving a structural purpose by forming base-paired contacts with the upstream PBS region[65]. Many different structures have been proposed for the entire region, spanning the 5' end of Gag and the 5' UTR, and although many of the details are still controversial, it seems likely that in fact it can assume multiple conformations. This region is highly conserved, and it may in fact play a regulatory role, switching from a conformation in which NC-binding and dimerization regions are sequestered to one in which they are exposed[66-68].
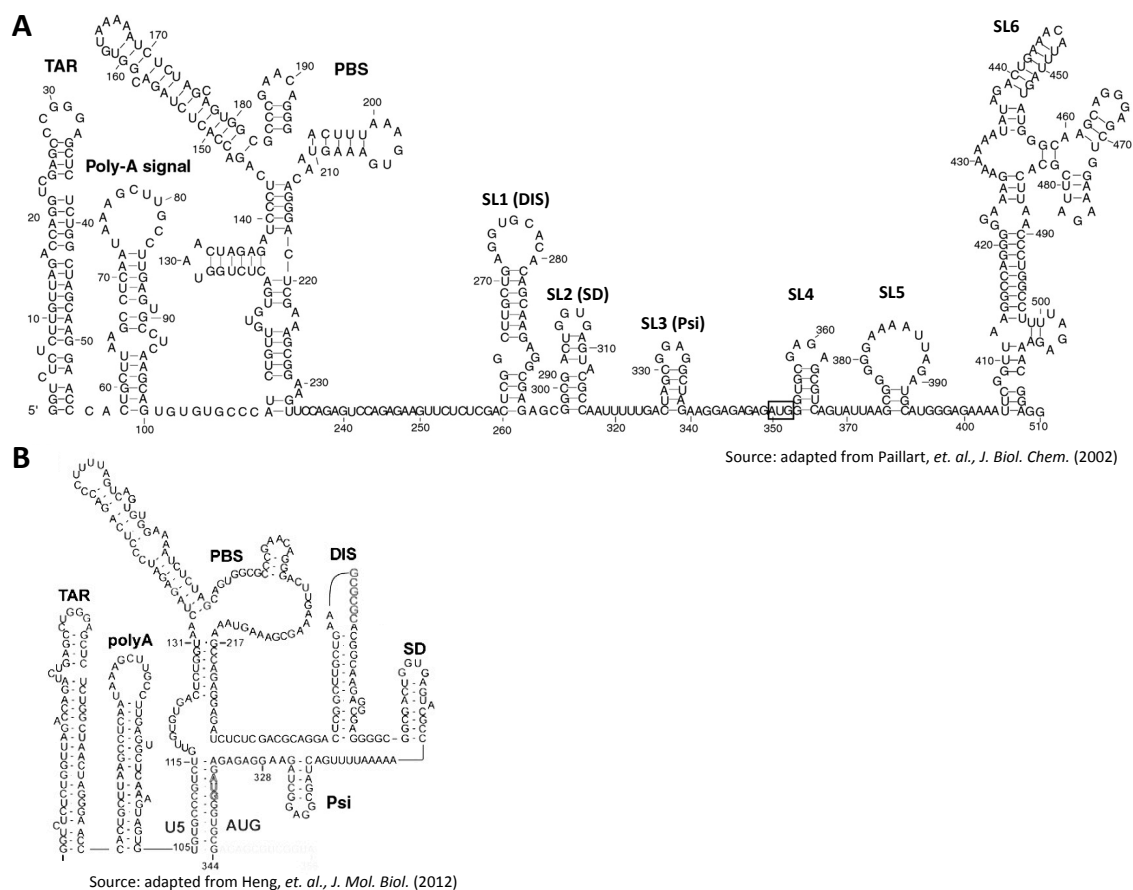
A

B

Fig.5.2. The 5'UTR of HIV-1: proposed structures for the Gag-binding region of the genomic RNA. The proposed conformation in **A**. includes putative stem-loops SL5 and SL6 which are deleted in the ΔMA Gag mutant described below. **B.** A more recent NMR-based structure of the upstream region, representing the conformation thought to promote dimerization and Gag-binding.

HIV-1 delays its own assembly

As described above, neither non-myristoylated Gag molecules or non-multimerizing Gag molecules are competent for robust membrane binding. Conversely, when the myristate is constitutively exposed, for instance by the deletion of the globular head region of MA which normally serves to sequester it, the requirement for multimerization is removed. In this case Gag molecules are targeted to the PM at low concentrations at which WT Gag is usually cytoplasmic[27,69]. This process is probably almost immediate; upon transfection of GFP-tagged derivatives of this mutant, only PM-bound signal is seen microscopically[27] and no cytoplasmic signal is detected even at very early time points (our unpublished observations).

This mutant, ΔMA HIV-1, lacks the majority of the MA domain, retaining only the N-terminal 7 residues the short stalk region that connects it to CA in the full-length Gag polyprotein. It has two remarkable characteristics. The first is that it is surprisingly functional. Full-length virus carrying this deletion is less infectious but remains replication-competent if paired with a deletion of the cytoplasmic tail of Env that is thought to be required in this case for envelope incorporation to proceed normally[70,71]. The second is that it leads to greatly enhanced virus release[27,69,70].This mutant produces virions both earlier and in greater quantities than does wild-type virus. It appears that the MA domain is not essential for replication, and also that

one of the few certain functions it does perform is to actively delay and inhibit

assembly.

The auto-inhibition that MA mediates by sequestering the myristate group at its N-

terminus probably represents both spatial and temporal regulation. The

requirement for PIP2 limits Gag targeting and assembly to the inner leaflet of the

PM, where PIP2 is highly enriched, and perhaps even to subdomains within the

PM[72,73]. Indeed, ΔMA Gag targets to all cellular membranes promiscuously[70]. This

auto-inhibition also represents a pronounced form of temporal regulation. The

concentration dependence of myristate exposure and membrane binding leads Gag

assembly to behave in a way that is switch-like[27,69]. In the absence of MA, this

cooperativity and the delay associated with it are absent. Gag is immediately

targeted to the PM, and virions bud both early and in greater quantities. The lack of

the myristate switch appears to make assembly independent both of initial

multimerization and of specific membrane interactions – and perhaps independent

of specific RNA binding as well. Under these circumstances Gag can drive extremely

productive and efficient assembly. Because increased production of virions would

presumably be strongly selected for, we hypothesize that there are likely to be

powerful functional reasons why this phenotype is inhibited in wild-type HIV-1.

We sought to make use of a ΔMA mutant to better understand the timing of the HIV-

1 assembly process. The fact that such a large deletion is compatible with even low-

level replication in tissue culture is surprising, given the compact and multi-functional nature of the majority of the HIV-1 genome. It is even more surprising that the primary role of this region appears to be the active inhibition of the assembly process. Given the short average lifetime of HIV-1 infected cells[74-76], it is reasonable to imagine that there would be strong selective pressure on HIV-1 to optimize itself for the rapid assembly and release of new virions. The presence of viral sequences that actively delay the process of assembly process point to the existence of an unknown but critical process, that requires some time to complete, prior to virion release.

These observations led us to design experiments intended to more carefully describe the kinetic parameters of the assembly process, and, in particular, to discover what downstream effects the deletion of MA would have. We reasoned that if auto-inhibition of assembly was an important process, forced acceleration of assembly (as in the ΔMA mutant) would lead to a deficit of some kind in the released virions, and that uncovering the nature of this deficit would provide an indication of the nature of the process enabled by the natural delay in assembly.

We first constructed variants of HIV-1 designed to allow the study of a single-cycle of infection and virion release. The ΔMA mutation was previously shown to be capable of multiple rounds of infection if paired with an envelope lacking the C-terminal cytoplasmic tail. We therefore constructed the ΔMA virus and a matched

control carrying full-length MA, on the background of an X4-tropic HIV-1 clone with this deletion of the C-terminal 142 residues of Env. In addition, we replaced the V3 region of Env with the V3 region from YU2 HIV-1, an R5-tropic strain not capable of infecting MT-4 cells[77]. The V3 region is the tropism determining region responsible for the ability of HIV-1 to utilize either the CCR5 co-receptor or the CXCR4 co-receptor[78,79]. All infectious stocks of virus were produced by co-transfection of the viral genome with a plasmid expressing the VSV-G envelope, thus allowing for efficient initial infection of MT-4 cells leading to the production of R5-tropic virions incapable of initiating a second round of infection. These virions, however, could be harvested and titrated on CCR5-expressing cells. The HIV-1 clone used as the backbone for these constructs was the replication-competent construct NHG, which carries GFP in place of Nef.

To follow the time course of assembly, infections were initiated by synchronized spinoculation, incubated for two hours at 37°C, washed three times, and split into plates for collection. At regular intervals samples of the cultures were taken for flow cytometry, infectivity assays, and for Western blot analysis of both lysates and supernatants. Representative experiments are shown in Figs. 3. and 4. The ΔMA virus releases virions into the supernatant both more rapidly and in greater total quantities than the control virus. However, this phenotype is highly variable. Fig. 5.3 shows an example of an experiment in which the ΔMA virus displayed an especially

strong phenotype. Fig. 5.4 shows an experiment in which it displays a much more
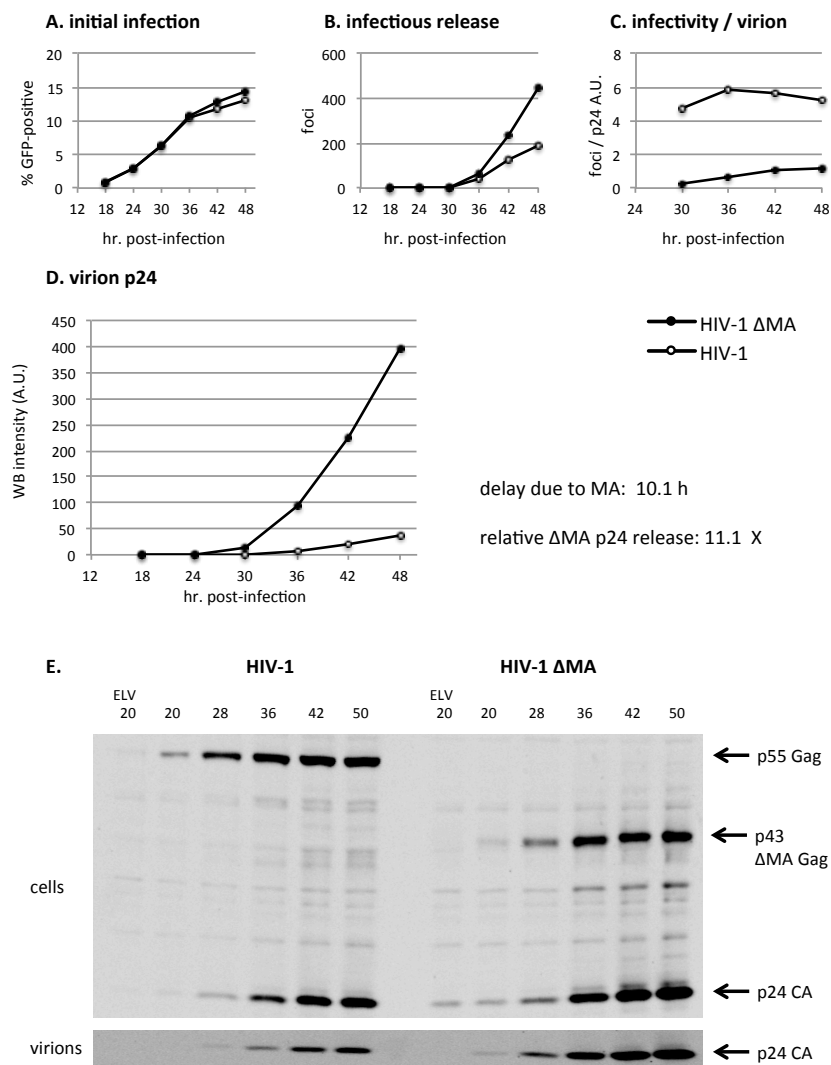
moderate phenotype.

Fig.5.3. Representative assembly time course: high ΔMA release efficiency. **A.** GFP reporter gene expression. **B.** Infectivity in supernatant, as assessed by infection of TZM-bl indicator cells and counting of foci. Western blots (WB) were quantitated using the Odyssey quantitation software and integrated fluorescence intensities were assigned arbitrary units (A.U.). This repetition of the experiment is the only one, of 9 in this cell type, in which the ΔMA-infected cells produced more infectious supernatant than the cells infected with WT HIV-1. **C.** Infectivity normalized to virion p24. **D.** Virion release into supernatant, quantitated from the Western blot in E. Delay and total release fold-change due to MA are calculated as described in the text. **E.** Western Blot of lysates and virions collected at time points post-infection. ELV, Elvitegravir. Elvitegravir is an RT-inhibitor added to some samples as a control for input virus contamination. Any visible virion p24 in ELV samples is due to the initial inoculum.
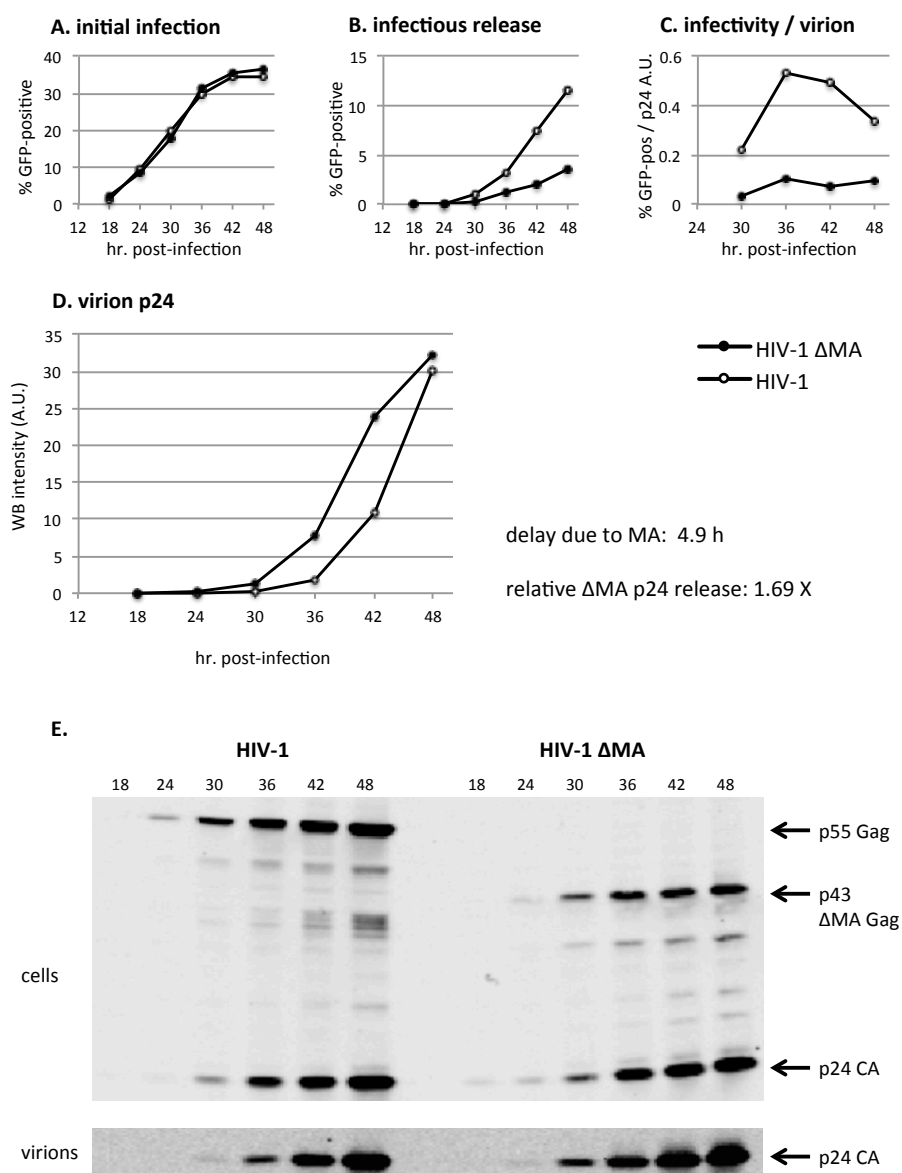
Fig.5.4. Representative assembly time course: low ΔMA release efficiency. **A.** GFP reporter gene expression. **B.** Infectivity in supernatant, as assessed by infection of MT2-R5 cells and flow cytometry analysis. Western blots (WB) were quantitated using the Odyssey quantitation software and integrated fluorescence intensities were assigned arbitrary units (A.U.). **C.** Infectivity normalized to virion p24. **D.** Virion release into supernatant. **E.** Western Blot of lysates and virions collected at time points post-infection.

In order to quantitate the kinetics of HIV-1 assembly, GFP expression and p24

release was monitored at each time point, over multiple experiments, and the data

was plotted as a percent of maximum value. A 4-parameter logistic curve was fit to

the data for each virus and the delay between early-gene GFP expression and p24

release was calculated between the half-maximal points on the curves using a

simple Matlab script (described in Materials and Methods). Plotting the data in this

way allows comparison of GFP and p24 release but is a poor method for quantifying

the difference between WT and ΔMA assembly. The typical strength of this

phenotype was such that it was not straightforward to calculate the kinetic delay

due to the presence of the MA domain. Frequently the ΔMA construct would release

as much as ten times more virions than the control at all time points, and this ratio

would remain relatively constant over the course of the experiment. One result of

this was that virion release from both the ΔMA and WT viruses can appear to

increase at the same rate over time if the data is plotted as a percentage of

maximum. In Fig. 5.6B, the WT and ΔMA curves are separated by 5 hr at their half-

maximal points. This is not realistic; plotting the raw data without scaling allows an

actual comparison of the phenotypes. However, scaling the data to a max of 100 in

this way does allow the straightforward comparison of the WT GFP and assembly

curves, and an estimate for 15.4 hours as the delay between the midpoints of these

stages of the viral life cycle.

To quantitate the effects of MA deletion on assembly, we chose to measure the time it took both the ΔMA and WT viruses to reach a fixed quantity of virion release after infection. The time point at which a WT HIV-1 infection reaches half of its maximum value is an easily quantifiable point and a reasonable estimate for the kinetic moment at which the infection has been successful enough that it should lead to second rounds of infection in susceptible cultures. We therefore calculated the time required to reach it by both viruses and the distance between them, using a Matlab script. Data are shown in Fig. 5.6, and give a mean estimate of 12.5 hr (+/- 5.4) for the acceleration of assembly caused by the deletion of MA. In order to quantitate the overall enhancement of virion release, we calculated the area under the p24 release curves generated by plotting the intensity of the Western blot virion bands from each time point. The mean enhancement obtained in this manner is 4.4-fold (+/- 3.2). In sum, the presence of MA in HIV-1 leads to a delay of about 13 hours in assembly and a 4-fold decrease in total virion release. This is a very large loss in viral fitness, and there must be strong functional reasons for it. Indeed in almost all cases the total infectious yield in the supernatant of cells infected with the ΔMA virus is much lower than for cells infected with WT HIV-1, despite the much greater concentration of virions.

Fig. 5.5. shows the blots used to calculate these results. Control samples treated after infection with Elvitegravir (ELV), an IN inhibitor, were included as a control. This drug blocks integration and therefore de novo virus production, and any signal

on Western Blots of these supernatants will represent contaminating input virus. In some cases a Neflinavir (NEL) control was used, in order to allow production of new virus that was not infectious, and to serve as a negative control for re-infection with collected supernatant. It is clear from these data that the earliest time point at which we can detect p24 in the supernatant of cells infected with WT HIV-1 is 24 hours post-infection. Maximum levels are reached near 48 hours, but the quantity of released virus rises steeply between 36 and 48 hours. In the case of ΔMA, we can sometimes detect virus as early as 18 hours post-infection, and a sharp increase is typically evident by at least 30 hours post-infection. The infectious titer of the released ΔMA virions is greatly reduced, to about 20% of the level of the WT control.

ΔMA HIV-1 incorporates envelope efficiently

We reasoned that this impaired infectivity was likely to be the result of failure at a critical stage of assembly that could not be completed properly without the delay caused by the presence of the MA domain. One likely possibility was that proper incorporation of Envelope was impaired. A failure of this sort could occur because of Gag targeting to assembly sites more rapidly than Envelope, or it could occur because of targeting to incorrect sites.

However, we did not find any defect in Envelope incorporation by ΔMA HIV-1. Fig. 5.7 shows time course data for MT-4 cell infections, and Fig. 5.8 shows similar data for both 293T and HOS cells. In all cases, Envelope is robustly incorporated into assembling virions, even at the earlier time points of virion release driven by the ΔMA construct. It does appear that Env incorporation increases over time, but this is the case for both the WT and the ΔMA viruses.

ΔMA HIV-1 does not incorporate genome efficiently

Another possible source of the infectivity defect displayed by the ΔMA mutant could be a failure to properly package the genomic RNA. This was more plausible in several respects than was the envelope-incorporation hypothesis. Monomeric Gag with a normally sequestered myristate group is thought to remain in the cytoplasm for some length of time, during which it both initiates early Gag-Gag multimerization interactions and engages the RNA genome. Constitutively myristate-exposed mutants are capable of PM targeting essentially at once, as indicated by the absence of any cytoplasmic fluorescence in studies of fluorescent derivatives of ΔMA Gag[27,69], and indeed we detect virion p24 in the supernatant of cells infected with the ΔMA mutant almost as soon as it is detectable in the lysates. The time between detectability of PM Gag puncta and virion release has been shown to be only

minutes[30,33]. This rapid movement to the PM could potentially take place prior to the

sequence of cytoplasmic interactions required for genome packaging.
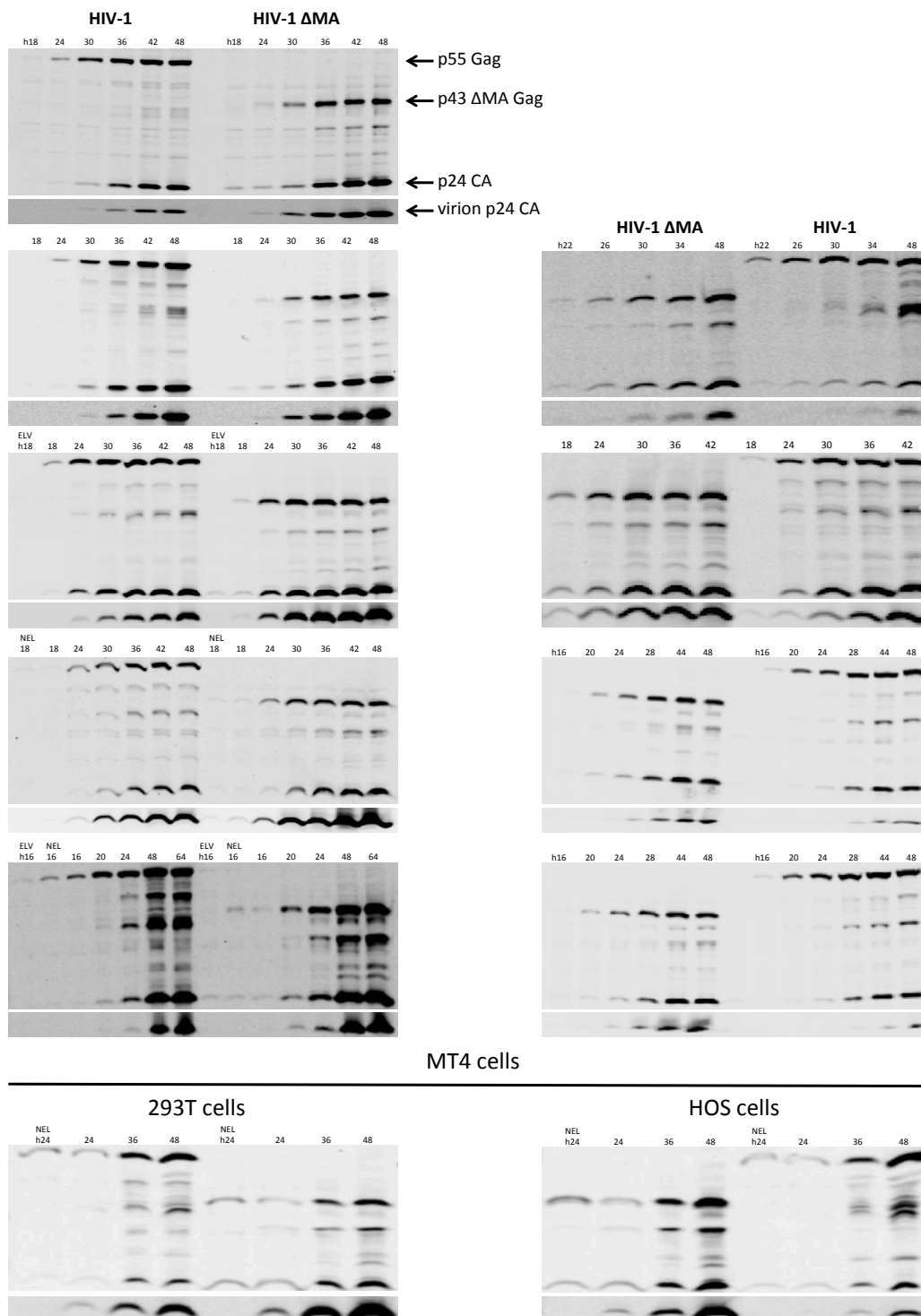
Fig. 5.5. Western blot time courses comparing HIV-1 and ΔMA HIV-1 Gag production and virion release. ELV, elvitegravir control; NEL, Nelfinavir control.
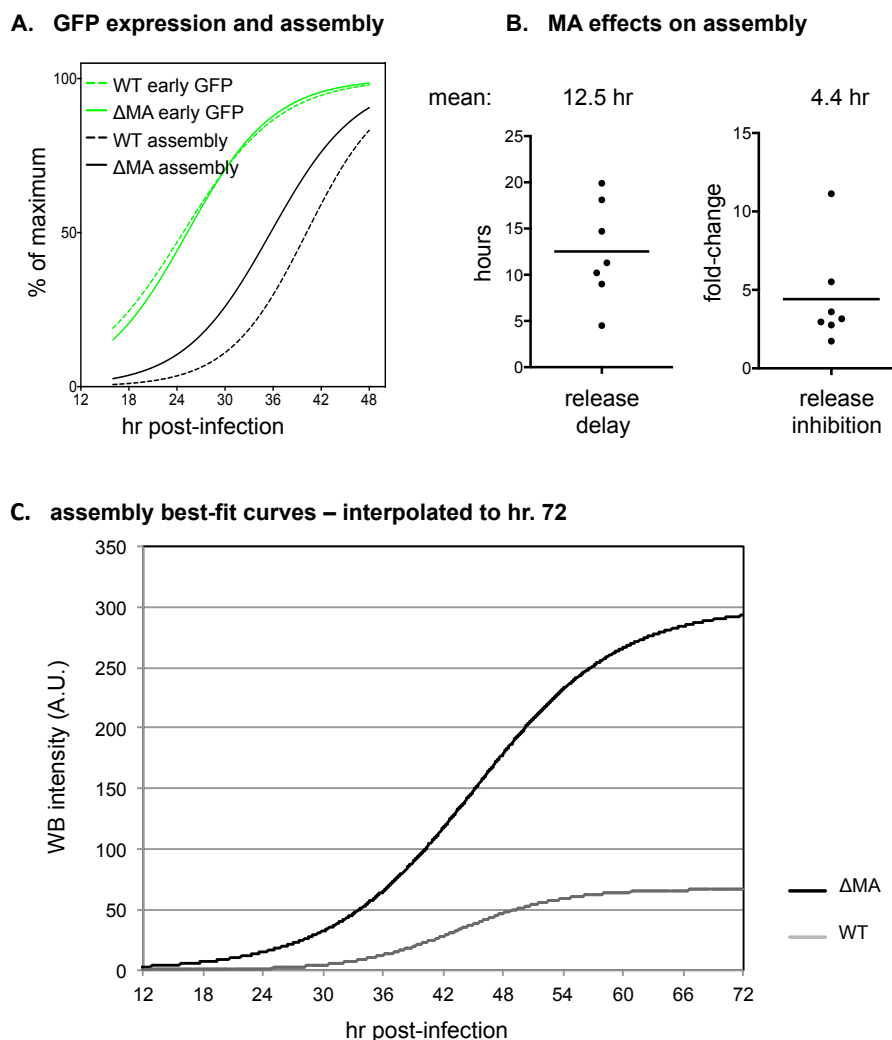
A. GFP expression and assembly

B. MA effects on assembly

mean: 12.5 hr 4.4 hr

C. assembly best-fit curves – interpolated to hr. 72

Fig.5.6. (A) For seven experiments comparing the kinetics of p24 release from infected MT-4 cells, GFP expression and Western blot p24 intensity data was charted over time. Data was plotted as a percentage of maximum, and 4-parameter logistic functions were fit to each data set. The delay between the half-maximum point of WT early GFP expression and WT assembly was calculated to be 15.4 hr. **(B)** The delay between WT and ΔMA assembly was determined by plotting the raw unscaled p24 data, generating point-to-point interpolations of these curves and calculating the distance between the points at which each curve reached a value equal to half of the WT intensity at 48 hr. Overall release inhibition was determined by calculating the area under each curve (AUC) and the relative fold-change in AUC between WT and ΔMA. Mean values are shown +/- SD at the top of the charts. (B) **(C)** 4-parameter logistic functions were fit to to the unscaled data set, to generate representative curves for WT and ΔMA release, and interpolated out to hr. 72.
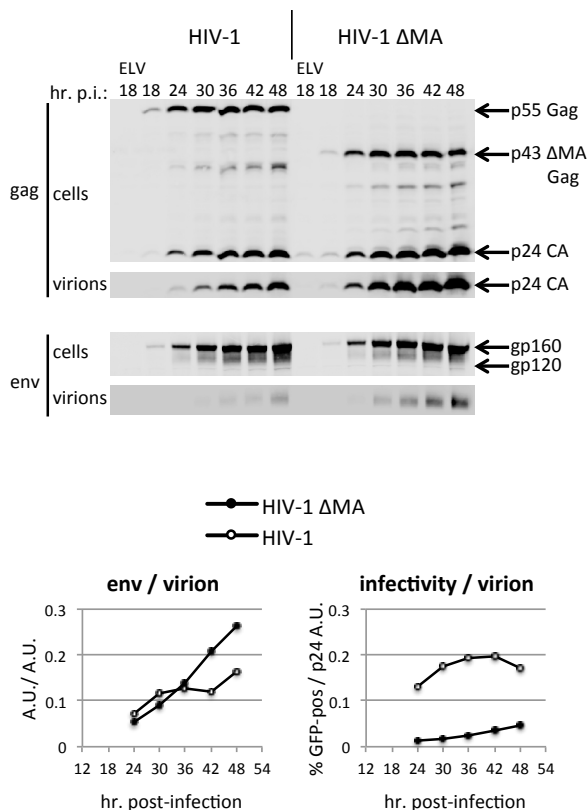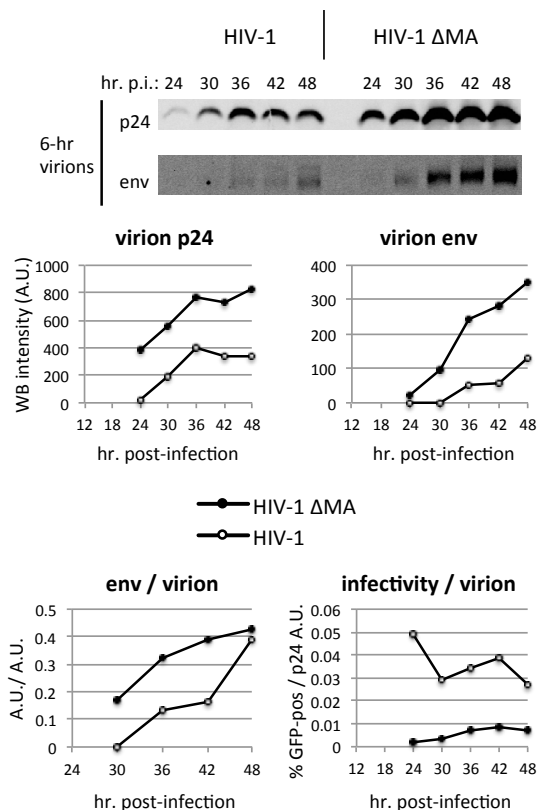
Fig. 5.7. Envelope incorporation in MT-4 cells. A representative Gag and Envelope production and virion release time course is shown in **A.**, with each sample representing cumulative production to the indicated time point. Normalized envelope and infectivity levels over time are shown in the bottom panels. **B.** Blots and quantitation of virions from the same experiment collected after washing cells and culturing for 6 hours between the indicated time points. The middle panels show raw p24 and Env levels in the virions; the bottom panels show normalized Env and infectivity levels. Infectivity in supernatant was assessed by infection of MT2-R5 cells and flow cytometry analysis. Western blots (WB) were quantitated using the Odyssey quantitation software and integrated fluorescence intensities were assigned arbitrary units (A.U.).
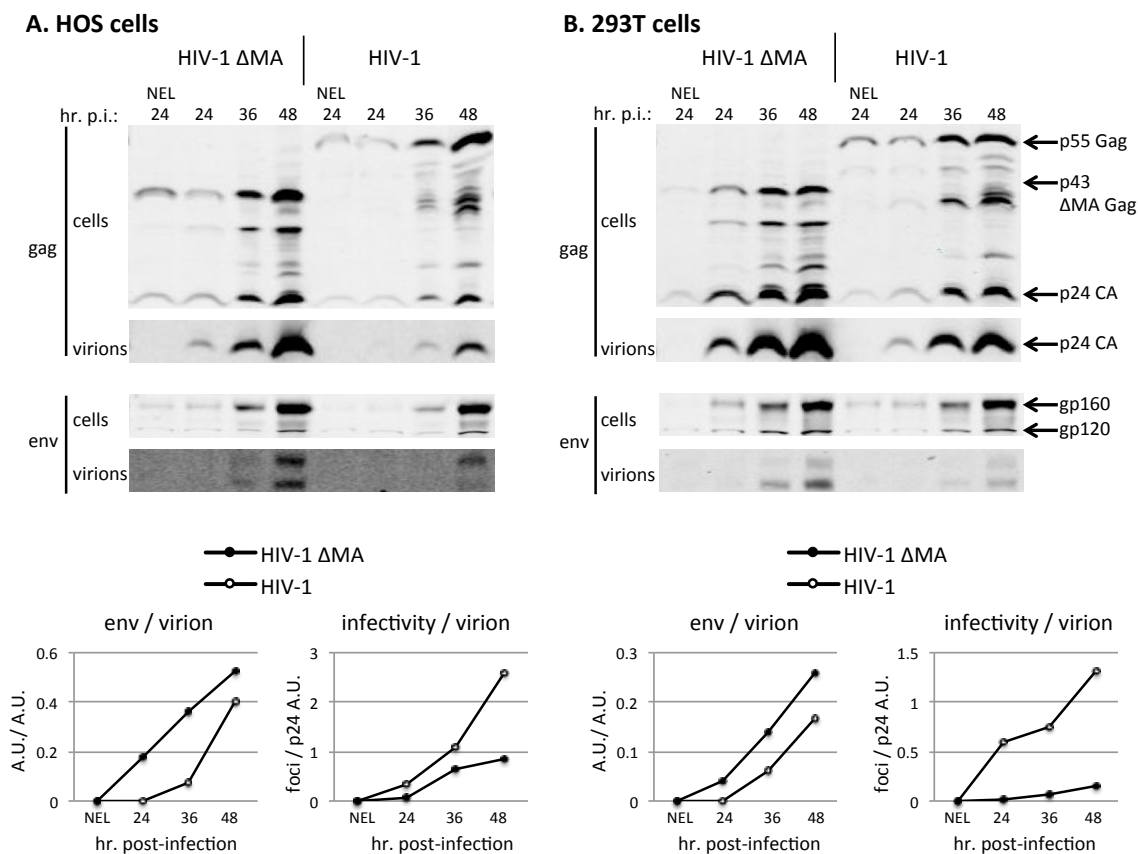
Fig. 5.8. Envelope incorporation in adherent cells. Representative Gag and Envelope production and virion release time courses are shown, with normalized Env and infectivity levels per virion shown in the bottom panels. **A**., HOS cells. **B**., 293T cells. NEL, Nelfinavir. Nelfinavir is a Protease inhibitor added to some samples as a control for input virus contamination. Any visible processed virion p24 in NEL samples is due to the initial inoculum. Infectivity in supernatant was assessed by infection of TZM-bl indicator cells and counting of foci. Western blots (WB) were quantitated using the Odyssey quantitation software and integrated fluorescence intensities were assigned arbitrary units (A.U.).

To examine this, we harvested virions at time points post-infection and used quantitative RT-PCR to analyze their RNA content. When we used primers specific for the GFP sequence carried by these viruses in the early-gene Nef position, we found only modestly reduced levels of HIV-1 RNA in virions. However, HIV-1 is known to nonspecifically package a wide variety of cellular RNAs, and also to package many of its own spliced transcripts. This primer set is not able to distinguish between partial transcripts and full-length genomes.

We therefore used primers specific for the 5'UTR of the genome as a control. These are targeted to a site that that spans the upstream splice site in every spliced viral message, and would therefore only be present in unspliced full-length genomic RNA molecules. In this experiment it was clear that the reduction in the packaging of full genomes by ΔMA virus was much more significant than the overall reduction in viral RNA packaging. Fig. 5.9 (C&D) show that the RNA levels in the supernatant samples are significantly lower when normalized to virion quantity (lower panels) and lower again when using primers for unspliced RNA (right panels). This distinction is even more marked when analyzing the virions collected after washing and culturing for discrete 8hr periods, as in D.

At least at later time points, ΔMA virions packaged close to 80% less genomic RNA per virion as WT – a fraction that corresponds precisely to the defect in infectivity. It was not as straightforward to interpret the data collected from earlier time points,

as we unexpectedly found that WT HIV-1 packaged less genomic RNA at earlier time points than later ones. At these earlier times, the difference between the control and mutant viruses is less marked. Were ΔMA Gag to have a defect in genome packaging relate to its early rapid assembly, we would have expected to see precisely the opposite: that WT Gag would package about the same amount of genomic RNA per virion at every time point, and that ΔMA Gag would package genome poorly at first but more efficiently at later time points. Instead, ΔMA Gag appears to have a similar packaging defect at all times and WT Gag appears to improve over time (Fig. 5.9D, bottom panels).
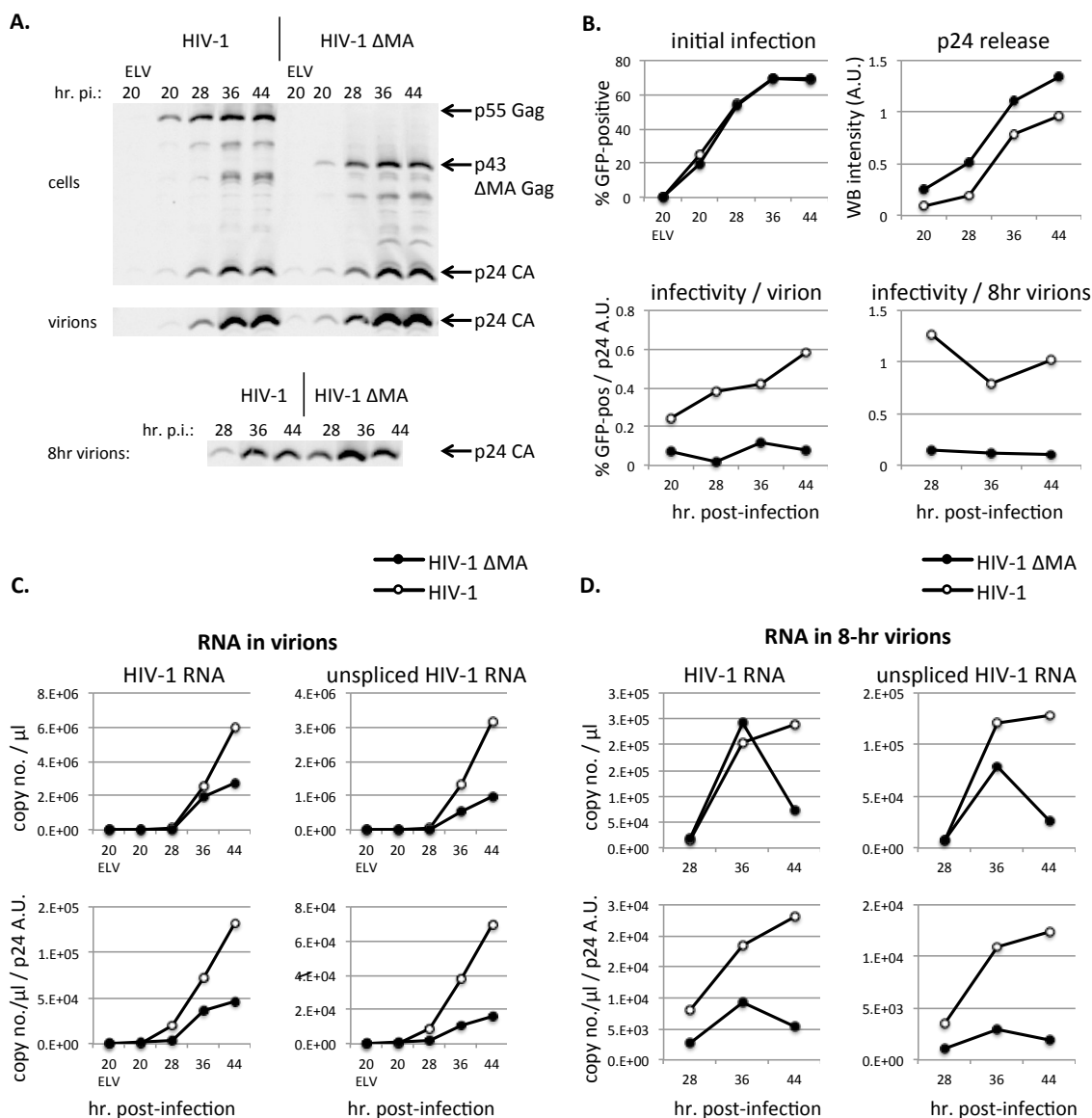
Fig. 5.9. Genomic RNA incorporation in in infected MT-4 cells. A Western blot time course is shown in **A.,** with non-cumulative virions collected by washing and replating for 8hr periods shown in the bottom panel. **B.** The top row shows the progress of the initial infection as cells become GFP positive over time, and the release of p24 into the supernatant. The bottom row shows normalized infectivity over time of both cumulative and non-cumulative virions. Infectivity in supernatant was assessed by infection of MT2-R5 cells and flow cytometry analysis. Western blots (WB) were quantitated using the Odyssey quantitation software and integrated fluorescence intensities were assigned arbitrary units (A.U.). **C.** RNA in cumulative virions. Total HIV-1 RNA using GFP as the target is

on the left; unspliced full-length genomic RNA is on the right. The top row is raw copy numbers; the bottom row is normalized per virion. **D.** The same data is plotted as in **C.,** but for non-cumulative virions. RNA was quantitated by qRT-PCR and is represented as number of copies of cDNA per µl of PCR template.

ΔMA Gag can package WT genome

We reasoned that it should be possible to distinguish between possible causes of this failure on the part of ΔMA Gag to package genomic RNA, by analyzing the concentration dependence of the process. If ΔMA Gag were simply leaving the cytoplasm too rapidly for the normal packaging process to take place, it might still be functional for packaging if it could be brought together with the genome before assembly. Raising the intracellular concentration of genomes should accomplish this and partially restore both packaging and infectivity. If, on the other hand, there was an obligatory mechanistic block to packaging, then it would potentially be insensitive to genome concentration.

To differentiate between these possibilities we provided genome and Gag separately by co-transfecting 293T cells with the components necessary to make infectious virus. We transfected, in increasing amounts, a packageable HIV-1 vector genome (CSGW), and co-transfected a VSV-G envelope and a GagPol plasmid expressing either WT NL4-3 GagPol, or ΔMA NL4-3 GagPol. CSGW is an HIV-1 based gene

transduction vector. It carries a GFP reporter, the viral LTRs, and the viral 5'UTR and packaging sequence, including the majority of MA.

Our initial hypothesis was that at low genome concentrations only the WT Gag would effectively package genomes and generate infectious particles, but that at higher concentrations the ΔMA Gag would potentially be restored to similar levels of packaging as WT. We also thought it possible that the ΔMA Gag would be inefficient at packaging across all concentrations. What we observed (Fig. 5.10) was quite different than either of these potential results. In this context, there was no defect in RNA packaging by ΔMA Gag. ΔMA Gag released higher levels of virions, and packaged correspondingly higher levels of RNA. When normalized, both spliced and unspliced RNA targets were detected at similar levels in WT and ΔMA virions. The infectiousness of both types of particles was approximately equal.

This HIV-1 genomic vector could be packaged equivalently, at all concentrations of genome, by Gag either carrying or lacking the MA region. In the experiments involving infection with full-length virus, assembly of infectious virions by the ΔMA virus required that MA-deleted Gag package genomic RNA molecules that also carried the corresponding deletion at the nucleic acid level. This deletion begins after the 18th nucleotide of the Gag coding region and removes amino acids 7-110 of the 132 amino acid MA gene. The HIV-1 genomic vector used in these transfection experiments, CSGW, carries this entire sequence. The packaging signal that directs

NC-RNA interactions leading to virion incorporation begins in the 5'UTR immediately 5' of MA and runs into the MA coding region. SL4 begins with the initiation codon of MA and is thought to form a base-paired RNA stem-loop structure that maintains base-pairing up until nucleotide 17. Thus, the ΔMA deletion removes a large section of RNA immediately adjacent to this complex structure. SL4 is thought to provide long-range structural interactions that contribute to the overall stability of the Psi region. In addition, stem-loops SL5 and SL6 are absent in ΔMA and are also thought to serve a similar structural role.

In our infection experiments we find greatly reduced infectivity and genomic RNA levels when ΔMA gag is required to package ΔMA genomes. In these transfection experiments, the genome being packaged into virions contains all of MA, is packaged efficiently, and leads to wild-type infectivity levels. In this setting, the deletion of MA from the Gag protein does not have any negative effect on virion assembly. We think it reasonable to conclude from these results that the ΔMA HIV-1 infectivity defect results from a failure to properly package genomic RNA simply as a result of the effect of the ΔMA deletion at the RNA level.
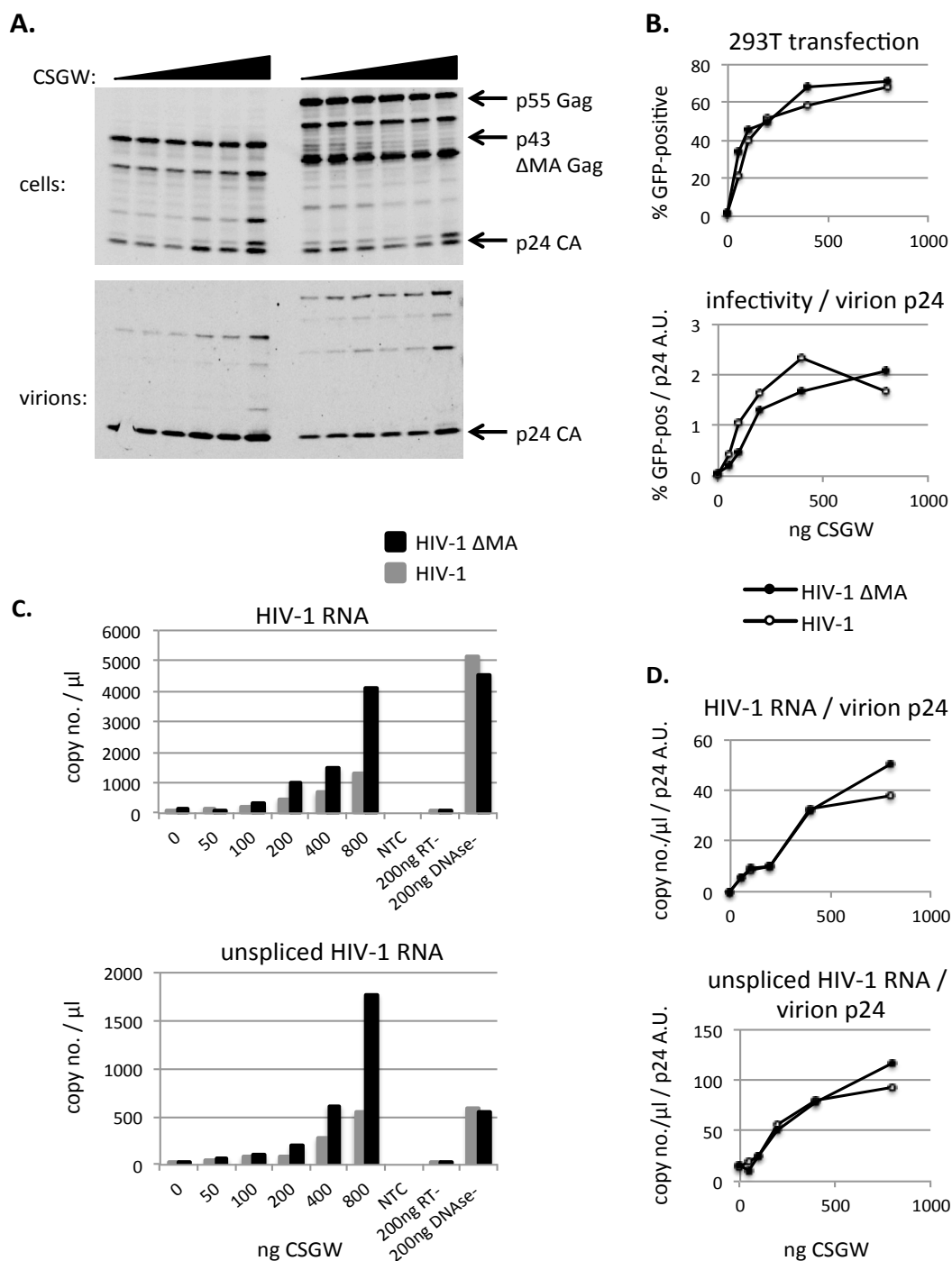
Fig. 5.10. Incorporation by ΔMA Gag of genomic RNA carrying full-length MA sequence. 293T cells were transfected with HIV-1 Gag or ΔMA HIV-1 Gag, VSV-G envelope, and increasing amounts of an HIV-1 vector genome, CSGW, that does

not produce Gag but provides a packageable genome containing the entire Psi sequence and MA region. Lysate and virion Gag production is shown in **A. B.** CSGW carries a GFP coding region; transfected cells fixed at time points were analyzed by flow cytometry to ensure equal transfection in both time courses. The bottom panel shows normalized infectivity data from supernatant collected at time points and titrated on MT-4 cells. Western blots (WB) were quantitated using the Odyssey quantitation software and integrated fluorescence intensities were assigned arbitrary units (A.U.). **C.** Raw RNA copy number data from virion samples, including no-template controls (NTC), Reverse-Transcriptase-negative controls (RT-), and DNAse- controls. RNA was quantitated by qRT-PCR and is represented as number of copies of cDNA per μl of PCR template. **D.** Normalized RNA levels per virion.

References, Chapter 5

1. Schwedler, Von, U. K., Stray, K. M., Garrus, J. E. & Sundquist, W. I. Functional surfaces of the human immunodeficiency virus type 1 capsid protein. *J. Virol.* **77**, 5439–5450 (2003).

2. Gheysen, D. *et al.* Assembly and release of HIV-1 precursor Pr55gag virus-like particles from recombinant baculovirus-infected insect cells. *Cell* **59**, 103–112 (1989).

3. Hogue, I. B., Grover, J. R., Soheilian, F., Nagashima, K. & Ono, A. Gag induces the coalescence of clustered lipid rafts and tetraspanin-enriched microdomains at HIV-1 assembly sites on the plasma membrane. *J. Virol.* **85**, 9749–9766 (2011).

4. Chukkapalli, V., Oh, S. J. & Ono, A. Opposing mechanisms involving RNA and lipids regulate HIV-1 Gag membrane binding through the highly basic region of the matrix domain. *Proceedings of the National Academy of Sciences* **107**, 1600–1605 (2010).

5. Kong, L. B. *et al.* Cryoelectron microscopic examination of human immunodeficiency virus type 1 virions with mutations in the cyclophilin A binding loop. *J. Virol.* **72**, 4403–4407 (1998).

6. Briggs, J. A. G. *et al.* The stoichiometry of Gag protein in HIV-1. *Nat. Struct. Mol. Biol.* **11**, 672–675 (2004).

7. Li, S., Hill, C. P., Sundquist, W. I. & Finch, J. T. Image reconstructions of helical assemblies of the HIV-1 CA protein. *Nature* **407**, 409–413 (2000).

8. Berkowitz, R., Fisher, J. & Goff, S. P. RNA packaging. *Curr. Top. Microbiol. Immunol.* **214**, 177–218 (1996).

9. Lever, A., Göttlinger, H., Haseltine, W. & Sodroski, J. Identification of a sequence required for efficient packaging of human immunodeficiency virus type 1 RNA into virions. *J. Virol.* **63**, 4085–4087 (1989).

10. Freed, E. O. & Martin, M. A. Domains of the human immunodeficiency virus type 1 matrix and gp41 cytoplasmic tail required for envelope incorporation into virions. *J. Virol.* **70**, 341–351 (1996).

11. Camaur, D. & Trono, D. Characterization of human immunodeficiency virus type 1 Vif particle incorporation. *J. Virol.* **70**, 6106–6111 (1996).

12. Zhu, H., Jian, H. & Zhao, L.-J. Identification of the 15FRFG domain in HIV-1 Gag p6 essential for Vpr packaging into the virion. *Retrovirology* **1**, 26 (2004).

13. Jenkins, Y. *et al.* Biochemical analyses of the interactions between human immunodeficiency virus type 1 Vpr and p6(Gag). *J. Virol.* **75**, 10537–10542 (2001).

14. Zhang, F., Zang, T., Wilson, S. J., Johnson, M. C. & Bieniasz, P. D. Clathrin facilitates the morphogenesis of retrovirus particles. *PLoS Pathog.* **7**, e1002119 (2011).

15. Eastman, S. W., Martin-Serrano, J., Chung, W., Zang, T. & Bieniasz, P. D. Identification of human VPS37C, a component of endosomal sorting complex required for transport-I important for viral budding. *J. Biol. Chem.* **280**, 628–636 (2005).

16. Strack, B., Calistri, A., Craig, S., Popova, E. & Gottlinger, H. G. AIP1/ALIX is a binding partner for HIV-1 p6 and EIAV p9 functioning in virus budding. *Cell* **114**, 689–699 (2003).

17. Martin-Serrano, J., Zang, T. & Bieniasz, P. D. Role of ESCRT-I in retroviral budding. *J. Virol.* **77**, 4794–4804 (2003).

18. Garrus, J. E. *et al.* Tsg101 and the vacuolar protein sorting pathway are essential for HIV-1 budding. *Cell* **107**, 55–65 (2001).

19. Lehmann, M., Nikolic, D. S. & Piguet, V. How HIV-1 takes advantage of the cytoskeleton during replication and cell-to-cell transmission. *Viruses* **3**, 1757–1776 (2011).

20. Sheehy, A. M., Gaddis, N. C., Choi, J. D. & Malim, M. H. Isolation of a human gene that inhibits HIV-1 infection and is suppressed by the viral Vif protein. *Nature* **418**, 646–650 (2002).

21. Neil, S. J. D., Zang, T. & Bieniasz, P. D. Tetherin inhibits retrovirus release and is antagonized by HIV-1 Vpu. *Nature* **451**, 425–430 (2008).

22. Perlman, M. & Resh, M. D. Identification of an intracellular trafficking and assembly pathway for HIV-1 gag. *Traffic* **7**, 731–745 (2006).

23. Tritel, M. & Resh, M. D. Kinetic analysis of human immunodeficiency virus type 1 assembly reveals the presence of sequential intermediates. *J. Virol.* **74**,

5845–5855 (2000).

24. Jouvenet, N., Simon, S. M. & Bieniasz, P. D. Visualizing HIV-1 assembly. *J. Mol. Biol.* **410**, 501–511 (2011).

25. Ganser-Pornillos, B. K., Yeager, M. & Sundquist, W. I. The structural biology of HIV assembly. *Curr. Opin. Struct. Biol.* **18**, 203–217 (2008).

26. Kutluay, S. B. & Bieniasz, P. D. Analysis of the initiating events in HIV-1 particle assembly and genome packaging. *PLoS Pathog.* **6**, e1001200 (2010).

27. Perez-Caballero, D., Hatziioannou, T., Martin-Serrano, J. & Bieniasz, P. D. Human immunodeficiency virus type 1 matrix inhibits and confers cooperativity on gag precursor-membrane interactions. *J. Virol.* **78**, 9560–9563 (2004).

28. Datta, S. A. K. *et al.* Conformation of the HIV-1 Gag protein in solution. *J. Mol. Biol.* **365**, 812–824 (2007).

29. Zhou, W. & Resh, M. D. Differential membrane binding of the human immunodeficiency virus type 1 matrix protein. *J. Virol.* **70**, 8540–8548 (1996).

30. Jouvenet, N., Bieniasz, P. D. & Simon, S. M. Imaging the biogenesis of individual HIV-1 virions in live cells. *Nature* **454**, 236–240 (2008).

31. Ono, A., Waheed, A. A. & Freed, E. O. Depletion of cellular cholesterol inhibits membrane binding and higher-order multimerization of human immunodeficiency virus type 1 Gag. *Virology* **360**, 27–35 (2007).

32. Nermut, M. V. *et al.* Time course of Gag protein assembly in HIV-1-infected cells: a study by immunoelectron microscopy. *Virology* **305**, 219–227 (2003).

33. Ivanchenko, S. *et al.* Dynamics of HIV-1 assembly and release. *PLoS Pathog.* **5**, e1000652 (2009).

34. Goila-Gaur, R., Demirov, D. G., Orenstein, J. M., Ono, A. & Freed, E. O. Defects in human immunodeficiency virus budding and endosomal sorting induced by TSG101 overexpression. *J. Virol.* **77**, 6507–6519 (2003).

35. Spearman, P., Wang, J. J., Vander Heyden, N. & Ratner, L. Identification of human immunodeficiency virus type 1 Gag protein domains essential to membrane binding and particle assembly. *J. Virol.* **68**, 3232–3242 (1994).

36. Saad, J. S. *et al.* Structural basis for targeting HIV-1 Gag proteins to the plasma membrane for virus assembly. *Proc. Natl. Acad. Sci. U.S.A.* **103**, 11364–11369

(2006).

37. Spearman, P., Horton, R., Ratner, L. & Kuli-Zade, I. Membrane binding of human immunodeficiency virus type 1 matrix protein in vivo supports a conformational myristyl switch mechanism. *J. Virol.* **71**, 6582–6592 (1997).

38. Bryant, M. & Ratner, L. Myristoylation-dependent replication and assembly of human immunodeficiency virus 1. *Proc. Natl. Acad. Sci. U.S.A.* **87**, 523–527 (1990).

39. Sandefur, S., Smith, R. M., Varthakavi, V. & Spearman, P. Mapping and characterization of the N-terminal I domain of human immunodeficiency virus type 1 Pr55(Gag). *J. Virol.* **74**, 7238–7249 (2000).

40. Ono, A., Demirov, D. & Freed, E. O. Relationship between human immunodeficiency virus type 1 Gag multimerization and membrane binding. *J. Virol.* **74**, 5142–5150 (2000).

41. Zhang, W. H., Hockley, D. J., Nermut, M. V., Morikawa, Y. & Jones, I. M. Gag-Gag interactions in the C-terminal domain of human immunodeficiency virus type 1 p24 capsid antigen are essential for Gag particle assembly. *J. Gen. Virol.* **77 (Pt 4)**, 743–751 (1996).

42. Carrière, C., Gay, B., Chazal, N., Morin, N. & Boulanger, P. Sequence requirements for encapsidation of deletion mutants and chimeras of human immunodeficiency virus type 1 Gag precursor into retrovirus-like particles. *J. Virol.* **69**, 2366–2377 (1995).

43. Li, H., Dou, J., Ding, L. & Spearman, P. Myristoylation is required for human immunodeficiency virus type 1 Gag-Gag multimerization in mammalian cells. *J. Virol.* **81**, 12899–12910 (2007).

44. Burniston, M. T., Cimarelli, A., Colgan, J., Curtis, S. P. & Luban, J. Human immunodeficiency virus type 1 Gag polyprotein multimerization requires the nucleocapsid domain and RNA and is promoted by the capsid-dimer interface and the basic region of matrix protein. *J. Virol.* **73**, 8527–8540 (1999).

45. Ono, A., Orenstein, J. M. & Freed, E. O. Role of the Gag matrix domain in targeting human immunodeficiency virus type 1 assembly. *J. Virol.* **74**, 2855–2866 (2000).

46. Ono, A. & Freed, E. O. Binding of human immunodeficiency virus type 1 Gag to membrane: role of the matrix amino terminus. *J. Virol.* **73**, 4136–4144 (1999).

47. Alfadhli, A. *et al.* HIV-1 matrix protein binding to RNA. *J. Mol. Biol.* **410**, 653–

666 (2011).

48. Alfadhli, A., Still, A. & Barklis, E. Analysis of human immunodeficiency virus type 1 matrix binding to membranes and nucleic acids. *J. Virol.* **83**, 12196–12203 (2009).

49. Ott, D. E., Coren, L. V. & Gagliardi, T. D. Redundant roles for nucleocapsid and matrix RNA-binding sequences in human immunodeficiency virus type 1 assembly. *J. Virol.* **79**, 13839–13847 (2005).

50. Purohit, P., Dupont, S., Stevenson, M. & Green, M. R. Sequence-specific interaction between HIV-1 matrix protein and viral genomic RNA revealed by in vitro genetic selection. *RNA* **7**, 576–584 (2001).

51. Ono, A., Ablan, S. D., Lockett, S. J., Nagashima, K. & Freed, E. O. Phosphatidylinositol (4,5) bisphosphate regulates HIV-1 Gag targeting to the plasma membrane. *Proc. Natl. Acad. Sci. U.S.A.* **101**, 14889–14894 (2004).

52. Poon, D. T., Li, G. & Aldovini, A. Nucleocapsid and matrix protein contributions to selective human immunodeficiency virus type 1 genomic RNA packaging. *J. Virol.* **72**, 1983–1993 (1998).

53. Datta, S. A. K. *et al.* HIV-1 Gag extension: conformational changes require simultaneous interaction with membrane and nucleic acid. *J. Mol. Biol.* **406**, 205–214 (2011).

54. Jones, C. P., Datta, S. A. K., Rein, A., Rouzina, I. & Musier-Forsyth, K. Matrix domain modulates HIV-1 Gag's nucleic acid chaperone activity via inositol phosphate binding. *J. Virol.* **85**, 1594–1603 (2011).

55. Datta, S. A. K. *et al.* Interactions between HIV-1 Gag molecules in solution: an inositol phosphate-mediated switch. *J. Mol. Biol.* **365**, 799–811 (2007).

56. Berkowitz, R. D., Luban, J. & Goff, S. P. Specific binding of human immunodeficiency virus type 1 gag polyprotein and nucleocapsid protein to viral RNAs detected by RNA mobility shift assays. *J. Virol.* **67**, 7190–7200 (1993).

57. Roldan, A. *et al.* In vitro identification and characterization of an early complex linking HIV-1 genomic RNA recognition and Pr55Gag multimerization. *J. Biol. Chem.* **279**, 39886–39894 (2004).

58. Wang, S.-W. & Aldovini, A. RNA incorporation is critical for retroviral particle integrity after cell membrane assembly of Gag complexes. *J. Virol.* **76**, 11853–11865 (2002).

59.   Khorchid, A., Halwani, R., Wainberg, M. A. & Kleiman, L. Role of RNA in facilitating Gag/Gag-Pol interaction. *J. Virol.* **76**, 4131–4137 (2002).

60.   Clever, J., Sassetti, C. & Parslow, T. G. RNA secondary structure and binding sites for gag gene products in the 5' packaging signal of human immunodeficiency virus type 1. *J. Virol.* **69**, 2101–2109 (1995).

61.   Paoletti, A. C., Shubsda, M. F., Hudson, B. S. & Borer, P. N. Affinities of the nucleocapsid protein for variants of SL3 RNA in HIV-1. *Biochemistry* **41**, 15423–15428 (2002).

62.   Shubsda, M. F., Paoletti, A. C., Hudson, B. S. & Borer, P. N. Affinities of packaging domain loops in HIV-1 RNA for the nucleocapsid protein. *Biochemistry* **41**, 5276–5282 (2002).

63.   Roldan, A., Liang, C. & Wainberg, M. A. Structural changes in the SL5 and SL6 leader sequences of HIV-1 RNA following interactions with the viral mGag protein. *Virus Res.* **155**, 98–105 (2011).

64.   Paillart, J.-C., Skripkin, E., Ehresmann, B., Ehresmann, C. & Marquet, R. In vitro evidence for a long range pseudoknot in the 5'-untranslated and matrix coding regions of HIV-1 genomic RNA. *J. Biol. Chem.* **277**, 5995–6004 (2002).

65.   Amarasinghe, G. K. *et al.* Stem-loop SL4 of the HIV-1 psi RNA packaging signal exhibits weak affinity for the nucleocapsid protein. structural studies and implications for genome recognition. *J. Mol. Biol.* **314**, 961–970 (2001).

66.   Spriggs, S., Garyu, L., Connor, R. & Summers, M. F. Potential intra- and intermolecular interactions involving the unique-5' region of the HIV-1 5'-UTR. *Biochemistry* **47**, 13064–13073 (2008).

67.   Heng, X. *et al.* Identification of a minimal region of the HIV-1 5'-leader required for RNA dimerization, NC binding, and packaging. *J. Mol. Biol.* **417**, 224–239 (2012).

68.   Lu, K. *et al.* NMR detection of structures in the HIV-1 5'-leader RNA that regulate genome packaging. *Science* **334**, 242–245 (2011).

69.   Hatziioannou, T., Martin-Serrano, J., Zang, T. & Bieniasz, P. D. Matrix-induced inhibition of membrane binding contributes to human immunodeficiency virus type 1 particle assembly defects in murine cells. *J. Virol.* **79**, 15586–15589 (2005).

70.   Reil, H., Bukovsky, A. A., Gelderblom, H. R. & Göttlinger, H. G. Efficient HIV-1 replication can occur in the absence of the viral matrix protein. *EMBO J.* **17**,

2699–2708 (1998).

71. Rescue of human immunodeficiency virus type 1 matrix protein mutants by envelope glycoproteins with short cytoplasmic domains. **69**, 3824–3830 (1995).

72. Ono, A. & Freed, E. O. Plasma membrane rafts play a critical role in HIV-1 assembly and release. *Proc. Natl. Acad. Sci. U.S.A.* **98**, 13925–13930 (2001).

73. Lindwasser, O. W. & Resh, M. D. Multimerization of human immunodeficiency virus type 1 Gag promotes its localization to barges, raft-like membrane microdomains. *J. Virol.* **75**, 7913–7924 (2001).

74. Perelson, A. S., Neumann, A. U., Markowitz, M., Leonard, J. M. & Ho, D. D. HIV-1 dynamics in vivo: virion clearance rate, infected cell life-span, and viral generation time. *Science* **271**, 1582–1586 (1996).

75. Coombs, D., Gilchrist, M. A., Percus, J. & Perelson, A. S. Optimal viral production. *Bull. Math. Biol.* **65**, 1003–1023 (2003).

76. Dixit, N. M., Markowitz, M., Ho, D. D. & Perelson, A. S. Estimates of intracellular delay and average drug efficacy from viral load data of HIV-infected individuals under antiretroviral therapy. *Antivir. Ther. (Lond.)* **9**, 237–246 (2004).

77. Li, Y. *et al.* Molecular characterization of human immunodeficiency virus type 1 cloned directly from uncultured human brain tissue: identification of replication-competent and -defective viral genomes. *J. Virol.* **65**, 3973–3985 (1991).

78. Meister, S. *et al.* Basic amino acid residues in the V3 loop of simian immunodeficiency virus envelope alter viral coreceptor tropism and infectivity but do not allow efficient utilization of CXCR4 as entry cofactor. *Virology* **284**, 287–296 (2001).

79. Kato, K., Sato, H. & Takebe, Y. Role of naturally occurring basic amino acid substitutions in the human immunodeficiency virus type 1 subtype E envelope V3 loop on viral coreceptor usage and cell tropism. *J. Virol.* **73**, 5520–5526 (1999).

Chapter 6. Materials and Methods

Cells and tissue culture

293T (ATCC #: CRL-11268) and HOS (ATCC #: CRL-1543) cells were obtained from

ATCC and grown in DMEM supplemented with 10% fetal bovine serum. MT-4 cells,

obtained from the NIH AIDS Research and Reference Reagent Program, were

cultured in RPMI supplemented with 10% fetal bovine serum. HOS and MT-4 cells

stably expressing cherry-APOBEC3G (cherry-A3G) or a chimeric tetherin gene

(humoTeth[1]) were generated by transduction with a retroviral vector (pBMN-IRES-

Blasti) that allowed production of the gene of interest and the selectable marker

Blasticidin from the same transcript and were grown in DMEM supplemented with

10% fetal bovine serum and 10μg/ml Blasticidin. The plasmids pBMN-IRES-Blasti

and pBMN-humoTeth-IRES-Blasti were kindly provided by Bieniasz lab member

Fengweng Zhang. pBMN-A3G-IRES-Blasti was kindly provided by Bieniasz lab

member Steven Soll, and the mCherry coding sequence was placed in frame as an N-

terminal fusion to A3G using XhoI and NotI sites. Retroviral stocks of pBMN-cherry-

A3G-IRES-Blasti or pBMN-humoTeth-Blasti were produced by co-transfection of the

genomic vector plasmid with a plasmid expressing MLV Gag-Pol, a plasmid

expressing the VSV-G envelope protein from the VSV virus, and also (in the case of

pBMN-cherry-A3G-IRES-Blasti) a plasmid expressing HIV-1 Vif to block A3G-

mediated effects on the retroviral virions themselves. HumoTeth is a chimeric human tetherin that carries the extracellular domain of mouse tetherin. This tetherin has the same restrictive and Vpu-counteraction properties as human tetherin, but is very easily detectable on the surface of cells using an anti-mouse-tetherin antibody. At the time these experiments were performed there was no effective antibody available against human tetherin. Human PBMCs were isolated from blood using Ficoll-paque gradient centrifugation, stimulated with phytohemagglutinin for 2 days, and then grown in RPMI with 10% fetal bovine serum in the presence of IL-2 (20 U/ml, Roche) for a further 3 days before use.

Viruses

The HIV-1 reporter viruses NL4.Nef:GFP, NL4.MA-GFP, NL4.MA-GFP.Nef:cherry, NL4.MA-cherry.Nef:GFP were constructed using overlap PCR to insert GFP or cherry in either the Nef or Gag positions within the full-length HIV-1 proviral clone NL4.3.dINdRTdEnv., kindly provided by Bieniasz lab member Noulwenn Jouvenet. This virus does not produce Envelope, and carries inactivating mutations in both the Integrase and Reverse Transcriptase genes, rendering it both replication-incompetent and safe to work with in non-BSL-3 environments. Fluorophores in the Nef position were inserted directly in frame, beginning with the native start codon of Nef. Fluorophores internal to Gag were inserted at the protease site between MA

and CA by duplicating this site (with amino acid sequence "VSQNYPIVQ") so that the ten amino acid linker "PIVQNAAAGS" is upstream of the fluorophore coding sequence, immediately after the final codon of MA, and the ten amino acid linker "GSAAAVSQNY" is downstream of the fluorophore coding sequence, immediately before the first codon of CA.

For assembly experiments, the viruses used were constructed in the context of the full-length HIV-1 proviral clone NHG[2] (*GenBank: JQ585717.1*). NHG is a replication-competent virus carrying GFP in the Nef position. It includes Gag-Pol sequence from NL4.3{Westervelt:1991tl} (*GenBank: U26942.1*), and is otherwise derived from proviral clone HXB2[3] *(GenBank: K03455.1).* NHG was modified by the addition of a stop codon after nucleotide 2133 of the env gene, effectively removing the 142 C-terminal residues of the cytoplasmic tail of the Env protein, and by replacement of the V3 region of env (nucleotides 915:975) with the V3 region from the R5-tropic proviral clone YU2[4] (*GenBank: M93258.1*). This virus, NHG. ΔCT.YU2V3 was used as the control for all experiments involving the ΔMA mutant, and served as the backbone for the construction of NHG.ΔMA.ΔCT.YU2V3 (referred to as in the text as ΔMA.HIV-1) by the deletion of residues 7-110 of the Gag gene. The ΔMA deletion in NHG.ΔMA.ΔCT.YU2V3 and in ΔMA.NLGagPol was generated by replacing the BssHII-SpeI fragment with the corresponding fragment from ΔMA.NL4-3, kindly provided by Trinity Zang. All plasmid construction was performed using overlap PCR and standard molecular biology techniques.

Transfections and infections

All viral stocks used in these studies were pseudotyped with the VSV-G envelope

protein[5] from the VSV virus and produced by transfection of semiconfluent 10cm

plates of 293T cells with 10ug of proviral plasmid and 1ug of VSV-G expression

vector, using polyethyleneimine (PEI; PolySciences, Warrington, Pennsylvania,

United States)at a DNA:PEI ratio of 1:4. Cells were incubated overnight and medium

containing the transfection mixture was replaced with fresh medium the following

day. Reporter viruses that carried deletions in the Pol gene and/or fluorophore

insertions in the MA region were produced by transfection of the proviral plasmid,

the VSV-G plasmid, and an NL4-3 GagPol-expressing plasmid at a ratio of 5:1:5.

These insertions and/or deletions can be complemented in trans by provision of WT

GagPol, allowing production of infectious virus competent for a single round of

infection. Viral supernatants were harvested on the following two days, filtered

through a .22 micron filter and stored in aliquots at -80°. All viruses carried at least

one fluorescent reporter gene, and viral titers were determined by infection of MT-4

cells in serial dilutions, collection of cells at 48 hours post-infection, and flow

cytometry to quantify the percentage of infected cells.

For the assembly experiments utilizing transfection of subgenomic plasmids, co-

transfections of 293T cells in 12 well plates were performed with PEI, using

increasing amounts (50-800ng) of the HIV-1-derived vector CSGW[6], 20ng of the

VSV-G envelope, and 100ng of NLGag-Pol or ΔMA.NLGagPol. Infectious virions were titrated on MT-4 cells.

All infection time courses used a synchronized infection protocol as follows: virus was added to cells in 6 well or 12 well dishes, in the presence of 5µg/ml polybrene, cells were centrifuged at 15℃ for 45minutes, moved to a 37℃ incubator for 2 hours and then washed three times and fed with fresh medium. MT-4 cells were washed by resuspension and centrifugation, and replated in the appropriate dishes. Supernatant and lysate samples were collected at regular time point intervals and analyzed by Western blotting. Infectivity in the supernatant was analyzed by infection in serial dilutions of MT2-R5 target cells carrying the HIV-1 receptor CD4 and the co-receptor CCR5. In some cases, infectivity was analyzed by infection of Hela-TZM indicator cells, which also carry CD4 and CCR5, and in addition carry the HIV-1 LTR promoter region upstream of the gene encoding *E. coli* β-galactosidase (lacZ). Expression of the lacZ gene is dependent upon Tat transactivation of the LTR. Once a cell is infected, Tat is produced, activating the LTR to drive β-galactosidase production, which can then be detected with the chromogenic substrate X-gal. Hela-TZM cells are plated in 24-well plates, infected with limiting dilutions of infectious supernatant, and fixed in 0.2% glutaraldehyde in PBS at 48hr post-infection. They are then stained with X-gal staining solution and and the blue foci generated for each infection event are enumerated by microscope.

Staining and Flow cytometry

Cells expressing the human-mouse chimeric tetherin were collected at time points after infection and washed twice by centrifugation and resuspension in PBS. Adherent cells were collected using PBS with 5mM EDTA. Cells were suspended in a 50X dilution of APC-conjugated antibody to mouse tetherin (anti-mouse-mPDCA1; Miltenyi Biotec) in PBS, incubated at 4° for 90 minutes, washed three times in PBS with 0.2% BSA and fixed in PBS with 2% PFA.

Cells not requiring staining were collected, by trypsinization for adherent cells, and fixed in a 2% final concentration of PFA. Flow cytometry was performed on a CyFlow Space flow cytometer (PARTEC) using a blue 488nm laser for the excitation of GFP, a yellow 561nm laser for excitation of mCherry and a red 638nm laser for excitation of APC. Samples were loaded using a connected Hypercyte Autosampler 96well plate-sampling machine (Intellicyt). Results were analyzed using FlowJo flow cytometry analysis software (Treestar Inc.). All gates were set to include less than 1% of the negative population. GFP v. mCherry plots represent cells previously gated on FSC v SSC plots to remove dead cells from analysis, and on FSC H v FSC W plots to remove doublets from analysis.

Western blotting

Cells were grown in 12 or 24 well plates, collected at time points (by trypsinization or PBS-EDTA if adherent) centrifuged, resuspended in SDS-PAGE loading buffer and stored at -80℃. 10% of the cells were first set aside for PFA fixation and flow cytometry analysis. Viral supernatants were clarified by centrifugation at 1000 rpm for 5 min. The cleared supernatants were filtered (0.22 μm), layered over 20% sucrose in 1X PBS and centrifuged at 14,000 rpm in an Eppendorf 5417R microfuge for 2 hours at 4°. After aspiration of supernatant pellets were resuspended in 80 ul SDS-PAGE loading buffer and stored at -80°.

Prior to loading on gels, samples were thawed and heated to 70 for 15 minutes. Cell lysate samples were further disrupted by sonication. Cell lysates and virion samples were separated on 4–12% acrylamide gels (Novex) and proteins transferred to nitrocellulose membranes which were then probed with antibodies against HIV-1 Gag (183-H12-5C) and HIV-1 Env (ID6), both from the NIH AIDS Research and Reference Reagent Program. The blots were then probed with anti-mouse IgG conjugated to IR Dye800 CW (LiCOR). They were scanned using the LiCOR Odyssey IR imager and quantified using Odyssey quantification software.

Quantitation and comparison of time course Western blot data for p24 release was done with a simple Matlab script. In order to determine the delay in assembly caused by MA it was not possible to measure between p24 release curves expressed

as a percent of maximum, because the similar rates of change, although in different intensity ranges, caused these curves to resemble each other. Instead we plotted the raw values for p24 intensity over time for both WT and ΔMA and calculated the distance between these curves at this point, to determine how long it takes ΔMA viral release to reach half of the WT release value. We used a simple Matlab script to fit point-to-point interpolations to these curves, to identify points closest to the 50% value on the WT release curve, and to calculate the distance in hours between the WT and ΔMA curves at this intensity value. We calculated this delay value for seven experiments performed in MT-4 cells with identical time points (Fig. 5.6A). The values for 293T and HOS cells were not included, but they were quite similar, as can be seen in Fig. 5.5. To determine the magnitude of enhanced virus release in the absence of MA we use the same interpolated p24 release curves and calculated the area under each curve. In addition we fit 4-parameter logistic curves to the entire WT data set and the entire ΔMA data set (Fig. 5.6B), and calculated the release delay (13.5 hr) and total release difference (4.5 hr) between these two fit-curves in the same way as we did for the individual curves. These values are almost identical with those obtained by analyzing the experiments individually and taking the mean.

Real-Time PCR

Viral RNA was isolated from virions after pelleting as described above for Western

blotting. Virion pellets were resuspended in 80μl PBS, 20μl of which was used for RNA isolation with the QIAmp Viral RNA kit (Qiagen). The remaining 60μl was lysed with 60μl of 2X SDS-PAGE loading buffer, and processed for Western blotting. RNA samples were reverse-transcribed using the ImProm-II Reverse Transcription system (Promega). The resulting cDNA was used as template for quantitative real-time PCR (qRT-PCR) using the ABI 7500 Fast RT-PCR system. Viral RNA was quantitated using a SYBR Green-based assay (Roche) with the following primer pairs: GFP.FWD: AAGTTCATCTGCACCACCGGCAA; GFP.REV: TGCACGCCGTAGGTCAGG; 5'UTR-FWD: CGGCGACTGGTGAGTACG; 5'UTR-REV: GACGCTCTCGCACCCAT. A standard curve using known copy numbers of NL4-3 plasmid was generated for quantitation of copy numbers of RNA in virions.

Microscopy

Live-cell time-lapse microscopy was performed using a VivaView FL incubator microscope (Olympus). MT-4 cells and PBMC were infected as described above, washed, and adhered to glass-bottom dishes using Cell-Tak adhesive (BD Biosciences). Cell-Tak coated plates were prepared on the day of use by an adsorption method, as follows. 10μl Cell-Tak is added to 285μl sodium bicarbonate pH 8.0 and 5 μl 1M NaOH and this solution is dispensed onto the glass regions of the microscopy plates. These are incubated for 20min at room temperature, the solution

is aspirated, and the plates are washed 3X with sterile water and allowed to air-dry at room temperature. This procedure is carried out inside a sterile tissue culture hood. After infection and washing in plastic tissue culture plates, cells were dispensed into these plates, centrifuged at 1500RPM for 8 minutes and immediately transferred to the microscope incubator. Images of MT-4 cells and PBMC were captured every 4-8 minutes.

Preparation of movies and quantitation of microscope data was performed using Metamorph software (Molecular Devices). For quantitation over time, regions were drawn closely around immobilized cells and max intensity at each frame was logged. Control regions next to each cell were also logged. Background-corrected plots of intensity over time for each cell were generated by subtracting the control region intensity from the cell intensity at each time point. These curves were then fit to 5-parameter logistic equations using a custom Matlab script. The script then defined the point in time at which the intensity trace rose above background levels as the first point on the fit curve at least seven intensity units above the lower horizontal asymptote, and these points were used to calculate the time difference between the GFP and mCherry intensity traces for each cell.

Anti-retroviral drugs

Anti-retrovirals were used in the inhibitor time course experiments and as controls

in the assembly assays. Elvitegravir, an Integrase inhbitor was used at 400nM.

Efavirenz and Nevirapine, Reverse-Transcriptase inhibitors, were used at 200nM

and 2μM, respectively. Nelfinavir, a Protease inhibitor was used at 5μM.

References, Chapter 6

1. Zhang, F. *et al.* SIV Nef proteins recruit the AP-2 complex to antagonize Tetherin and facilitate virion release. *PLoS Pathog.* **7**, e1002039 (2011).

2. Wilson, S. J. *et al.* Inhibition of HIV-1 particle assembly by 2',3"-cyclic-nucleotide 3"-phosphodiesterase. *Cell Host Microbe* **12**, 585–597 (2012).

3. Ratner, L. *et al.* Complete nucleotide sequences of functional clones of the AIDS virus. *AIDS Res. Hum. Retroviruses* **3**, 57–69 (1987).

4. Li, Y. *et al.* Molecular characterization of human immunodeficiency virus type 1 cloned directly from uncultured human brain tissue: identification of replication-competent and -defective viral genomes. *J. Virol.* **65**, 3973–3985 (1991).

5. Aiken, C. Pseudotyping human immunodeficiency virus type 1 (HIV-1) by the glycoprotein of vesicular stomatitis virus targets HIV-1 entry to an endocytic pathway and suppresses both the requirement for Nef and the sensitivity to cyclosporin A. *J. Virol.* **71**, 5871–5877 (1997).

6. High-level transduction and gene expression in hematopoietic repopulating cells using a human immunodeficiency [correction of imunodeficiency] virus type 1-based lentiviral vector containing an internal spleen focus forming virus promoter. **13**, 803–813 (2002).

Chapter 7. Discussion.

Kinetic optimization

Early in the HIV-1 epidemic Alan Perelson, Marty Markowitz and David Ho used a combination of mathematical modeling and experimental data obtained from patients in the first hours and days of anti-retroviral therapy to determine that both viral production and clearance were far higher than had initially been supposed[1-4]. This approach relied upon the fact that the rate with which viremia drops upon treatment initiation is a function of both the virion production rate and the death rate of infected cells, and it provided the theoretical basis upon which the now-standard multidrug HAART therapy approach would be founded. However, the earliest versions of these models assumed that cells could produce virus immediately upon infection. Only in the following years were they expanded to take into account the "eclipse time" — the time between infection and viral production[5-7]. Successive refinements led to the conclusion that this intracellular delay period was about 24 hours, and that the lifetime of infected cells was on average another 24 hours once production began[8-11]. It was understood that such models were of necessity oversimplifications, and that in particular they failed to take into account the fact that viral production was unlikely to begin at the same rate it would ultimately attain. It was also apparent that the rate of viral production was itself subject to natural selection, and would presumably be optimized to maximize the

amount of infectious virions produced before the death of the infected cell[12,13]. Still, for the purposes of mathematical modeling of infection, there was no reason why the eclipse time could not remain a black box. What mattered was exactly when the intracellular delay would come to an end and infectious virus would begin to emerge from cells, and what the dynamics of viral production would be from that moment on. The work presented in this thesis tries to clarify the timing of the events that take place during the intracellular eclipse. It is these events that will dictate the dynamics of virion production from cells, when it does begin, and ultimately the course that viral pathogenesis will take in an infected host.

Just as theoretical work has suggested that viral pathogenesis and replication rates in a host organism are likely to reflect the balance between transmission and death rate[14-19], the kinetics of viral production from an infected cell are expected to reflect a balance between the time available for production and the possibility that high viral replication may itself contribute to a shorter cellular lifetime available for that production[12,20,21]. Viral protein synthesis may have direct cytotoxic effects and also generate increased visibility to immune surveillance leading to cytotoxic T-cell killing of infected cells. Newer models of HIV-1 replication that take these facts into account[12,13] find that in such cases the optimal levels of production may be lower than the theoretical maximum. They also find that the rates of change of viral production are themselves subject to optimization based on the rate of cell death and the ways in which replication impacts that rate[12,22]. In some cases steady-state

production is optimal; in others, gradually increasing production rates are optimal.

The root causes of HIV-1 related cell-death remain poorly understood[23-32], and
without better data on the subject it will not be possible to adjust such models to
reflect the underlying biology. In particular, it is still unclear how much direct
toxicity of viral replication contributes to cell death in vivo, compared to the rate at
which cytotoxic T cells kill infected cells[33-36]. But what all models of viral dynamics
make clear is that different kinetic strategies that pathogens adopt have concrete
effects on their fitness and success. The known tendency of HIV-1 Gag to assemble in
a cooperative and switch-like manner[37,38] is consistent with one version of such
models[22] because switch-like behavior can cause a rapid transition to plateau levels
of production, and also that, in the presence of MA, these levels will be suppressed
below a maximum that could be attained. However, all approaches to such models
emphasize the importance of maximizing the viral burst size (the total amount of
viral production per cell). Inhibition of viral production as extreme as that caused by
the MA domain of Gag is not consistent with this requirement. Nor does it appear
that deletion of MA disrupts the switch-like nature of assembly—in fact
translational production of Gag occurs rapidly enough that the immediate release
associated with the ΔMA mutant actually generates virions with a steeper initial
increase than is seen with WT Gag. It also does not appear that the ΔMA mutant is
associated with a higher level of cell death, at least in tissue culture (our
unpublished observations; if anything, the reverse is the case). Therefore it is

unlikely that the assembly inhibition due to MA is involved in optimization of virion

production with respect to the short lifetime of the infected cell. Rather, this

inhibition appears to operate in opposition to this time pressure. It is precisely this

requirement, for efficient viral production, that makes the behavior of the MA

domain so mysterious.

The development of a clear picture of the dynamics of HIV-1 intracellular

replication, both by modeling and experiment, is important because those dynamics

may have repercussions on the course of disease. The dynamics of Gag production,

multimerization, and membrane targeting drive the kinetics of virus release. These

kinetics, in turn, can influence affect systemic pathogenesis. The dynamics of the

viral burst from the very first infected cell in a human can have an impact on

whether or not the virus will be cleared or infection will take hold[13]. These

production kinetics can then go on to structure the balance with immune clearance

that leads to the viral set point after the acute phase, and therefore to impact the

kinetic time course of the disease over years[39-45]. For these reasons, we sought to

map the timing of the intracellular events that constitute the eclipse phase in models

of viral replication, and to try to make sense of those events that do not fit with the

predictions of these models.

Why does HIV-1 encode a MA protein?

It appears that HIV-1 is not optimized with respect to the kinetic pressures that it faces. A mutant HIV-1, ΔMA, is much better optimized for those pressures, except that it is not very infectious. The inhibitory effect exerted by MA on the kinetics of viral release would be understandable if this infectivity defect were an unavoidable consequence of early assembly. The infectivity defect we discovered does not fit with this picture. Rather, it appears to be a consequence of this particular deletion in the RNA, which leads to poor infectivity even at later time points. This infectivity defect does not appear to be a necessary result of abrogation of the myristoyl switch mechanism[46-48]. In fact, multiple mutants have been described in MA that lead to a similar early release phenotype[49-54]. Most of these are point mutants, and are unlikely to have a defect packaging genomic RNA such as the one caused by the removal of all of MA. (Though it should be mentioned that we performed experiments with several of these, and did not see a significant release-enhancement phenotype).

Our goal here was to describe the kinetics of viral assembly and release, and, in addition, to use the ΔMA HIV-1 mutant as a tool to define aspects of retroviral kinetics that are autoregulated. The experiments we performed were not able to uncover the reason for MA-induced inhibition of assembly, although we ruled out several possibilities. We showed that in the absence of MA, HIV-1 Gag is still fully

able to incorporate envelope into virions, and that the low infectivity it shows is not related to envelope. We were also able to show that a full-length molecular clone of ΔMA HIV-1 is not able to package the viral genome efficiently, and that this correlates to a large degree with the infectivity defect. However, in a setting where the ΔMA deletion is present only in the Gag protein driving assembly and not in the RNA genome itself, this packaging defect is not present. Nor, at least in the setting of transfected 293T cells, is the infectivity defect present. Virions produced in this manner showed wild-type infectivity.

Therefore, the role served by the majority of the MA protein remains unclear. It remains reasonable to assume that a phenotype of increased viral production, of a magnitude such as that seen with the ΔMA mutant, would be linked to an infectivity defect related to the kinetics of assembly. The defect we found was large, but was not directly related to the Gag assembly process. One possible explanation is that the deletion of MA sequence in the RNA genome of the ΔMA mutant only accounts for a portion of the observed loss of infectivity, and that some other factor contributes a substantial portion as well. Both the infectivity and RNA packaging defects were close to 5-fold, and both were entirely restored to WT levels in a context where the RNA-level deletion was not present. However, this experiment was performed by transfection in 293T cells (Fig. 5.10). It is possible that in MT-4 cells a factor lacking in 293T cells contributed to the infectivity defect in addition to the RNA deletion. Were it feasible to perform a co-transfection based assay of this

type in MT-4 cells, it is possible that such an effect would be more apparent.

Alternatively, the nature of the defect we found in ΔMA virions may conceal another defect that would be apparent were RNA to be packaged efficiently. In particular, another genomic defect, such as A3G-mediated hypermutation, could be concealed by the effects of the RNA deletion in the ΔMA mutant. It is conceivable that WT HIV-1 requires a MA domain for the inhibition of rapid assembly because virions released prior to Vif-mediated A3G degradation would not be fully infectious and would therefore represent a loss of viral resources. Our use of a mutant that packages a decreased quantity of infectious genomes, for a reason entirely distinct from the effects of A3G, would have served to conceal any such phenotype.

If this were the case, we cannot assume that our result in 293T cells sheds light on this problem. 293T cells do express A3G, but if assembly driven by ΔMA Gag could result in early production of hypermutated virus, we would not have detected it. This particular experiment did not follow kinetics—it examined the effect of increasing quantities of genome on viral release and infectivity assessed at 48 hours post-transfection. As viral release can occur as early as 6 hours after transfection, these cells would have been producing virions for 42 hours prior to collection, and any decreased infectivity in the earliest virions packaged by the ΔMA Gag would have been unlikely to contribute a detectable signal.

It is puzzling why HIV-1 does not avail itself of this extremely rapid assembly rate that would appear to be possible with minor sequence modifications to a protein with few known essential roles. It is not hard to picture modifications of MA that would expose the myristate group and drive accelerated assembly without significantly disrupting the regions of the genomic RNA important for packaging. Indeed, the regions disrupted by the ΔMA mutation are not known to be among the most critical regions for genome packaging; the most important determinants for this process are upstream of the MA coding region.

As will be described in more detail below, the timing of viral production by ΔMA HIV-1 is such that it would actually be expected to sustain A3G-mediated damage, so we favor the hypothesis that avoidance of such damage provides at least part of the selective pressure that has led HIV-1 to maintain MA-induced auto-inhibition of assembly and egress.

A kinetic map

The timing of many parts of the viral life cycle, as well as assembly, may provide important information about basic replication mechanisms, and may be subject to viral regulation. Using a variety of different methods, we were able to map the timing of multiple stages of the viral lifecycle in MT-4 cells, and correlate them to

each other.

Drug-addition time courses allowed us to define the kinetics of reverse-transcription and integration. Completion of reverse transcription is detectable as early as 6 hr post-infection, half-complete by 14.4 hr (+/-0.4), and is largely finished by 24 hr. Integration follows reverse transcription with an average delay of 4.9 hr (+/- 1.2 h) and is complete in half the cells by 19.3 hr (+/- 1.1). After integration there is a significant delay prior to gene expression. Using reporter viruses with fluorophores in positions in the viral genome that are known to be expressed at different points in the replication cycle, we defined the kinetics of gene expression in more detail than has previously been done. Using flow cytometry to monitor these infections, we found that early gene expression reaches half its maximum value at 30.1 hr (+/-0.4) post-infection, 10.8 hours (+/- 1.2) after integration does.

We used quantitative single-cell microscopy to calculate more precise values for the kinetics of gene expression from these dual-reporter viruses. This method gave us a value of 2.8 hr (+/-0.6) for the delay between early and late gene expression, in agreement with the value obtained by flow cytometry. We then used the same microscopy approach to image MT-4 cells stably expressing a cherry-A3G fusion, which we infected with HIV-1 reporter viruses carrying GFP in either early or late gene positions. This gave us values of 4.9 hr (+/-1.2) and 2.5 hr (+/-0.6), respectively, for the delay between early or late gene expression and cherry-A3G

degradation. The difference between these two values, 2.4 hr, provides another estimate of the delay between early and late gene expression and is concordant with the average value of 2.8 hr found with dual-reporter viruses. Cherry-A3G itself is degraded rapidly as GFP expression begins to appear, often by the time the late gene reporter is actually visible. This fits will with the flow cytometry data in which cells infected with the late gene reporter appear green primarily only after cherry signal has disappeared. Tetherin follows a similar down-regulation pattern, at least as followed by flow cytometry. It seems clear that both tetherin and A3G are cleared rapidly and efficiently from HIV-1 infected cells, in a process that takes place in the brief window of time directly surrounding late gene expression (as reported by a fluorescently tagged MA fusion). Our microscopy data indicates in a qualitative way that the duration of A3G degradation, from the beginning of loss of mCherry signal to the reduction of this signal to background levels, takes place in about three hours. Our quantitative data measuring the time between late gene expression and A3G removal indicate that it is complete less than three hours after late gene expression begins to be detectable. The total time of the process cannot be much longer than this, because Vif is a Rev-dependent late gene[55] and cannot be made as early as the viral early genes are. Thus, Vif is potentially present, and the A3G degradation process underway, for a period of time longer than 2.5 hr, but significantly shorter than the 4.9 hr we have shown as the delay between early gene expression and A3G degradation. Vpu is also a late, Rev-dependent, viral gene, and its target, tetherin, is degraded by it with similar kinetics. Therefore, within 2 – 4 hours from the time late

gene expression begins, Vif (and probably tetherin as well) have been cleared from HIV-1 infected cells.

Fig. 7.1 shows the kinetic map of the various stages of the HIV-1 life cycle. The completion midpoints of these first five stages are indicated, as well as the delays between them. The reverse transcription, integration and early gene expression curves are derived from the flow cytometry data presented in Chapter 3. The curve for late gene expression is from this data as well, but is positioned half an hour earlier to reflect the more accurate data obtained from single-cell microscopy. The A3G degradation curve is a copy of the late gene expression curve, positioned as the microscopy data indicates, 2.5 hours after late gene expression. All of these curves indicate percentages of maximum values. The curves for the progression of WT and ΔMA assembly and release are derived from Western blot time courses of p24 release, as described in the figure legend. There is a 4-5 fold difference in the areas beneath these two curves, and thus also in the total amount of p24 produced in this time by both viruses. Despite this, because they follow similar rates of change, when expressed as a percentage of maximum they lie very close to each other in a way that does not reflect the actual data. Therefore here the ΔMA assembly curve is scaled so its maximum is at 100, like the rest of the data on this graph, and the WT assembly curve is scaled proportionally, to indicate the relationship between them.

It is important to keep in mind that these curves do not all represent the same kind

of information. The progress of reverse transcription and integration were followed

in infected cell cultures by adding inhibitory drugs at time points. The cells from

each time point were analyzed by flow cytometry at 48hr post infection, and each

increase in green cells from one time point to the next indicates cells that have

completed the given process and are no longer susceptible to stage-specific

inhibition. The gene expression curves generated by flow cytometry, on the other

hand, indicate the percentage of cells in the culture that have just *begun* early or late

gene expression—or, to be more specific, have completed the transcription,

translation, folding, and some minimal level of accumulation, of the viral reporter

protein. In contrast again, the curve for cherry-A3G degradation represents the

endpoint of that process (although it is a very short process). The assembly curves

represent neither the end nor the beginning of the assembly process, but rather

track the total accumulation of extracellular virus.

Because these are different types of processes these time course curves should be

compared with care. However we can safely say that WT virus rarely produces

detectable virions any sooner than 24 hours post-infection, whereas ΔMA virus

generally already displays significant levels of production by then. At this point, 24

hr. post-infection, the process of A3G degradation has barely begun and destructive

A3G is likely to still be present. Our infection time courses used a virus carrying a

GFP early-gene reporter and allowed us to correlate the process of early gene

expression and p24 assembly and release. We calculated, from the data in Fig.s 5.5

and 5.6 (See text and Materials and Methods), that WT assembly takes place an average of 15.4 hr (+/-3.9) after early GFP expression. We also calculated that WT assembly is delayed an average of 12.5 hr (+/- 5.4) with respect to ΔMA virus. Therefore ΔMA takes place about 2.9 hr after early gene expression. This is an average value, of course, but it indicates that assembly in the absence of the MA domain is almost certainly taking place almost immediately upon late gene expression, and that it is therefore taking place while A3G is still functional in the cell. Our unpublished observations of fluorescent fusions with ΔMA Gag, transfected into cells and visualized by live cell microscopy, are in agreement with this. These constructs appear in puncta at the plasma membrane as soon as they appear at all, and display almost no detectable cytoplasmic background signal.

Taken together, our data indicate that WT HIV-1 assembly begins about 12 hours later than both late gene expression and ΔMA assembly. This timing fits well with a straightforward model of the kinetic regulation of HIV-1 assembly: Late gene expression produces both structural proteins, and accessory proteins that counteract cellular restriction factors, at about the same time. The process of restriction factor removal begins immediately and efficiently, while the process of assembly is delayed, ensuring that newly produced virions are not damaged or restricted by remaining antiviral factors. After a delay long enough to account for even slow restriction factor clearance, assembly begins. We have not provided definitive proof that this process is the basis of the requirement for a delay in

assembly. It remains to be shown if there is an infectivity phenotype common to all myristate-exposing mutations of the HIV-1 MA domain. However, we have shown that WT assembly takes place after the clearance of restriction factors from the cell, and that in the absence of the delay imposed by the MA domain, assembly proceeds while these factors are still present.
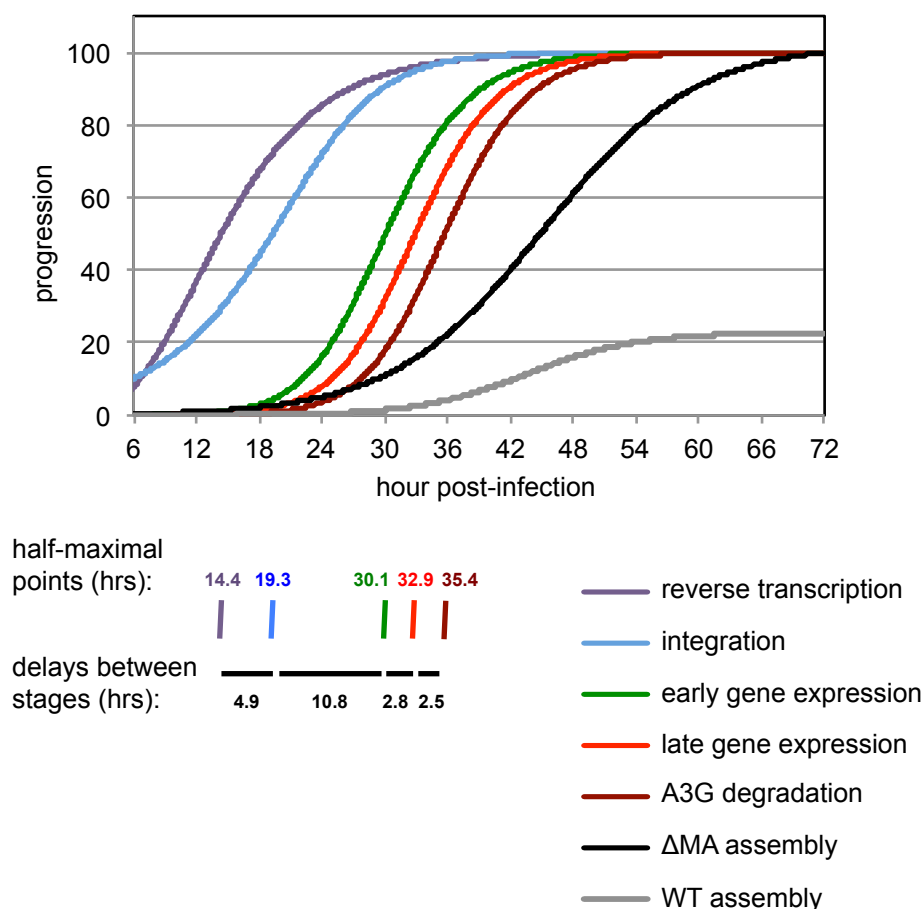
Figure 7.1. The time line of HIV-1 replication. A schematic representation of the timing of the major events in the HIV-1 life cycle. The reverse-transcription, integration, and early and late gene expression curves are 5-parameter logistic functions fit to the data in Fig. 3.9, in which inhibitor-addition and dual-reporter infection experiments were carried out in parallel at 4 different titers, analyzed by flow cytometry, and expressed as a percentage of maximum. The late-gene expression curve is shifted slightly earlier to reflect the more accurate value obtained for the delay between early and late gene expression using single-cell microscopy. The cherry-A3G degradation curve (A3G) is a duplicate of the curve fit to the late-gene expression data, shifted 2.5 hr later to reflect the delay between these stages calculated by single-cell microscopy. The WT and ΔMA curves are the 4-parameter logistic functions fit to 7 repetitions of the assembly experiment in Fig. 5.5, and interpolated to 72 hr. They are not expressed as a percentage of maximum but are instead scaled proportionally to each other with the maximum of the ΔMA curve set at 100 for clarity. The times post-infection at which each of the first five stages reaches half its maximum value are shown at bottom, as well as the delays between these points.

Future directions

The timing of the intracellular events of retroviral infection will vary widely from cell type to cell type. Therefore for a kinetic map of the life cycle to be complete it should be defined in multiple relevant cell types, and ideally in primary cells. In addition there are several stages that we did not explore. It would be worthwhile to complete more of the type of time course experiments shown here, for every amenable stage of the viral life cycle, in way that allows correlation of two or more stages at a time. For instance, it would not be difficult to follow the kinetics of entry at the same time as those of reverse transcription. We have done so preliminarily, by adding the entry inhibitor dextran sulfate at timepoints soon after infection (unpublished data), and we believe that the spinoculation protocol we use leads to the majority of infectious entry events taking place within 2-3 hours, even when the inoculum is not washed off. But this experiment should be performed in conjunction with an entry assay[56,57], that can allow sensitive detection of actual entry events.

More information on the relative kinetics of the post-entry stages is sorely needed, but much more difficult to obtain. Uncoating in particular is a complex process to follow, and requires biochemical assays that can be complicated by the presence of Gag molecules that are not part of an active infection pathway. Performing these at low enough MOI to minimize such effects would result in levels of material too small

to perform most assays with. Even at effective MOIs of much less than 1, this is still

a potential issue. The experiments performed here were all done at an MOI of less

than 0.5 to avoid effective co-infection - but this still does not bypass the potential

interference of hundreds of non-functional viral particles. These may be on the

outer surface of the cell, or have successfully navigated cellular and even nuclear

entry[58-60]. The particle to infectious unit ratio for HIV-1 is very high, and many of

these viral particles attain the nucleus and form extrachromosomal DNA circles[60]. It

is not known what effects these non-productive virions may have on kinetic studies.

In the worst case scenario, they can contribute to the detection of early events such

as reverse transcription (if DNA products are measured), without going on to

contribute to the signal for later ones. However, this is thought to be the nature of

HIV-1 infection – that the infection of a cell simply involves many particles but

usually only one provirus[58,61,62]. These extra viral particles may play a relevant role

in the life cycle, for instance by serving as decoy targets for TRIM5alpha[63,64].

Completion of a full kinetic map of the HIV-1 life cycle will require the

determination of the precise relative timing of the interrelated uncoating, transport,

and reverse transcription events that take place after entry. Innovative

combinations of microscopy and drug-inhibition approaches have proven useful

with respect to these questions[65-68].

However, even the simpler assays for uncoating, for instance timed cyclosporine

addition or washout[65,69], could be done using viruses carrying early or late gene

reporters, or both, and this will allow the determination of the relative timing between these stages. In these experiments it is necessary to infect cultures and then split them, collecting one arm at time points for reporter kinetics. The other arm is then used for addition or removal of drug at the same timepoints, and is collected at 48 hr post-infection. Thus the two data sets represent the same infection of the same culture and can be precisely correlated.

There is also a large gap in the data provided here with respect to gene expression. Our reporter viruses indicate the appearance of mature folded proteins, but we can only make inferences about how this reflects the underlying processes of transcription, splicing, and mRNA export. Techniques are available for following the actual kinetics of transcriptional RNA production[70], and these would allow us to answer critical questions such as: does the appearance of reporter gene proteins take place immediately post-transcription, or is there a significant delay associated with the splicing and export processes? Are these delays the same for different viral genes, or do they vary widely? We can also perform such experiments in tandem with integration-inhibition time courses. Together these would give us a picture of the relative timing of integration, transcription, and gene expression. At the moment we cannot say with certainty where the transcriptional process takes place within the 11 hr gap between integration and protein production.

In addition, our reporter viruses carry a single late gene reporter, and a single early

gene reporter, produced from positions in the viral genome that are thought to be representative of these stages. We are forced to speculate about the actual timing of the production of viral proteins such as Rev and Vif. Rev is produced as an early gene, by definition, but it may not follow the same kinetics as the reporter we have in the Nef early gene position. Following the actual appearance of Rev would give us not only more information about early gene production, but would allow us to set an early limit on the possible timing of Rev-dependent late gene production. Likewise, following the kinetics of Vif production at the same time as we follow A3G degradation will be vastly superior than simply following a general late gene reporter. Vif is partially spliced, and therefore Rev-dependent. However, it is possible that partially spliced transcripts may appear earlier than unspliced ones, and this would be quite significant with regard to the conclusions we will draw about the A3G counteraction process. Vif or Rev or other viral proteins can be followed by fixing and staining cells at timepoints, though this has obvious drawbacks. New techniques utilizing small tags may become feasible for live cell imaging[68,71-73]. Live cell imaging of viral proteins as fluorescent fusions is vastly preferable, but of course this requires modifying the viral genome with insertions in ways that are not always possible.

Determining the nature of the role played by the MA domain is still necessary. Firstly, it needs to be established beyond a reasonable doubt that the deletion in the

genomic RNA is the cause of the infectivity defect of the ΔMA mutant. This is straightforward to determine, as the deletion can be made in a genome that is provided in trans by transfection and packaged by WT Gag into virions. If an envelope plasmid is also provided, these virions can be assessed for infectiousness on target cells. The converse experiment will then be a starting point for assessing the role of the deletion of MA in the Gag protein itself: full-length genome can be provided in trans to ΔMA Gag, much as was done in the 293T experiment described in Fig. 5.10. However, in order to use this setup to understand the *kinetic* effect of the deletion, the experiment would now consist of harvesting virus at time points post-infection (beginning as early as hr. 4), and analyzing it for p24 content, RNA content, and infectivity. This would not recapitulate the kinetics of an actual infection. But the MA-deleted Gag will still produce virions far more efficiently, and they will now carry completely healthy genomes. The hypothesis would be that they will still not be fully infectious – that at the very least, the early time points will show a defect with respect to a WT Gag control. It would be very surprising if fixing the RNA alone allowed this mutant to generate high quantities of virions that are infectious as WT virus. The goal would simply be to determine exactly what defect does remain after the RNA is repaired. The experiment should be done in cells carrying A3G, by transfection with genomes that are +/- Vif. It should also be done in cells lacking A3G. If the hypothesis that A3G hypermutation is involved is correct, only in absence of A3G will the ΔMA Gag package fully infectious virions. Even in the presence of A3G and Vif as well, ΔMA Gag would still show an infectivity defect, at

least at early time points. A3G avoidance is only one plausible explanation for the role of MA; and it may not be a good enough one, given the powerful effects of Vif so soon after late gene expression begins (See Ch. 4). Of course, the question of A3G involvement can also be addressed quite easily in a different way: by sequencing genomic RNA from virions and looking for the signs of A3G hypermutation.

It will be quite important to discover whether any remaining infectivity defect to ΔMA Gag assembly (in the presence of a non-deleted genome) is present only at early time points or applies to virions produced later as well. At later time points, presumably Vif will have removed A3G from cells, and therefore any ongoing defect cannot be explained by A3G-directed hypermutation. But in order to carefully compare the infectiousness of virus collected at varying points in the assembly process, it is much preferable to perform the experiments in the context of an infection with natural kinetics. This is not straightforward in this case, as we are attempting to study a virus in which the structural Gag protein carries a deletion not present in the genome. There are complex methods by which this could be accomplished, such as infecting stable cells lines carrying ΔMA GagPol with virus lacking the Gag start codon. This arrangement would allow the production of virus with partially normal infection kinetics, although the Gag production kinetics would be atypical. It would be preferable to identify a MA mutant that has the ΔMA phenotype without lacking so much of the MA sequence. It is reportedly possible to generate MA mutants with accelerated assembly using only point mutations[47,51,54].

Although we ourselves have seen no release enhancement with the MA point

mutants we have tested (unpublished results), an important next step toward

understanding the role of MA in the regulation of assembly kinetics would be to

construct a panel of smaller deletions in MA in order to narrow the region necessary

for the phenotype. This would potentially be both the most practical and the most

informative approach to bypassing the RNA incorporation defect while allowing

study of the accelerated assembly phenotype.

Finally, there is a tool that should be developed for the study of assembly, and would

be particularly useful for studying the timing of assembly and MA mutants. There is

no assay for studying the timing of Gag assembly on membranes at the single cell

level. Assembly and release are thought to take place so rapidly[74,75] that assessing

supernatant p24 levels is a good proxy for assembly itself. Fractionation techniques

can assess membrane binding. But each of these is a bulk cell culture technique, and

cannot tell us, for instance, how soon assembly proceeds in individual cells with

respect to initial late gene production and A3G degradation. The assembly of

individual virions can be imaged by TIRF microscopy[75], but these events can take

place at any point during the assembly process. It would be possible to set up an

assay for assembly, for instance a FRET or bimolecular fluorescence

complementation[76,77] assay using either two Gag constructs, or one Gag construct

and a membrane-bound Gag interactor, and use it in tandem with the quantitative

single-cell microscopy approach used here. This would allow high resolution

quantitation of assembly kinetics as they relate to prior processes in the viral life cycle. It would be possible to generate intensity traces for single cells that show the progression of late gene expression and then of the formation of assembly foci, or the progression of A3G degradation together with assembly. Biochemical approaches have given us general data on the rate of the assembly process, but these are still partially obscured by bulk effects, and by the fact that overall viral accumulation in the supernatant masks the actual rate of change of the assembly process in a cell.

The goal of all these studies is the same: a more detailed picture of the timing of HIV-1 replication in cells, and therefore a better understanding of the pressures faced by each viral process prior to release of new virions. Every point in the viral life cycle for which we discover new cellular requirements is a potential new point of intervention or inhibition that could lead to new treatment options for HIV-1 infection.

References, Chapter 7.

1. Perelson, A. S. *et al.* Decay characteristics of HIV-1-infected compartments during combination therapy. *Nature* **387**, 188–191 (1997).

2. Perelson, A. S., Essunger, P. & Ho, D. D. Dynamics of HIV-1 and CD4+ lymphocytes in vivo. *AIDS* **11 Suppl A**, S17–24 (1997).

3. Perelson, A. S., Neumann, A. U., Markowitz, M., Leonard, J. M. & Ho, D. D. HIV-1 dynamics in vivo: virion clearance rate, infected cell life-span, and viral generation time. *Science* **271**, 1582–1586 (1996).

4. Ho, D. D. *et al.* Rapid turnover of plasma virions and CD4 lymphocytes in HIV-1 infection. *Nature* **373**, 123–126 (1995).

5. Nelson, P. W., Murray, J. D. & Perelson, A. S. A model of HIV-1 pathogenesis that includes an intracellular delay. *Math Biosci* **163**, 201–215 (2000).

6. Mittler, J. E., Markowitz, M., Ho, D. D. & Perelson, A. S. Improved estimates for HIV-1 clearance rate and intracellular delay. *AIDS* **13**, 1415–1417 (1999).

7. Mittler, J. E., Sulzer, B., Neumann, A. U. & Perelson, A. S. Influence of delayed viral production on viral dynamics in HIV-1 infected patients. *Math Biosci* **152**, 143–163 (1998).

8. Dixit, N. M. & Perelson, A. S. Complex patterns of viral load decay under antiretroviral therapy: influence of pharmacokinetics and intracellular delay. *J. Theor. Biol.* **226**, 95–109 (2004).

9. Nelson, P. W. & Perelson, A. S. Mathematical analysis of delay differential equation models of HIV-1 infection. *Math Biosci* **179**, 73–94 (2002).

10. Nelson, P. W., Mittler, J. E. & Perelson, A. S. Effect of drug efficacy and the eclipse phase of the viral life cycle on estimates of HIV viral dynamic parameters. *JAIDS Journal of Acquired Immune Deficiency Syndromes* **26**, 405–412 (2001).

11. Dixit, N. M., Markowitz, M., Ho, D. D. & Perelson, A. S. Estimates of intracellular delay and average drug efficacy from viral load data of HIV-infected individuals under antiretroviral therapy. *Antivir. Ther. (Lond.)* **9**, 237–246 (2004).

12. Gilchrist, M. A., Coombs, D. & Perelson, A. S. A. S. Optimizing within-host viral fitness: infected cell lifespan and virion production rate. *J. Theor. Biol.* **229**, 281–288 (2004).

13. Pearson, J. E., Krapivsky, P. & Perelson, A. S. Stochastic theory of early viral infection: continuous versus burst production of virions. *PLoS Comp Biol* **7**, e1001058 (2011).

14. May, R. M. & Nowak, M. A. Coinfection and the evolution of parasite virulence. *Proc. Biol. Sci.* **261**, 209–215 (1995).

15. May, R. M. & Anderson, R. M. Epidemiology and genetics in the coevolution of parasites and hosts. *Proc. R. Soc. Lond., B, Biol. Sci.* **219**, 281–313 (1983).

16. Nowak, M. A. & May, R. M. Superinfection and the evolution of parasite virulence. *Proc. Biol. Sci.* **255**, 81–89 (1994).

17. Shirreff, G., Pellis, L., Laeyendecker, O. & Fraser, C. Transmission selects for HIV-1 strains of intermediate virulence: a modelling approach. *PLoS Comp Biol* **7**, e1002185 (2011).

18. Müller, V., Fraser, C. & Herbeck, J. T. A strong case for viral genetic factors in HIV virulence. *Viruses* **3**, 204–216 (2011).

19. Hill, A. L., Rosenbloom, D. I. S. & Nowak, M. A. Evolutionary dynamics of HIV at multiple spatial and temporal scales. *J. Mol. Med.* **90**, 543–561 (2012).

20. Woolhouse, M. E. J., Webster, J. P., Domingo, E., Charlesworth, B. & Levin, B. R. Biological and biomedical implications of the co-evolution of pathogens and their hosts. *Nat. Genet.* **32**, 569–577 (2002).

21. Lenski, R. E. & May, R. M. The evolution of virulence in parasites and pathogens: reconciliation between two competing hypotheses. *J. Theor. Biol.* **169**, 253–265 (1994).

22. Coombs, D., Gilchrist, M. A., Percus, J. & Perelson, A. S. Optimal viral production. *Bull. Math. Biol.* **65**, 1003–1023 (2003).

23. Balamurali, M. *et al.* Does cytolysis by CD8+ T cells drive immune escape in HIV infection? *J. Immunol.* **185**, 5093–5101 (2010).

24. Ribeiro, R. M., Mohri, H., Ho, D. D. & Perelson, A. S. In vivo dynamics of T cell activation, proliferation, and death in HIV-1 infection: why are CD4+ but not CD8+ T cells depleted? *Proc. Natl. Acad. Sci. U.S.A.* **99**, 15572–15577 (2002).

25. Petit, F. *et al.* Productive HIV-1 infection of primary CD4+ T cells induces mitochondrial membrane permeabilization leading to a caspase-independent cell death. *J. Biol. Chem.* **277**, 1477–1487 (2002).

26. Piller, S. C., Jans, P., Gage, P. W. & Jans, D. A. Extracellular HIV-1 virus protein R causes a large inward current and cell death in cultured hippocampal neurons: implications for AIDS pathology. *Proc. Natl. Acad. Sci. U.S.A.* **95**, 4595–4600 (1998).

27. Sylwester, A., Murphy, S., Shutt, D. & Soll, D. R. HIV-induced T cell syncytia are self-perpetuating and the primary cause of T cell death in culture. *J. Immunol.* **158**, 3996–4007 (1997).

28. Alimonti, J. B., Ball, T. B. & Fowke, K. R. Mechanisms of CD4+ T lymphocyte cell death in human immunodeficiency virus infection and AIDS. *J. Gen. Virol.* **84**, 1649–1661 (2003).

29. Gougeon, M. L. & Montagnier, L. Programmed cell death as a mechanism of CD4 and CD8 T cell deletion in AIDS. Molecular control and effect of highly active anti-retroviral therapy. *Ann. N. Y. Acad. Sci.* **887**, 199–212 (1999).

30. Estaquier, J. *et al.* Programmed cell death and AIDS: significance of T-cell apoptosis in pathogenic and nonpathogenic primate lentiviral infections. *Proc. Natl. Acad. Sci. U.S.A.* **91**, 9431–9435 (1994).

31. Renan, M. J. T-cell depletion following HIV infection: a case of c-myc-induced cell death? *Res. Virol.* **144**, 173–174 (1993).

32. Ameisen, J. C. & Capron, A. Cell dysfunction and depletion in AIDS: the programmed cell death hypothesis. *Immunol. Today* **12**, 102–105 (1991).

33. Klenerman, P. *et al.* Cytotoxic T lymphocytes and viral turnover in HIV type 1 infection. *Proc. Natl. Acad. Sci. U.S.A.* **93**, 15323–15328 (1996).

34. Pantaleo, G. & Fauci, A. S. Immunopathogenesis of HIV infection. *Annu.*

Rev. Microbiol. **50**, 825–854 (1996).

35. Zinkernagel, R. M. Are HIV-specific CTL responses salutary or pathogenic? *Curr. Opin. Immunol.* **7**, 462–470 (1995).

36. Zinkernagel, R. M. & Hengartner, H. T-cell-mediated immunopathology versus direct cytolysis by virus: implications for HIV and AIDS. *Immunol. Today* **15**, 262–268 (1994).

37. Yadav, S. S., Wilson, S. J. & Bieniasz, P. D. A facile quantitative assay for viral particle genesis reveals cooperativity in virion assembly and saturation of an antiviral protein. *Virology* (2012).doi:10.1016/j.virol.2012.04.008

38. Perez-Caballero, D., Hatziioannou, T., Martin-Serrano, J. & Bieniasz, P. D. Human immunodeficiency virus type 1 matrix inhibits and confers cooperativity on gag precursor-membrane interactions. *J. Virol.* **78**, 9560–9563 (2004).

39. Stilianakis, N. I. & Schenzle, D. On the intra-host dynamics of HIV-1 infections. *Math Biosci* **199**, 1–25 (2006).

40. Cheng-Mayer, C., Seto, D., Tateno, M. & Levy, J. A. Biologic features of HIV-1 that correlate with virulence in the host. *Science* **240**, 80–82 (1988).

41. Soriano, V., Heredia, A., Bravo, R., Gutiérrez, M. & González-Lahoz, J. [Rapid progression to AIDS in a patient with infection from a strain of syncytium forming HIV-1]. *Med Clin (Barc)* **105**, 99–100 (1995).

42. Barbour, J. D. & Grant, R. M. The role of viral fitness in HIV pathogenesis. *Curr HIV/AIDS Rep* **2**, 29–34 (2005).

43. Lobritz, M. A., Lassen, K. G. & Arts, E. J. HIV-1 replicative fitness in elite controllers. *Curr Opin HIV AIDS* **6**, 214–220 (2011).

44. Barbour, J. D. & Grant, R. M. The Clinical Implications of Reduced Viral Fitness. *Curr Infect Dis Rep* **6**, 151–158 (2004).

45. Anastassopoulou, C. G. & Kostrikis, L. G. Viral correlates of HIV-1 disease. *Curr. HIV Res.* **3**, 113–132 (2005).

46. Resh, M. D. A myristoyl switch regulates membrane binding of HIV-1 Gag. *Proc. Natl. Acad. Sci. U.S.A.* **101**, 417–418 (2004).

47. Paillart, J. C. & Göttlinger, H. G. Opposing effects of human immunodeficiency virus type 1 matrix mutations support a myristyl switch model of gag membrane targeting. *J. Virol.* **73**, 2604–2612 (1999).

48. Spearman, P., Horton, R., Ratner, L. & Kuli-Zade, I. Membrane binding of human immunodeficiency virus type 1 matrix protein in vivo supports a conformational myristyl switch mechanism. *J. Virol.* **71**, 6582–6592 (1997).

49. Chukkapalli, V., Oh, S. J. & Ono, A. Opposing mechanisms involving RNA and lipids regulate HIV-1 Gag membrane binding through the highly basic region of the matrix domain. *Proceedings of the National Academy of Sciences* **107**, 1600–1605 (2010).

50. Ono, A., Demirov, D. & Freed, E. O. Relationship between human immunodeficiency virus type 1 Gag multimerization and membrane binding. *J. Virol.* **74**, 5142–5150 (2000).

51. Ono, A., Orenstein, J. M. & Freed, E. O. Role of the Gag matrix domain in targeting human immunodeficiency virus type 1 assembly. *J. Virol.* **74**, 2855–2866 (2000).

52. Kiernan, R. E., Ono, A. & Freed, E. O. Reversion of a human immunodeficiency virus type 1 matrix mutation affecting Gag membrane binding, endogenous reverse transcriptase activity, and virus infectivity. *J. Virol.* **73**, 4728–4737 (1999).

53. Ono, A. & Freed, E. O. Binding of human immunodeficiency virus type 1 Gag to membrane: role of the matrix amino terminus. *J. Virol.* **73**, 4136–4144 (1999).

54. Saad, J. S. *et al.* Point mutations in the HIV-1 matrix protein turn off the myristyl switch. **366**, 574–585 (2007).

55. Cullen, B. R. Regulation of HIV-1 gene expression. *FASEB J.* **5**, 2361–2368 (1991).

56. Cavrois, M., de Noronha, C. & Greene, W. C. A sensitive and specific enzyme-based assay detecting HIV-1 virion fusion in primary T lymphocytes. *Nat. Biotechnol.* **20**, 1151–1154 (2002).

57. Saeed, M. F., Kolokoltsov, A. A. & Davey, R. A. Novel, rapid assay for measuring entry of diverse enveloped viruses, including HIV and

rabies. *J. Virol. Methods* **135**, 143–150 (2006).

58. Bell, P., Montaner, L. J. & Maul, G. G. Accumulation and intranuclear distribution of unintegrated human immunodeficiency virus type 1 DNA. *J. Virol.* **75**, 7683–7691 (2001).

59. Saenz, D. T. *et al.* Unintegrated lentivirus DNA persistence and accessibility to expression in nondividing cells: analysis with class I integrase mutants. *J. Virol.* **78**, 2906–2920 (2004).

60. Pang, S. *et al.* High levels of unintegrated HIV-1 DNA in brain tissue of AIDS dementia patients. *Nature* **343**, 85–89 (1990).

61. Suspène, R. & Meyerhans, A. Quantification of unintegrated HIV-1 DNA at the single cell level in vivo. *PLoS ONE* **7**, e36246 (2012).

62. Sloan, R. D. & Wainberg, M. A. The role of unintegrated DNA in HIV infection. *Retrovirology* **8**, 52 (2011).

63. Stremlau, M. *et al.* The cytoplasmic body component TRIM5alpha restricts HIV-1 infection in Old World monkeys. *Nature* **427**, 848–853 (2004).

64. Shi, J. & Aiken, C. Saturation of TRIM5 alpha-mediated restriction of HIV-1 infection depends on the stability of the incoming viral capsid. *Virology* **350**, 493–500 (2006).

65. Hulme, A. E., Perez, O. & Hope, T. J. Complementary assays reveal a relationship between HIV-1 uncoating and reverse transcription. *Proceedings of the National Academy of Sciences* **108**, 9975–9980 (2011).

66. Arfi, V. *et al.* Characterization of the behavior of functional viral genomes during the early steps of human immunodeficiency virus type 1 infection. *J. Virol.* **83**, 7524–7535 (2009).

67. Arhel, N. J. *et al.* HIV-1 DNA Flap formation promotes uncoating of the pre-integration complex at the nuclear pore. *EMBO J.* **26**, 3025–3037 (2007).

68. Arhel, N. *et al.* Quantitative four-dimensional tracking of cytoplasmic and nuclear HIV-1 complexes. *Nat. Methods* **3**, 817–824 (2006).

69. Perez-Caballero, D., Hatziioannou, T., Zhang, F., Cowan, S. & Bieniasz, P. D. Restriction of human immunodeficiency virus type 1 by TRIM-CypA

occurs with rapid kinetics and independently of cytoplasmic bodies, ubiquitin, and proteasome activity. *J. Virol.* **79**, 15567–15572 (2005).

70. Maiuri, P., Knezevich, A., Bertrand, E. & Marcello, A. Real-time imaging of the HIV-1 transcription cycle in single living cells. *Methods* **53**, 62–67 (2011).

71. Lelek, M. *et al.* Superresolution imaging of HIV in infected cells with FlAsH-PALM. *Proceedings of the National Academy of Sciences* **109**, 8564–8569 (2012).

72. Whitt, M. A. & Mire, C. E. Utilization of fluorescently-labeled tetracysteine-tagged proteins to study virus entry by live cell microscopy. *Methods* **55**, 127–136 (2011).

73. Andresen, M., Schmitz-Salue, R. & Jakobs, S. Short tetracysteine tags to beta-tubulin demonstrate the significance of small labels for live cell imaging. *Mol. Biol. Cell* **15**, 5616–5622 (2004).

74. Jouvenet, N., Bieniasz, P. D. & Simon, S. M. Imaging the biogenesis of individual HIV-1 virions in live cells. *Nature* **454**, 236–240 (2008).

75. Ivanchenko, S. *et al.* Dynamics of HIV-1 assembly and release. *PLoS Pathog.* **5**, e1000652 (2009).

76. Jin, J., Sturgeon, T., Weisz, O. A., Mothes, W. & Montelaro, R. C. HIV-1 matrix dependent membrane targeting is regulated by Gag mRNA trafficking. *PLoS ONE* **4**, e6551 (2009).

77. Chen, C. *et al.* Association of gag multimers with filamentous actin during equine infectious anemia virus assembly. *Curr. HIV Res.* **5**, 315–323 (2007).